University of Alberta

Hydrology, microbiology and carbon cycling at a high Arctic polythermal glacier, (John Evans Glacier, Ellesmere Island, Canada).

by

Mark Leslie Skidmore ©

A thesis submitted to the Faculty of Graduate Studies and Research in partial fulfillment of the requirements for the degree of Ph.D.

Department of Earth and Atmospheric Sciences

Edmonton, Alberta

Fall 2001

National Library of Canada
Acquisitions and Bibliographic Services
395 Wellington Street
Ottawa ON K1A 0N4
Canada

Bibliothèque nationale du Canada
Acquisitions et services bibliographiques
395, rue Wellington
Ottawa ON K1A 0N4
Canada

Your file Votre référence

Our file Notre référence

The author has granted a non-exclusive licence allowing the National Library of Canada to reproduce, loan, distribute or sell copies of this thesis in microform, paper or electronic formats.

L'auteur a accordé une licence non exclusive permettant à la Bibliothèque nationale du Canada de reproduire, prêter, distribuer ou vendre des copies de cette thèse sous la forme de microfiche/film, de reproduction sur papier ou sur format électronique.

The author retains ownership of the copyright in this thesis. Neither the thesis nor substantial extracts from it may be printed or otherwise reproduced without the author's permission.

L'auteur conserve la propriété du droit d'auteur qui protège cette thèse. Ni la thèse ni des extraits substantiels de celle-ci ne doivent être imprimés ou autrement reproduits sans son autorisation.

0-612-68994-8

Canada

University of Alberta

Library Release Form

Name of Author: Mark Leslie Skidmore

Title of Thesis: Hydrology, microbiology and carbon cycling at a high Arctic polythermal glacier, (John Evans Glacier, Ellesmere Island, Canada).

Degree: Doctor of Philosophy

Year this Degree Granted: 2001

Permission is hereby granted to the University of Alberta Library to reproduce single copies of this thesis and to lend or sell such copies for private, scholarly or scientific research purposes only.

The author reserves all other publication and other rights in association with the copyright in the thesis, and except as herein before provided, neither the thesis nor any substantial portion thereof may be printed or otherwise reproduced in any material form whatever without the author's prior written permission.

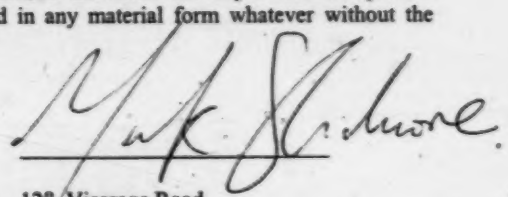

128, Vicarage Road,
Wollaston,
Stourbridge,
West Midlands
DY8 4QY
United Kingdom

24th September 2001

"It is important that students bring a certain ragamuffin barefoot irreverance to their studies; they are not here to worship what is known, but to question it."

Jacob Bronowski, The Ascent of Man

University of Alberta

Faculty of Graduate Studies and Research

The undersigned certify that they have read, and recommend to the Faculty of Graduate Studies and Research for acceptance, a thesis entitled Hydrology, microbiology and carbon cycling at a high Arctic polythermal glacier, (John Evans Glacier, Ellesmere Island, Canada) by Mark Skidmore in partial fulfillment of the requirements for the degree of Doctor of Philosophy.

Dr. Martin Sharp

Dr. Karlis Muehlenbachs

Dr. Robert Creaser

Dr. Marvin Dudas

Dr. Alexander Wolfe

For Dr. Warwick Vincent

Date: 24 September 2001

This thesis is dedicated to the memories of
Paul Wolfe and Charles Andriashek.

Abstract

Analysis of the hydrology, hydrochemistry and microbiology at polythermal John Evans Glacier and geochemical and isotopic data from Haut Glacier d'Arolla demonstrates that certain subglacial chemical weathering processes are microbially mediated.

Subglacial drainage is likely an annual occurrence beneath John Evans Glacier and solute rich subglacial waters indicate over winter storage at the glacier bed. Subglacial microbial populations are also present, and are viable under simulated near *in situ* conditions at 0.3°C. This suggests that temperate subglacial environments at a polythermal glacier, which are isolated by cold ice above and around them, provide a viable habitat for life where basal water and organic carbon are present throughout the year. Thus, a subglacial microbial ecosystem based upon legacy carbon, (from old soils or surface inputs) rather than primary production may exist, where redox processes are a key component, and seasonal anoxia may occur. The existence of anoxic environments is supported by the presence of strictly anaerobic bacteria (sulphate reducing bacteria and methanogens) in the basal sediments, - which are viable in culture at 4°C - and also argues that these bacteria are not washed in with oxygenated surface meltwaters, but are present in the subglacial environment.

During the summer meltseason there is a large input of surficial waters to the subglacial system and water residence times are drastically reduced. Hence, kinetic weathering processes dominate, resulting in light δ^{13}C-DIC (dissolved inorganic carbon) in glacial

runoff, as verified by experimental work on $CaCO_3$ and John Evans Glacier sediments. The experiments demonstrate kinetic bedrock fractionation (KBF) during carbonate hydrolysis and that kinetic fractionation of CO_2 (KFC) is proportional to the rate of CO_2 draw down during the carbonation of carbonates. This results in significantly depleted δ^{13}C-DIC values (≤ -16 ‰) relative to the bedrock carbonate. Incorporating KBF and KFC processes into geochemical weathering models makes it possible to distinguish between kinetic effects and microbial CO_2 as causes of light δ^{13}C-DIC in glacial runoff. However, where kinetically produced DIC dominates, this can potentially mask small microbial respiration signatures. Only in the distributed system waters at Haut Glacier d'Arolla is light δ^{13}C-DIC clearly due to microbial respiration.

Acknowledgements

Science: I am deeply indebted to Martin Sharp for his guidance, enthusiam and encouragement for my research throughout my Ph.D. Thanks. Karlis Muehlenbachs has also offered me a great deal of insight into the world of scientific investigation and the odd crazy lunch. Julia Foght too has been an incredible mentor and has significantly improved my understanding of microbiology. Finally, thanks to Martyn Tranter for his belief in me to complete the thesis and patience in achieving that end. Viva Wolves. I have also benefitted considerably from interactions with the wonderful graduate student community at U of A, most notably Dave Selby, Devon Rowe, Jo Molyneux, Scott Lamoureux, Melissa Lafreniere, Karen Fallas, John Paul Zonneveld and Murray Gingras, however, many others have contributed along the way, e.g. Ted and Dean.

Fun stuff: So the folks who have kept me psuedo sane during the thesis, include the grad students above plus a few others. So the notables in this field are Mole City, Chris, John, Devo and Charles and Cap'n Nemo too, especially Rod. I have shared many a pint/scotch with numerous friends during the Ph.D. So in no particular order, thanks go to Joel, Anixia, Gwen, Lynn,Vaughn, Darryl, Vinny, Claude, Jeff and Leyla, Shandy and Chris, Rob and Shady, Jase, Leslie Driver, Candace, Andrea, Craig, Anna-Liisa, Mandy, Rick, Leslie Dawson, George, Betsy & the BWC, Dr Mann, Mike C., Karin, the Bristol Crew + Dave R., Russ, Chris, Ian, Amy and Cesco. A special mention is due to Jez D., Andy and Dave E. who kept my spirits alive over the final stretch, and of course Plops and Snoop and for keeping me far from the straight and narrow.

Field and technical assistance: Field assistance was ably provided by Anthony Arendt, Christina MacIssac, and Rick Young, thanks for saving my life mate. John England's help and words of wisdom during some tough field work also proved invaluable. Thanks also to Martin Sharp, Joel Barker, Wendy Davis, Luke Copland and Darek Glowacki for collection of additional field samples. Sara Ebert provided technical help with the culture work and Rakesh Bhatnagar assisted with the TEM imaging. DOC and TOC analyses of the ice samples were kindly performed by Kristen Leckrone, Biogeochemical Laboratories, Indiana University. Jenny Mills performed the Si analyses. Shawn Marshall kindly provided me with unpublished ice sheet model output data which was skilfully transformed into maps by Guy Munhoven.

Funding and logistics: The research was supported by Canadian Circumpolar Institute and two Geological Society of America grants to myself and NSERC operating grants to Martin Sharp and Julia Foght. During my Ph.D. I was also the recipient of a Teaching Assistantship, GL Cumming Scholarship for Isotope Geochemistry, and J Gordin Kaplan Travel Award, all from University of Alberta and a Graduate Travel Award, Lunar and Planetary Institute, Houston, Texas, U.S.A. Logistical field support was provided by the Polar Continental Shelf Project (PCSP), Natural Resources Canada. Fieldwork was carried out with the kind permission of the Nunavut Research Institute and the peoples of Resolute Bay and Grise Fiord.

Finally. Thanks to my parents and brother for their support and encouragement.

Table of Contents

Chapter 1. Introduction 1

1.1. PREVIOUS WORK AT JOHN EVANS GLACIER 2

1.2. JOHN EVANS GLACIER MELTWATER CHEMISTRY 3

1.3. THESIS OBJECTIVES 4

1.4. ADDITIONAL Ph.D. RESEARCH 8

1.5. REFERENCES 9

Chapter 2. Drainage system behaviour of a high Arctic polythermal glacier. 14

2.1. INTRODUCTION 14

2.2. FIELD SITE 16

2.3. METHODS 16

2.4. RESULTS 18
2.4.1. Evidence for subglacial drainage 18
2.4.2. Release of subglacial water 19
2.4.3. Subglacial outflow hydrographs 20
2.4.4. Evidence for subglacial water storage 21
2.4.5. Synthesis 23

2.5. DISCUSSION 24
2.5.1. Implications for subglacial hydrology 24
2.5.2. Inter-annual variations in subglacial drainage system behaviour 25
2.5.3. Comparison to other studies 25

2.6. CONCLUSIONS 26

2.7. REFERENCES 27

Chapter 3. Microbial life beneath a High Arctic Glacier 34

3.1. INTRODUCTION 34

3.2. MATERIALS AND METHODS 36
3.2.1. Field site. 37
3.2.2. Definition of ice and water types. 37
3.2.3. Water samples 1996. 38
3.2.4. Ice samples 1997. 39
3.2.5. 1998 Ice samples. 41
3.2.6. Microscopy. 42
3.2.7. Organic carbon concentrations. 42

3.3. RESULTS 43
3.3.1. 1996 water samples. 43
3.3.2. 1997 ice samples. 44
3.3.3. 1998 ice samples. 45
3.3.4. Microscopy. 46
3.3.5. Allochthonous organic carbon. 47

3.4. DISCUSSION 47
3.4.1. Glacial/interglacial carbon cycling. 50
3.4.2. Ice core gases. 51
3.4.3. Martian polar analogue. 51

3.5. REFERENCES 52

Chapter 4. Fractionation of carbon isotopes during the weathering of carbonates in glaciated catchments: Implications for the detection of subglacial microbial activity. 62

4.1. INTRODUCTION 62
4.1.1. Chemical weathering reactions in glacial environments 64
4.1.2. Isotopic fractionation and carbonate equilibria. 67
4.1.2.1. Chemical equilibria in the carbonate system 67
4.1.2.2. Equilibrium isotope fractionations in the carbonate system 68
4.1.2.3. Kinetic fractionations in the carbonate system 68

2. STUDY AREAS 69
4.2.1. John Evans Glacier 69
4.2.1.1. Site description 69
4.2.1.2. Hydrology and access to atmospheric gases 70
4.2.2. Haut Glacier d'Arolla 70
4.2.2.1. Site description 70
4.2.2.2. Hydrology and access to atmospheric gases 71

4.3. METHODS 71
4.3.1. John Evans Glacier 72
4.3.1.1. Water sampling 72
4.3.1.2. δ^{13}C-DIC analysis 72
4.3.1.3. Isotopic analysis of rock and sediment samples 73
4.3.1.4. δ^{34}S analysis 73
4.3.2. Haut Glacier d'Arolla 73
4.3.2.1. Water sampling 74
4.3.2.2. Rock samples 74
4.3.2.3. δ^{13}C-DIC and rock samples 75
4.3.3. Laboratory free drift weathering experiments 76
4.3.4. δ^{13}C-DIC geochemical and biogeochemical models 77
4.3.4.1. Weathering processes and δ^{13}C - DIC 78
4.3.4.2. Carbonate hydrolysis and carbonation of carbonates. 78
4.3.4.3. Contribution of protons via sulphide oxidation (SO) 79

4.3.4.4. Subglacial carbonate precipitation 80
4.3.4.5. Bedrock carbonate $\delta^{13}C$ variability 81
4.3.4.6. Model assumptions 82
4.3.4.7. Physical environments represented by models 1-5 83

4.4. RESULTS *85*
4.4.1. Field data 85
4.4.1.1. John Evans Glacier 85
4.4.1.2. Haut Glacier d'Arolla 86
4.4.2. $\delta^{13}C$–DIC values predicted using geochemical/biogeochemical models 86
4.4.2.1. John Evans Glacier 87
4.4.2.2. Haut Glacier d'Arolla 87
4.4.2.3. Interpretation of δ^{13}-DIC data based on Bio- and geochemical models 88
4.3.2.4. Summary 91
4.4.3. Free drift weathering experiments 92
4.4.3.1. Alkalinity variations 92
4.4.3.2. Chemical and isotope equilibrium 92
4.4.3.3. Isotopic fractionation. 93
4.4.3.4. $\delta^{13}C$ variations in relation to weathering reactions 94
4.4.3.5. Effect of carbonate concentration on ε_b and ε_k 96

4.5. INTERPRETATION OF FIELD DATA *98*
4.5.1. John Evans Glacier 99
4.5.1.1 Subglacial stream water geochemistry 99
4.5.1.2. Marginal stream water geochemistry 100
4.5.1.3. Seasonal changes in subglacial $\delta^{13}C$–DIC 100
4.5.2. Haut Glacier d'Arolla 101
4.5.2.1. Distributed and channelised system $\delta^{13}C$-DIC. 102
4.5.2.2. Comparison of field and laboratory ε_b values 107
4.5.2.3. PCO_2 v $\delta^{13}C$-DIC relationships 108
4.5.3. Summary 108

4.6. CONCLUSIONS *110*

4.7. REFERENCES *112*

Chapter 5. Summary **136**

5.1. REFERENCES *140*

List of Tables

Table 1.1. Average chemical composition of John Evans Glacier streams 1994, 1996, 1998 and 1999. 12

Table 1.2. Positive degree days (PDD) in 1994, 1996, 1998 and 1999 at the lower automatic weather station at John Evans Glacier. 13

Table 2.1. Average chemical composition of the eight streams studied. 29

Table 2.2. Comparison of characteristics of drainage events in 1994 and 1996. 30

Table 3.1 Concentration of headspace gases generated during 12 months incubation at 4°C generated by 1997 thawed ice samples amended with 0.25X R2A medium. 57

Table 4.1 Geochemical and isotopic field data and output from Models 1-5 118

Table 4.2. Predicted quickflow (Q_q) geochemistry for JD 205 at Haut Glacier d'Arolla 119

List of Figures

Fig. 2.1 (a) John Evans Glacier and (b) Configuration of the outflowing streams at the glacier terminus 31

Fig. 2.2 (a) SO_4^{2-} concentrations in the supraglacial, proglacial and west marginal streams, 1994 and (b) SO_4^{2-} concentrations in the supraglacial, west marginal and subglacial streams, 1996. 32

Fig. 2.3 Subglacial discharge hydrographs for (a) 1994 and (b) 1996. 33

Fig. 3.1 Anaerobic incubations of thawed ice samples at 4°C in the dark, amended with: (a) nitrate medium (5 mM NO_3^-) (b) sulfate medium (14 mM SO_4^{2-}). 58

Fig. 3.2 Aerobic incubations of thawed ice samples in the dark. 59

Fig. 3.3 Aerobic incubation of 1998 ice samples in the dark at increasing temperatures (-4.8°C, -1.8°C and 0.3°C). 60

Fig. 3.4 TEM images of bacteria in meltwater from basal ice samples. 61

Fig 4.1 Study areas, (a) John Evans Glacier and (b) Haut Glacier d'Arolla 120

Fig 4.2 John Evans Glacier $\delta^{13}C$-DIC field data. 121

Fig 4.3 Haut Glacier d'Arolla a) $\delta^{13}C$-DIC and discharge 122

b) $\delta^{13}C$-DIC and PCO_2 123

Fig 4.4. "Free drift" weathering experiments. (a) Alkalinity vs time 124

(b) PCO_2 vs time 125

(c) $\delta^{13}C$ 5 g l^{-1} closed system vs time 126

(d) $\delta^{13}C$ 5 g l^{-1} open system vs time 127

(e) $\delta^{13}C$ 0.01 g l^{-1} open system vs time 128

Fig 4.5 Predicted ε_k and ε_b to achieve isotope mass balance for 5 g l^{-1} $CaCO_3$ weathering experiment. 129

Fig. 4.6 Rate of CO_2 drawdown in the 5 g l^{-1} weathering experiments. (sediment and $CaCO_3$) 130

Fig 4.7 ε_k v CO_2 draw down rate for 5 g l^{-1} $CaCO_3$ weathering experiments. 131

Fig 4.8 (a) John Evans Glacier $\delta^{13}C$-DIC vs DIC 132

(b) Haut Glacier d'Arolla $\delta^{13}C$-DIC vs DIC. 133

Fig. 4.9 John Evans Glacier and Haut Glacier d'Arolla $\delta^{13}C$–DIC vs PCO_2 134

Glossary of terms used in the thesis

CB	Carbonation (Equation 2 chapter 4)
CB-CD	Carbonate dissolution driven by the carbonation reaction
CD	Carbonate dissolution (Equation 4 chapter 4)
CFIRMS	Continuous flow isotope ratio mass spectrometry
CH	Carbonate hydrolysis (Equation 6 chapter 4)
DIC	Dissolved inorganic carbon
DOC	Dissolved organic carbon
GD	Gypsum dissolution (Equation 7 chapter 4)
KFC	Kinetic fractionation of carbon isotopes associated with CO_2 dissolution across the gas-water interface
KBF	Kinetic fractionation of carbon isotopes associated with the dissolution of carbonate minerals
MR	Microbial respiration (Equation 3 chapter 4)
MR-CD	Microbial respiration coupled to carbonate dissolution
NRB	Nitrate reducing bacteria
OC	Organic carbon
PCO_2	Partial pressure of CO_2
PDD	Positive degree day
PHREEQC	A computer program for speciation, batch-reaction, one-dimensional transport, and inverse geochemical calculations
PMR	Post-mixing reactions
POC	Particulate organic carbon
SI_{cc}	Saturation index for calcite
SO	Sulfide oxidation (Equation 1 chapter 4)
SO-CD	Sulfide oxidation coupled to carbonate dissolution
SRB	Sulfate reducing bacteria
SSC	Suspended sediment concentration
TEM	Transmission electron microscopy
TOC	Total organic carbon
VPDB	Vienna Pee Dee Belemnite

Chapter 1. Introduction

The overall objective of the thesis is to determine whether microbially mediated chemical weathering occurs beneath glaciers. This requires an analysis of the hydrology, hydrochemistry and microbial processes occurring in a glaciated catchment. The study focuses on a large polythermal Arctic glacier (John Evans Glacier, Ellesmere Island, Canada) for two reasons. First, little is known about hydrological and biogeochemical processes at polythermal glaciers relative to the more widely studied temperate glaciers. Second, polythermal glaciers are potentially good small scale analogues for the Pleistocene mid-latitude ice sheets due to greater similarity in thermal regime - a key component of ice sheet behaviour – in comparison with small temperate valley glaciers. However, the study does also consider biogeochemical processes in a temperate glacial environment (Haut Glacier d'Arolla, Switzerland) as a contrast to those in polythermal glacial environments.

The thesis is presented as a series of three papers as follows, with a concluding summary chapter drawing together the main findings.

Paper 1. Drainage system behaviour of a high Arctic polythermal glacier.

Paper 2. Microbial activity beneath a high Arctic glacier

Paper 3. Fractionation of carbon isotopes during the weathering of carbonates in glaciated catchments: Implications for subglacial microbial activity.

The papers demonstrate that (a) subglacial drainage and chemical weathering does occur annually beneath John Evans Glacier, (b) microbial populations which oxidise organic carbon are present beneath John Evans Glacier and are viable under simulated *in situ* conditions and (c) δ^{13}C-DIC (dissolved inorganic carbon) of glacial runoff can be used to detect microbial oxidation of organic carbon as a DIC source beneath glaciers. This isotopic technique is effective in identifying microbial CO_2 sources beneath Haut Glacier d'Arolla, but not beneath John Evans Glacier.

1.1. PREVIOUS WORK AT JOHN EVANS GLACIER

Preliminary work at John Evans Glacier in 1994 examined the hydrology and the hydrochemistry of a number of the outflowing meltwater streams (Skidmore, 1995). The main findings of the study are briefly outlined. The work demonstrated that there is good evidence for the existence of a subglacial drainage system beneath the glacier on the basis of the high crustal solute content of the waters exiting the glacier subglacially. Meltwater chemistry indicates that waters routed subaerially in the supraglacial, proglacial and marginal streams have a dominant Ca^{2+}/HCO_3^- chemistry. These waters plot on a similar weathering pathway and reflect a progressive increase in calcite dissolution. By contrast waters routed subglacially are dominated by Ca^{2+}/SO_4^{2-}, reflecting dissolution of both calcite and anhydrite/gypsum in the subglacial environment. Subglacial drainage is initiated at least three weeks after surficial melt begins, as a sudden outburst-break flood event. The chemistry of the initial 'burst' waters indicates that storage of water at the bed occurs on the timescale of at least 5 days, however, it is possible that this water has been stored over winter. Drainage of the water from the store is complex and three modes of water outflow are observed in different locations; an artesian fountain, upwelling of waters through the subglacial sediments and channelised subglacial drainage. The chemistry of the waters outflowing in these three locations is similar, likely indicating a common source. The existence of subglacial drainage strongly suggests that the glacier has a polythermal regime. Additional work using radio echo sounding techniques supports the hydrochemical inferences that the glacier is polythermal, (Copland and Sharp, in press).

1.2. JOHN EVANS GLACIER MELTWATER CHEMISTRY

Paper 1 includes an analysis of 1994 and 1996 meltwater chemistry data. In addition to this there are meltwater chemistry measurements for John Evans Glacier from 1998 and to a lesser extent for 1999. The results from the latter years are not published or included in full in any of the papers; however, reference is made to some of the geochemistry

measurements for 1998 in Paper 3. Thus, there follows a synthesis of the main features of the full geochemical dataset (Table 1.1) to provide a broader background to the study. The comparisons focus on the marginal and subglacial water chemistries, for which the largest datasets exist. In all years solute concentrations are higher in subglacial streams relative to the subaerial streams. The marginal stream has a dominant Ca^{2+}/HCO_3^- chemistry reflecting calcite dissolution and waters routed subglacially are dominated by Ca^{2+}/SO_4^{2-}, with minor Mg^{2+}/HCO_3^- reflecting dissolution of calcite, dolomite and anhydrite/gypsum in the subglacial environment (Table 1.1.). Little interannual variability is observed in solute concentrations in both the subglacial and marginal stream between 1994 and 1996. Similarly, there is little interannual variability between 1998 and 1999 in marginal and subglacial stream chemistries. However, solute concentrations are lower in the marginal and subglacial streams in 1998 and 1999 than in 1994 and 1996. This is most likely due to higher runoff levels in 1998 and 1999, reducing water:rock contact times in marginal and subglacial environments and the degree of chemical weathering. This is supported by positive degree day data, which provide a crude melt index for each year (Table 1.2.). The 1994 total is probably high in comparison with 1996, 1998 and 1999 data since the meteorological station was situated on the proglacial outwash plain rather than on the terminus region of the glacier, resulting in comparatively warmer air temperatures. A comparative figure for 1994 would therefore, likely be lower than 201 PDD. Generally the PDD data indicate lower melt energy and therefore runoff in 1994 and 1996 compared with 1998 and 1999.

HCO_3^- and PCO_2 levels in the subglacial streams are relatively low and constant, despite varying concentrations of SO_4^{2-} and cationic species. By contrast HCO_3^- concentrations in the marginal stream vary in conjunction with other ionic species. Geochemical analysis of the subglacial water chemistry using PHREEQC (Parkhurst and Appelo, 1999) indicates that waters are close to saturation with respect to calcite ($SI_{cc} \sim 0$), as also indicated by the constant HCO_3^- and PCO_2 values. Modelling of the subglacial waters using PHREEQC indicates that the common ion effect with gypsum will only affect SI_{cc} levels when Ca^{2+} concentrations from gypsum dissolution are ~ 20000 $\mu eq\ l^{-1}$ or higher, which is ~ 10 times higher than measured values. However, the combined effects of

calcite and dolomite hydrolysis cause $SI_{cc} \sim 0$ to occur extremely rapidly, resulting in low HCO_3^- concentrations and low PCO_2 values as observed in the field data. The average weighted mean for all the PCO_2 data is $10^{-4.50}$ in the subglacial stream relative to $10^{-3.75}$ in the marginal stream. This suggests that re-equilibration with atmospheric CO_2 is significantly limited in the subglacial environment relative to the marginal stream environment, most likely due to the restricted access to the atmosphere in the subglacial environment.

1.3. THESIS OBJECTIVES

The specific objectives of the three papers are as follows.

Paper 1. To determine whether subglacial drainage beneath John Evans Glacier is an annual occurrence, and what does the outflowing meltwater chemistry reveal about subglacial chemical weathering reactions.

A literature review on polythermal glacier hydrology (Skidmore, 1995) indicates that observations on polythermal glaciers have generally been opportunistic (e.g. Baranowski, 1973; Andreasen, 1985) and few studies exist on the interannual variability of the hydrology of such systems (Wadham et al., 2001.). The storage of water and its release as observed at John Evans Glacier in 1994 seems similar to other more limited observations on polythermal glaciers. However, the aim of this study was to determine whether the 1994 hydrological and hydrochemical observations were unique or reflect an annually repeated pattern of behaviour for a large polythermal glacier and if possible, to develop a simple model to explain the hydrological behaviour. An improved understanding of the hydrology of these polythermal systems has important broader consequences, since subglacial hydrology is recognised as having a fundamental control on ice mass dynamics. Polythermal glaciers with terrestrial termini are likely closer analogues for the marginal conditions of the Pleistocene mid-latitude ice sheets than the more intensively studied Alpine glaciers.

The subglacial hydrological system is a key factor in controlling geochemical weathering reactions, since it determines water:rock ratios, water:rock contact times and access to atmospheric gases (Sharp, 1991). This affects the outflowing bulk meltwater geochemistry on both seasonal and diurnal timescales (e.g. Tranter et al., 1993; Brown et al., 1996; Anderson et al., 1999). Hence, the chemical composition of the outflowing waters can be used to infer properties of the subglacial drainage system. This study examines the differences in the subglacial and marginal stream geochemistry at John Evans Glacier and demonstrates that the unique chemical composition of the subglacial waters can be used to trace hydrological links between the subglacial and marginal streams.

Paper 2 : To determine whether microbes capable of utilising organic carbon exist beneath John Evans Glacier and whether they are viable under simulated *in situ* conditions.

Prior to 1996, glacier systems, especially subglacial environments, were thought to be abiotic due to the cold temperatures and potential lack of light and nutrients. Unpublished data, (later Sharp et al., 1999) suggested that in alpine subglacial environments bacterial populations increased with sediment concentration. This work demonstrated that in laboratory experiments using subglacial sediments at 3°C, enhanced rates of pyrite oxidation above those predicted from experimental (abiotic) geochemical data (Nicholson et al., 1988) occurred. The enhanced rates of sulphate production were interpreted as being due to microbially mediated sulphide oxidation. Supraglacial algal growth has been documented both in the Arctic (e.g. Jones et al., 1994; Mueller et al., in press) and Antarctic (Ling and Seppelt, 1990, 1993; Mueller et al., in press). However, Jones et al., (1994) document that only 8% of the microbes were viable at 1-4°C and that they were aerobic and predominantly photosynthetic, therefore, could only exist on the glacier surface. Aerobic bacteria have also been observed and revived from deep ice cores (Vostok Ice core), however, incubation was at 20°C, considerably higher than *in situ* temperatures (Abyzov, 1993). Gilichinsky, (1993) revived aerobic bacteria, from 2 million year old permafrost, demonstrating growth at –5°C, closer to the *in situ*

temperature (-12°C). However, no systematic study of glacial bacterial populations had been undertaken and therefore, it remained unknown as to the range of bacterial types that may exist, especially in the subglacial environment. Moreover, the discovery of the full extent of Lake Vostok, beneath the Antarctic Ice Sheet (Kapitsa et al., 1996), provided an additional interest in the search for life in subglacial environments (Ellis-Evans and Wynn-Williams, 1996). Hence, the study sampled supraglacial, marginal and subglacial streams and clean (debris-free) glacier ice and basal (debris-rich) ice at John Evans Glacier to investigate its microbial content.

The wider implications of this work were fourfold.

1. The potential to demonstrate microbial activity at the base of an Arctic glacier (cf. the Alpine work)
2. The potential impact of subglacial microbial activity on aqueous geochemistry, especially on stable carbon isotopic signatures in DIC.
3. If polythermal Arctic glaciers are reasonable Pleistocene mid-latitude ice sheet analogues then subglacial microbial activity has the potential to impact on carbon cycling on a continental scale during glacial periods.
4. If subglacial habitats are viable for microbial life it opens the possibility of microbial life on other planets, specifically Mars, where two large ice caps exist.

Paper 3. To determine whether measurements of δ^{13}C-DIC in glacial meltwaters can be used to provide independent evidence of *in situ* subglacial microbial activity.

This paper differs from the previous two in that it is a comparison study between John Evans Glacier and Haut Glacier d'Arolla, Switzerland. However, a greater proportion of the data is from John Evans Glacier and from experimental work using John Evans Glacier sediments and $CaCO_3$. John Evans Glacier water samples in 1998 were collected by Martin Sharp and Joel Barker. The laboratory experiments and the analytical work for the laboratory experiments and the John Evans Glacier field samples were carried out by myself. The unpublished isotope and geochemical data for Haut Glacier d'Arolla were supplied by Martyn Tranter and Simon Bottrell and are taken from (Lamb, 1997). Martyn

Tranter also supplied the description of the sampling and analytical methodology for Haut Glacier d'Arolla. All other writing and work on the paper is my own.

In unglaciated catchments, $\delta^{13}C$ of dissolved inorganic carbon (DIC) in runoff has been utilised to determine the relative importance of microbial (soil) and atmospheric CO_2 sources (e.g. Richey et al., 1988; Buhl et al., 1991). The main potential sources of DIC in glacial runoff (carbonate minerals, atmospheric CO_2 and CO_2 from microbial respiration) generally have significantly different $\delta^{13}C$ values (Faure, 1986). Hence, $\delta^{13}C$–DIC of glacial runoff has the potential to provide direct evidence of in situ subglacial microbial activity. Subglacial microbial activity is likely occurring beneath John Evans Glacier as demonstrated in Paper 2, (Skidmore et al., 2000). The absence of nitrate in runoff at Haut Glacier d'Arolla during parts of the meltseason (Tranter et al., 1994) was interpreted as potential geochemical evidence of microbial activity, by nitrate reducing bacteria. Laboratory studies on subglacial sediments from Haut Glacier d'Arolla have demonstrated significant microbial populations of 10^7 cells ml^{-1}, including 5-24 % as actively dividing cells, providing more direct evidence of viable and active subglacial microbes (Sharp et al., 1999). The unpublished 1994 data from Haut Glacier d'Arolla indicated isotopically light $\delta^{13}C$-DIC values ($\leq$ -10.2 ‰). However, interpretation of the data using the existing geochemical model for Haut Glacier d'Arolla (Tranter et al., 1993), indicated rapid increases (< 2 hours) in the input of isotopically light DIC associated with increasing diurnal discharge. This required physically unfeasible scenarios, for example, a 4 fold increase in microbial weathering rates in < 2 hours, in 0°C waters. However, the rapidity of the isotopic changes suggested that kinetic fractionation processes might be important in determining $\delta^{13}C$–DIC values. Previous experimental laboratory studies on $\delta^{13}C$–DIC variations in the carbonate system only identified a small (-1 ‰) kinetic fractionation of CO_2 (ε_k), in the initial stages of CO_2 transfer across the gas-water interface (Vogel et al., 1970; Zhang et al., 1995). However, this is not sufficient to account for the Haut Glacier d'Arolla data.

Haut Glacier d'Arolla is underlain by silicate bedrock and DIC is generated from weathering of trace calcite phases in the bedrock. At John Evans Glacier the underlying

bedrock is predominantly carbonate and thus provides a complimentary and possibly contrasting dataset to the one from Haut Glacier d'Arolla. John Evans Glacier field $\delta^{13}C$-DIC values were generally isotopically lighter than atmospheric $\delta^{13}C$-CO_2, also suggesting that kinetic fractionation processes were important. Therefore, a series of laboratory weathering experiments investigating kinetic isotopic effects were also undertaken using both $CaCO_3$ and glacial suspended sediment from John Evans Glacier to aid interpretation of the isotopic field data. The aim of the experiments was to determine the occurrence and magnitude of isotopic fractionation during the weathering of carbonates by carbonate hydrolysis and carbonation driven by atmospheric CO_2.

The paper demonstrates that by determining the isotopic shifts associated with kinetic weathering processes it is possible to use complimentary geochemical and isotopic data to identify glacial waters where light $\delta^{13}C$-DIC is due to kinetic effects and where it reflects input of microbial CO_2. Thus, it demonstrates an independent geochemical and isotopic technique for detecting subglacial microbial activity in addition to standard microbiological tests.

1.4. ADDITIONAL Ph.D. RESEARCH

I have undertaken both field and analytical work during my Ph.D. studies that is not described in the thesis, since I was not the primary author. However, this additional research has resulted in two papers: -

Sharp, M.J., Creaser, R. and **Skidmore, M.** (in press) Controls on the strontium isotope composition of runoff from a glacierised carbonate terrain. *Geochimica Cosmochimica Acta*

Sharp, M.J., **Skidmore, M.** and Nienow, P. (submitted) The chemistry of a high Arctic supraglacial snowcover. *Journal of Glaciology*.

1.5. REFERENCES

Abyzov S. S. (1993) Microorganisms in the Antarctic ice. In *Antarctic Microbiology* (ed. I. E. Friedmann), pp. 634. Wiley-Liss.

Andreasen, J.-O. (1985) Seasonal surface-velocity variations on a sub-polar glacier in West Greenland. *Journal of Glaciology*, **31** (109), 319-323.

Baranowski, S. (1973) Geyser-like water spouts at Werenskioldbreen, Spitsbergen. International Association of Hydrological Sciences **95**, 131-133.

Buhl D., Neuser R. D., Richter D. K., Riedel D., Roberts B., Strauss H., and Veizer J. (1991) Nature and nuture: environmental isotope story of the river Rhine. *Naturwissenschaften* **78**, 337-346.

Copland L. and Sharp M. J. (in press) Mapping thermal and hydrological conditions beneath a polythermal glacier with radio-echo sounding. *Journal of Glaciology*.

Ellis-Evans J. C. and Wynn-Williams D. (1996) A great lake under the ice. *Nature* **381**, 644-646.

Faure G. (1986) *Principles of isotope geology*. Wiley.

Gilichinsky D. A., Rivkina E. M., and Samarkin V. A. (1993) The microbiological and biogeochemical research in permafrost: Paleoecological implications. *6th International Conference on Permafrost*, 869-874.

Holland, H. (1978) *The chemistry of the atmospheres and oceans*, Wiley-Interscience, New York.

Jones H. G., Duchesneau M., and Handfield M. (1994) Nutrient cycling on the surface of an arctic ice cap: snow-atmosphere exchange of N species and microbiological activity. *Snow and Ice Covers. Interactions with the Atmosphere and Ecosystems*, 331-339.

Kapitsa A. P., Ridley J. K., Robin G. d. Q., Siegert M. J., and Zotikov I. A. (1996) A large deep freshwater lake beneath the ice of central East Antarctica. *Nature* **381**, 684-686.

Lamb H. R. (1997) Chemical weathering in Alpine subglacial environments. Ph.D., Bristol.

Ling H. U. and Seppelt R. D. (1990) Snow algae of the Windmill Islands, continental Antarctica. *Mesotaenium berggrenii* (Zygnematales, Chlorophyta) the alga of grey snow. *Antarctic Science* **2**(2), 143-148.

Ling H. U. and Seppelt R. D. (1993) Snow algae of the Windmill Islands, continental Antarctica. 2. *Chloromonas rubroleosa* sp. nov. (Volvocales, Chlrophyta), an alga of red snow. *European Journal of Phycology* **28**, 77-84.

Mueller, D. R., Vincent, W. F., Pollard, W. H. and Fritsen, C. H. (in press) Glacial cryoconite ecosystems: A bipolar comparison of algal communities and habitats. *Nova Hedwigia* **123**.

Parkhurst D. L. and Appelo C. A. J. (1999) User's guide to PHREEQC (Version 2)--a computer program for speciation, batch-reaction, one-dimensional transport, and inverse geochemical calculations, pp. 312. U. S. Geological Survey.

Richey J. E., Devol A. H., Wofsy S. C., Victoria R., and Riberio M. N. G. (1988) Biogenic gases and the oxidation and reduction of carbon in Amazon River and floodplain waters. *Limnology and Oceanography* **33**, 551-561.

Sharp M.J. (1991) Hydrological inferences from meltwater quality data: the unfulfilled potential. *Proceedings, BHS 3rd National Hydrology Symposium*, Southampton 5.1 - 5.8.

Sharp M., Parkes J., Cragg B., Fairchild I. J., Lamb H., and Tranter M. (1999) Widespread bacterial populations at glacier beds and their relationship to rock weathering and carbon cycling. *Geology* **27**(2), 107-110.

Skidmore M. L. (1995) The hydrochemistry of a high Arctic glacier. MSc., University of Alberta.

Tranter M., Brown G. H., Hodson A., Gurnell A. M., and Sharp M. J. (1994) Variation in the nitrate concentration of glacial runoff in Alpine and sub-Polar environments. *Snow and Ice Covers: Interactions with the Atmosphere and Ecosystems*, 299-311.

Tranter M., Brown G. H., Raiswell R., Sharp M. J., and Gurnell A. M. (1993) A conceptual model of solute acquisition by Alpine glacial meltwaters. *Journal of Glaciology* **39**, 573-581.

Vogel J. C., Grootes P. M., and Mook W. G. (1970) Isotopic fractionation between gaseous and dissolved carbon dioxide. *Zeitschrift fur Physik* **230**, 225-238.

Wadham J. L., Hodgkins R., Cooper R. J., and Tranter M. (2001) Evidence for seasonal subglacial outburst events at a polythermal glacier, Finsterwalderbreen, Svalbard. *Hydrological Processes 15*, 2259-2280.

Zhang J., Quay P. D., and Wilbur D. O. (1995) Carbon isotope fractionation during gas-water exchange and dissolution of CO_2. *Geochimica et Cosmochimica Acta* **59**(1), 107-114.

Table 1.1. Average chemical composition of John Evans Glacier streams 1994, 96, 98 and 99.

	Stream	Ca^{2+}				Mg^{2+}				Na^{+}				K^{+}				Si	
		94	96	98	99	94	96	98	99	94	96	98	99	94	96	98	99	94	98
Subaerial	Supraglacial	46	30	40		13	8	7		9	3	0		1.9	0.5	0		1.5	0
streams	Proglacial	259				21				0				0.1				3.1	
	West marginal	711	616	418	492	70	61	26	31	3	6	0	0	3.1	3.1	0.3	0.6	3.5	0.3
	East marginal	662				119				1	0			2.8				3.6	
Subglacial	Fountain	2390	2618			246	635			60	193			9.6	38.5			11.0	
streams	Upwelling	2210	1734			214	205			53	55			7.4	13.4			8.0	
	Subglacial	1701	1610	852	1111	175	176	74	120	54	45	26	38	10.7	9.5	2.2	6.4	9.1	1.2
	East subglacial		1160				119				28				6.1				

	Stream	HCO_3^-				SO_4^{2-}				Cl^-				Sum solute			
		94	96	98	99	94	96	98	99	94	96	98	99	94	96	98	99
Subaerial	Supraglacial	52	60	38		7	4	5		18	18	12		137	117	90	
streams	Proglacial	174				59				18				524			
	West Marginal	641	680	398	366	69	62	42	29	28	25	12	11	1549	1439	885	919
	East Marginal	648				107				16				-			
Subglacial	Fountain	278	327			2399	3037			31	116			6043	6880		
streams	Upwelling	284	353			2186	1707			28	42			5013	4099		
	Subglacial	269	342	246	272	1810	1521	662	1005	25	22	12	15	4031	3736	1861	2552
	East Subglacial		274				1113				15				2741		

	Stream	Charge balance (%)				PH				Log PCO_2				n			
		94	96	98	99	94	96	98	99	94	96	98	99	94	96	98	99
Subaerial	Supraglacial	15	-11.5	-2.3		7.1	7.1	6.4		-4.0	-3.7	-2.9		75	15	11	
streams	Proglacial	7.0				9.1				-4.9				34			
	West marginal	24	-1.3	-1.0	9.7	8.3	8.3	7.9	8.6	-3.8	-3.8	-3.4	-4.1	57	15	11	1
	East marginal	17				-				-				19			
Subglacial	Fountain	1.4	1.2			8.4	8.3			-4.1	-4.1			7	1		
streams	Upwelling		-2.4			8.3	8.5			-4.5	-4.3			13	3		
	Subglacial	-2.0	-1.6	2.0	0.0	8.7	8.7	8.7	8.4	-4.6	-4.4	-4.4	-4.1	38	8	11	7
	East Subglacial		-4.2				8.5				-4.3				1		

Table 1.1. continued. All concentrations are in ueq l^{-1}, except Si (μmol l^{-1}). Concentrations of Ca^{2+}, Mg^{2+}, Na^{+}, K^{+}, HCO_3^{-} and SO_4^{2-} have been corrected for atmospheric input using sea salt ratios relative to Cl^{-} (Holland, 1978) and therefore reflect solute input from crustal sources. n indicates the number of measurements for a particular stream. Charge balances were calculated using the raw (uncorrected) values for all ionic species.

Table 1.2. Positive degree days (PDD) in 1994, 1996, 1998 and 1999 at the lower automatic weather station at John Evans Glacier. (http://arctic.eas.ualberta.ca)

Year	PDD
1994	201
1996	91
1998	265
1999	274

Chapter 2. Drainage system behaviour of a high Arctic polythermal glacier.[1]

2.1. INTRODUCTION

During the past two decades there has been increasing recognition of the influence of the hydrology of glaciers and larger ice masses on their dynamics (e.g. Iken, 1981; Iken and Bindschadler, 1986). Studies of temperate glacier flow have identified changing subglacial water pressures as a key influence on velocity fluctuations on a variety of timescales (Iken et al., 1983; Kamb, 1987; Willis 1995). Subglacial water pressure depends upon the meltwater flux, the ice mass geometry (which controls the hydraulic gradient and the tendency for ice flow to close down drainage pathways), the structure of the drainage system, and the hydraulic geometry, sinuosity and boundary roughness of the major drainage routeways (Sharp, 1991). Observations on polythermal glaciers, (glaciers with a central core of temperate ice at the bed surrounded by cold ice at the surface, margins and glacier terminus, (Blatter, 1987)) have also shown seasonal velocity variations, which have been attributed to changes in subglacial water pressure (Müller and Iken, 1973; Andreasen 1985; Rabus and Echelmeyer, 1997). However, there is limited understanding of the drainage system properties of polythermal glaciers and of the hydrological changes which might be responsible for variations in water pressure within them. This paper uses observations of meltwater runoff and hydrochemistry to investigate the drainage system behaviour of a polythermal glacier over two summer melt seasons.

[1] A version of this chapter has been published as Skidmore M. L. and Sharp M. J. (1999) Drainage behaviour of a high Arctic polythermal glacier. *Annals of Glaciology*, **28**, 209-215.

2.2. FIELD SITE

John Evans Glacier is a large valley glacier located at 79° 40' N; 74° 00' W, on eastern Ellesmere Island, Nunavut, Canada. The main arm of the glacier occupies the western part of a 220 km^2 catchment, and spans an elevation range from 100-1500 m (Fig. 2.1 a). The glacier is underlain by an Ordovician/Silurian carbonate/evaporite sequence with a minor clastic component (Kerr, 1972). The mean annual air temperature at a meteorological station located on the glacier snout (Fig. 2.1 a) is –14.7°C and the long term mean equilibrium line altitude is ~750 m (personal communication from A. Arendt, 1998). In the terminus region, below an elevation of 250 m, ice depths are <150 m and radio echo sounding reveals a widespread internal reflector located ~20 m above the bed. This is interpreted to represent the boundary between cold and temperate ice and to indicate that the glacier is polythermal (Copland and Sharp, in press). At the glacier terminus and margins the ice is believed to be cold-based and the glacier is frozen to its bed. Meltwater runoff from the glacier occurs primarily via two ice-marginal streams and another stream which appears to be subglacially-fed (Fig. 2.1 b). The catchments drained by each of these streams are demarcated on Fig. 2.1 a. The subglacial stream is believed to be fed by runoff from the central basin, which enters the glacier in a major crevasse field ca. 4 km from the snout. In addition to these major streams, five other streams were investigated (Fig. 2.1 b). These are referred to as the supraglacial, proglacial, upwelling, fountain and east subglacial streams. The proglacial area is covered with a layer of unconsolidated sediments at least 4 m thick, dissected by a large braided channel network.

2.3. METHODS

Fieldwork was conducted from June 15th to August 7th 1994 (Julian Days (JD) 166-219) and June 24th to July 18th 1996 (JD 176 – 199). In both years subglacial stream discharges were measured on a daily basis using the velocity-area method (Gardiner and Dackcombe, 1983). At discharges >10 m^3 s^{-1} velocity profile measurement was

impossible and discharge was estimated from observations of the channel width, depth and surface water velocity using the velocity-area method.

In both years, water chemistry measurements were made on samples from seven meltwater streams. Samples were collected at least once a day from the supraglacial and west marginal streams, and for parts of each season from the proglacial, upwelling, fountain, east marginal and subglacial streams. A 500 ml aliquot of water was vacuum filtered through a 0.45 μm cellulose nitrate membrane. Two 20 ml samples were retained for laboratory analysis of major anion and cation concentrations by ion chromatography, and a 100 ml sample was taken for analysis of total alkalinity. Total alkalinity (primarily bicarbonate (HCO_3^-)) was determined in the field within 24 hours of sampling by titration using a Hach digital titrator. In 1994 the titration endpoint was determined using a Ross Sure-flow electrode, connected to an Orion 290A pH meter. In 1996, the endpoint was determined colourimetrically. The major cation and anion concentrations were measured using a Dionex DX 500 ion chromatograph. Anion concentrations (chloride (Cl^-), nitrate (NO_3^-), sulphate (SO_4^{2-})) were determined using a Dionex Ionpac AS4 column and 1.7 mM sodium carbonate/1.8 mM sodium bicarbonate eluent. Cation concentrations (sodium (Na^+), potassium (K^+), magnesium (Mg^{2+}), and calcium (Ca^{2+})) were determined using a Dionex Ionpac CS12 column and 20 mM methanesulphonic acid eluent. The component of the ionic species Ca^{2+}, Mg^{2+}, Na^+, K^+, SO_4^{2-}, HCO_3^- derived from sea salt aerosol was calculated using standard sea water ratios of these species relative to Cl^- (Holland, 1978) and subtracted from the total, yielding an estimate of the concentration of each species derived from crustal sources. Silica (Si) concentrations were determined by flow injection analysis, using a FIAstar 5010 system, consisting of a FIAstar 5023 spectrophotometer, V100 injector and Chemifold III. Samples were injected into a stream of ammonium molybdate, oxalic acid and acidified stannous chloride. The amount of molybdate reactive Si was determined spectrophotometrically at a wavelength of 695 nm.

Air temperatures were measured using a Campbell Scientific 107B thermistor at a meteorological station in the terminus region (see Fig. 2.1 a for locations). Measurements

were made every 10 seconds and 30 minute averages were stored on a Campbell CR10 data logger. Cumulative positive degree-days (PDD) were calculated by summing mean daily air temperatures (where positive). For comparison with 1996 measurements, air temperatures measured at an elevation of 50 m in 1994 were corrected to an elevation of 250 m using a measured lapse rate of 0.06°C/100 m (Arendt, 1997).

2.4. RESULTS

2.4.1. Evidence for subglacial drainage

Firm evidence for the occurrence of subglacial drainage at John Evans Glacier is provided by observations of meltwater chemistry made in both 1994 and 1996. In both years, turbid water with a distinctive chemical composition emerged from the glacier at three discrete locations (Fig. 2.1 b, Table 2.1): (i) by an artesian fountain 1-2 m high, located on the glacier surface ca. 200 m from the terminus, where ice was ~30 m thick, (the "fountain stream"); (ii) by upwelling through proglacial sediments over an area ~30 m wide immediately in front of the glacier terminus, (the "upwelling" stream) and (iii) as a channelised flow located at the ice-bed interface, (the "subglacial" stream).

The chemistry of these turbid waters indicates that they had much greater water/rock contact times than did waters in the four subaerial streams (supraglacial, proglacial, west and east marginal streams). This is indicated by: (i) the higher total solute concentrations in the subglacial streams (~4000-5000 μeq l^{-1}) than in the subaerial streams (~1500 μeq l^{-1}; Table 2.1), and (ii) the higher concentrations of ionic species (Na^+, K^+ and Si) that are products of silicate mineral weathering. This implies that the turbid waters were routed subglacially, which is consistent with observations on the pattern of water outflow.

The water chemistry indicates a common source for the fountain, upwelling and subglacial streams, that is different from the source of the subaerial stream waters (Table 2.1). Subglacial waters are dominated by Ca^{2+} and SO_4^{2-}, while the subaerial waters

contain predominantly Ca^{2+} and HCO_3^-. This suggests that the majority of solute in the subglacial and subaerial streams is derived from the dissolution of gypsum/anhydrite and calcite respectively. The elevated concentrations of Mg^{2+}, Na^+, K^+ and Si in the subglacial waters indicate that there is enhanced weathering of minerals with relatively slow dissolution kinetics (dolomite and silicate minerals such as muscovite) in the subglacial environment. Since the kinetics of gypsum/anhydrite dissolution are more rapid than those of calcite dissolution, it is the enhanced weathering of silicate minerals that indicates longer residence times for the subglacial waters. However, the high SO_4^{2-} concentrations (at least 20 times subaerial values) are unique to subglacial waters. This is probably due to differences in the lithologies available for weathering in the subglacial and subaerial environments.

The SO_4^{2-} concentration therefore acts as a tracer for subglacially-routed waters. In 1994, the SO_4^{2-} concentration in the proglacial stream increased markedly on JD 191 (July 10th) (Fig. 2.2 a). This reflects the input of upwelling waters of subglacial origin. The SO_4^{2-} concentration remained high throughout the period of upwelling input (JD 191-196), and returned to previous levels when this input ceased. Neither the west marginal nor supraglacial streams showed any significant change in SO_4^{2-} concentrations during this period. In 1996, however, elevated SO_4^{2-} levels were recorded in the west marginal stream when subglacial drainage via the fountain and upwelling streams was initiated (JD 189) (Fig. 2.2 b). SO_4^{2-} concentrations remained higher than the background for the next three days, suggesting that there was input of subglacial waters into the marginal stream throughout that period. Thus, the SO_4^{2-} data provide evidence for a link between the subglacial reservoir and west marginal streams in 1996 which was not evident in 1994.

2.4.2. Release of subglacial water

In both melt seasons, outflow of subglacially routed waters was concentrated in a series of Events (Fig. 2.3). Three subglacial discharge Events were observed in 1994, and 2 in 1996 (Fig. 2.3, Table 2.2). The style of water outflow in Events 1 and 2 was broadly

similar in both years. In Event 1, the initial release of water occurred via an artesian fountain on the glacier surface, followed within 12-24 hours by the upwelling of waters from beneath the frozen toe of the glacier. Longitudinal fracturing of the glacier surface in the vicinity of the fountain occurred at the time of flow initiation, and audible fracturing of the ice preceded the onset of upwelling, especially close to the outflow location. Discharge was larger in Event 2 than in Event 1, and the outflow was channelised (the subglacial stream).

Despite these similarities, however, there were some differences in the outburst location(s), between 1994 and 1996 (Table 2.2). In 1994, the location of water outflow switched between Events 1 and 2. In Event 1 (1994), discharge occurred only via the fountain and upwelling streams, while in Event 2 discharge was via the subglacial stream (Table 2.2). In 1996, however, the fountain, upwelling and subglacial streams were all operative during Event 1, and there was leakage of subglacial waters into the west marginal stream (Fig. 2.2 b, Fig. 2.3). In Event 2, (1994) 4 subsidiary channels opened up at the ice-bed interface to the west of the subglacial stream (Fig. 2.1 b). Those located furthest from the subglacial stream were broad and flat in cross-section (slot-like conduits with a width:height ratio of 10:1), while those nearer the subglacial stream were semi-cylindrical in form. No subsidiary channels were observed in this location in 1996, but there was a small discharge of subglacial water in a single channel located towards the eastern edge of the glacier terminus, (the east subglacial stream, Fig. 2.1 b). In Event 3, (1994) only the subglacial stream was active.

2.4.3. Subglacial outflow hydrographs

Subglacial discharge hydrographs at John Evans Glacier display two characteristic shapes. The hydrographs of Events 1 and 2, (1994) were both positively skewed (Fig. 2.3 a, Table 2.2), while those of Event 3, (1994) and Event 1 and probably Event 2 (1996) were negatively skewed. (Fig. 2.3 a and b, Table 2.2). There is some uncertainty about the shape of the hydrograph in Event 2 (1996). The 1996 discharge record ends abruptly due

to heavy snowfall on JD 200, which was followed by a period of subzero temperatures. Although the shape of the hydrograph between JD 200 and 203 is unknown, subglacial discharge had dropped to ca. 0.2 m^3 s^{-1} by JD 203. Since the rising limb of this hydrograph lasted at least 3 days, it seems most likely that it was negatively skewed.

These hydrograph shapes reflect the mode of flow initiation in each Event. The positively skewed hydrographs resemble those associated with "sudden outburst-break" type floods resulting from water pocket ruptures on Alpine glaciers (Haeberli, 1983). However, the duration of the John Evans Glacier Events was 2-6 days, compared with minutes to a few hours for the Events described by Haeberli. The sudden onset of drainage and associated fracturing of the glacier suggest that the connection between the subglacial reservoir and the atmosphere was established rapidly by rupture of the cold ice barrier at the glacier terminus. In contrast, the gradual rise to peak flows in the negatively skewed hydrographs implies either that the connection between the reservoir and the atmosphere was opened gradually, perhaps by melting, or that outflow during these Events was not restricted by a barrier at the glacier terminus and simply reflects the discharge response to increasing inputs of water from the glacier surface.

Subglacial outflow effectively ceased after Events 1 and 2, (1994), although surface melt continued. This suggests that the drainage outlets closed down after each outflow Event. The switch in outflow location between Events 1 and 2 was probably a consequence of closure of the outlets used during Event 1. In 1996, however, the subglacial stream continued to flow between Events 1 and 2, suggesting that a more permanent connection was established between the subglacial reservoir and the atmosphere in Event 1 (1996) than was ever established in 1994.

2.4.4. Evidence for subglacial water storage

Meltwater input into the subglacial drainage reservoir was likely via a large crevasse field at an elevation of ca. 500 m (Fig. 2.1 a). Two large supraglacial streams are known to

sink into the glacier in this region. Hence, the meltwater supply to the subglacial reservoir was controlled predominantly by the rate of surface melt in the catchment draining into the crevasse field. The diurnal cycle of melt input to the subglacial system was not apparent in the discharge hydrographs. This implies that outflow occurred from a subglacial reservoir with sufficient storage capacity to damp out the daily input cycle.

Further evidence for subglacial water storage comes from a comparison of air temperature records and hydrograph characteristics. Cumulative positive degree days (ΣPDD) were used as an index of melt energy supplied to the glacier prior to the drainage Events in each season (Table 2.2). The melt season was much longer in 1994 than in 1996. A total of 201.5 ΣPDD was recorded up to JD 219 1994 (when melt was still occurring at the end of fieldwork), compared to a total of 91 ΣPDD prior to JD 200 in 1996 (when the melt season ended). When comparing the degree-day totals for each year it is important to note that the snow pack was ~1.5 times thicker in 1996 than in 1994. This delayed the onset of runoff at the terminus until JD 175 in 1996 compared to JD 166 in 1994. At higher elevations, the transition from snow to ice on the glacier surface was also delayed by at least 10-14 days in 1996 relative to 1994. Hence, for a given positive degree day total, runoff would have been greater in 1994 because (a) low albedo ice surfaces were exposed earlier in 1994 than in 1996 (melt rates at John Evans Glacier are ~4 mm water equivalent PDD^{-1} for snow surfaces, compared to ~7 mm water equivalent PDD^{-1} for ice surfaces (Arendt, 1997)) and (b) the proportion of snow melt refrozen as superimposed ice was probably lower in 1994 than in 1996.

The ΣPDD prior to Event 1 was 1.5 times higher in 1994 than in 1996, but, the amount of water released in Event 1 was similar in the two years (Table 2.2, Fig. 2.3 a and b). The spacing of Events 1 and 2 was 14 days in 1994 and 8 days in 1996, and ΣPDD for these periods was 62 and 34 % respectively of ΣPDD prior to Event 1. However, 2-10 times more water was released in Event 2 than in Event 1. There are three possible explanations for this, (a) increased exposure of low albedo ice surfaces resulted in greater total melt input per PDD later in each melt season, (b) the proportion of surface melt converted to

superimposed ice within the catchment feeding the subglacial reservoir decreased as the melt season progressed, hence supraglacial runoff (input) increased, and (c) some of the water released in Event 2 was stored in the glacier prior to Event 1. Given the observed ΣPDD and melting degree day factors cited above, the "albedo effect" (a), is insufficient to account for the increases in discharge observed between Events 1 and 2. This suggests that either liquid water storage or the cessation of superimposed ice formation are the main causes of the discharge increase in Event 2. Liquid water storage within the glacier is consistent with the suggestion that, in 1994 at least, the outlet channels closed down between Events 1 and 2.

2.4.5. Synthesis

The 1994 melt season was significantly warmer and longer than the 1996 season, and therefore more meltwater was supplied to the subglacial reservoir. Prior to the initiation of subglacial drainage, the subglacial reservoir was almost certainly larger in 1994 than 1996. Artesian outflow continued for longer in 1994 than in 1996 (4 days compared to 1 day), and fracturing played an important role in opening drainage outlets. This suggests that subglacial water pressures were sustained at higher levels for longer periods in 1994 than in 1996. It thus seems likely that in 1994 outlets could not develop rapidly enough to drain increasing meltwater inputs to the subglacial reservoir. Water pressures increased to levels at which pressure-induced uplift and hydrofracturing became important processes of outlet creation. This explains the sudden onset of Events 1 and 2 in 1994. Closure of the outlets used in Event 1 prior to Event 2, and switching of outlet locations in Event 2 may simply have resulted from settlement of the glacier onto its bed after subglacial water pressures were reduced by Event 1. In 1996, the onset of Events 1 and 2 was more gradual, and the subglacial stream continued to flow between the two Events. This suggests that when the reservoir filled more slowly, slower processes, such as ice-melt, were able to create drainage outlets before high subglacial water pressures developed. As a result, pressure-induced uplift and hydrofracturing played a less significant role in

developing connections between the reservoir and the atmosphere, and connections did not close so abruptly when drainage occurred.

2.5. DISCUSSION

2.5.1. Implications for subglacial hydrology

The subglacial hydrological system beneath John Evans Glacier is clearly very different from systems underlying Alpine glaciers. Subglacial outflow is initiated each year by an outburst Event which occurs at least 2 weeks after the onset of the melt season, and releases subglacial waters which have been stored at the bed for an extended time period (up to 2 weeks). This suggests that at the start of the melt season subglacial outflow is impeded, probably by the cold ice barrier and frozen sediments at the glacier margin. Once initiated, however, the pattern of subglacial outflow bears a qualitative resemblance to the unstable spiral regime of water flow modeled by Szilder et al., (1997) in a stability analysis of glacier lake drainage. In this flow regime, discharge oscillations of increasing amplitude occur over time, Eventually leading to complete lake drainage. As at John Evans Glacier, increases in the reservoir volume prior to drainage were associated with (i) an increase in the temporal spacing of drainage Events, (ii) more rapid rates of increase in discharge during drainage Events, and (iii) greater discharge volumes. It should, however, be noted that there are significant differences between the situation at John Evans Glacier and that treated in the model. The model deals with the consequences of perturbations to an equilibrium system consisting of an ice marginal lake with an existing subglacial outflow. At John Evans Glacier, however, the reservoir is subglacial and initially has no outlet. The outlet appears to develop relatively rapidly once water pressures within the reservoir exceed some threshold value. In the model, the mechanics of outlet growth and closure through wall melting and ice deformation determine the rate of water release and the overall hydrograph shape. The similarities between the observed and modeled behaviour are sufficient to suggest that the pattern of outflow is determined

by the mechanics that control the size of the outlet connecting the subglacial reservoir to the proglacial environment.

2.5.2. Inter-annual variations in subglacial drainage system behaviour

A number of observations suggest that subglacial drainage is an annual occurrence at John Evans Glacier. Aerial photographs taken on August 5th, 1959, show a highly turbid stream issuing from the glacier at the same location where the subglacial stream was observed in 1994, 1996 and 1998. Photographs of the glacier snout taken on July 17th, 1995 by I. R. Smith show channelised flow of turbid waters in this same location. These photographs also show a large artesian fountain emerging from the glacier surface ca. 400 m east of the location of the fountain in 1994 and 1996. The artesian fountain formed in a similar easterly location in 1998. Geyser-like waterspouts were also observed in July 1991 (personal communication from G. Henry, 1994). These observations suggest that the location of channelised subglacial outflow is the same every year, while the location of the artesian fountain is more variable.

2.5.3. Comparison to other studies

It is believed that this study is the first to document a cyclical pattern of subglacial water release from a polythermal glacier. However, a number of observations suggest that similar behaviour may occur elsewhere. Indirect evidence for a supraglacially-fed subglacial drainage system beneath a high Arctic glacier was presented by Müller and Iken (1973), who observed increased ice flow velocities in the ablation zone of White Glacier, Axel Heiberg Island, N.W.T., in summer. Iken (1972) argued that meltwater flowing into moulins penetrated to the bed and spread out over an area large enough to affect the basal velocity. Subsequent studies by Blatter (1987) and Blatter and Hutter (1991) showed that White Glacier had a polythermal regime, with a central core of temperate ice at the bed surrounded by cold ice at the surface, margins and glacier terminus. Although meltwater reaching the bed of a polythermal glacier must initially be

restricted to the zone of basal ice at the pressure melting point, it must breach the cold ice barrier at the terminus and margins to exit the glacier. Discharge of turbid water was observed from both the eastern and western margins of White Glacier, but not from the glacier terminus (Iken, 1974). This suggests that the barrier of cold ice at the snout of White Glacier is more effective in preventing the drainage of such waters than those at its margins. Andreasen (1985) also noted increases in summer ice velocities at Kitdlerssuaq glacier in West Greenland in 1982 and 1983. He attributed these to increased basal sliding resulting from subglacial water storage. Andreasen also described outbursts of turbid (presumably subglacial) water on July 7th 1982 and July 23rd 1983, but did not discuss the nature of these outburst Events or their effect on stream discharge.

2.6. CONCLUSIONS

Subglacial outflow of supraglacially-derived meltwaters is an annual occurrence at polythermal John Evans Glacier. The initiation of subglacial outflow is lagged by as much as two weeks relative to the onset of the summer melt season, probably because outflow is initially impeded by ice at the glacier margin which is frozen to the bed. Prior to the initiation of subglacial outflow, a reservoir develops at the glacier bed. Water pressures in this reservoir may exceed the ice overburden pressure, especially in "warm" summers when the reservoir fills relatively rapidly. Drainage from the reservoir occurs in a series of outflow Events, the characteristics of which seem to be controlled more by the mechanics of outlet creation and closure than by the temporal pattern of water input to the reservoir. The first outflow Event in each year occurs via an artesian fountain at the glacier surface, and by upwelling through sediments at the glacier margin. The second Event is usually larger than the first, and occurs via a subglacial channel which may develop at a different location to the initial upwelling. The location of the channel is constant from year to year, while that of the artesian fountain is more variable. The hydrograph shapes, discharge volumes and temporal separation of outflow Events vary from year to year in response to changes in the rate of reservoir filling. Warmer years, which result in more rapid filling, are associated with larger discharge volumes, more

widely spaced outflow Events and positively skewed hydrographs. Hydrofracturing and water pressure-induced ice-bed separation play an important role in the creation of drainage outlets in such years, whereas processes such as melt-enlargement of drainage channels may be more important in cooler years. In warmer years, subglacial drainage may shut down completely between outflow Events, probably because the glacier settles back on its bed and seals off the drainage outlets when water pressure is reduced by outflow. In cooler years, however, subglacial drainage continues at a reduced rate between outflow Events. There is evidence to suggest that this type of drainage system behaviour may occur at other polythermal glaciers.

2.7. REFERENCES

Andreasen, J.-O. (1985) Seasonal surface-velocity variations on a sub-polar glacier in West Greenland. *Journal of Glaciology* **31,** (109), 319-323.

Arendt, A. (1997) Mass balance modelling of an Arctic glacier. MSc. thesis, University of Alberta.

Blatter, H. (1987) On the thermal regime of an Arctic valley glacier: a study of White Glacier, Axel Heiberg Island, N.W.T., Canada. *Journal of Glaciology* **33,** (114), 200-211

Blatter, H. and Hutter, K. (1991) Polythermal conditions in Arctic glaciers. *Journal of Glaciology* **37,** (126), 261-269.

Copland L. and Sharp M. J. (in press) Mapping hydrological conditions beneath a polythermal glacier using radio-echo sounding. *Journal of Glaciology*.

Gardiner, V. and Dackcombe, R. (1983) *Geomorphological field manual*, Allen and Unwin, London.

Haeberli, W. (1983) Frequency and characteristics of glacier floods in the Swiss Alps. *Annals of Glaciology* **4,** 85-90.

Holland, H. (1978) *The chemistry of the atmospheres and oceans*, Wiley-Interscience, New York.

Iken, A. (1972) Measurements of water pressure in moulins as part of a movement study of the White Glacier, Axel Heiberg Island, Northwest Territories, Canada. *Journal of Glaciology* **11**, (61), 53-58

Iken, A. (1974) Glaciology No.5. Velocity fluctuations of an Arctic valley glacier, a study of the White Glacier, Axel Heiberg Island, Canadian Arctic Archipelago. *Axel Heiberg Island Research Reports, McGill University, Montreal.*

Iken, A. (1981) The effect of the subglacial water pressure on the sliding velocity of a glacier in an idealised numerical model. *Journal of Glaciology* **27**, (97), 407-421.

Iken, A., Röthlisberger, H., Flotron, A. and Haeberli, W. (1983) The uplift of Unteraargletscher at the beginning of the meltseason - a consequence of water storage at the bed? *Journal of Glaciology* **29**, (101), 28-47.

Iken, A. and Bindschadler, R. A. (1986) Combined measurements of subglacial water pressure and surface velocity of Findelengletscher, Switzerland: conclusions about drainage system and sliding mechanism. *Journal of Glaciology* **32**, (110), 101-119.

Kamb, B. (1987) Glacier surge mechanism based on linked cavity configuration of the basal water conduit system. *Journal of Geophysical Research* **92 (B9)**, 9083-9100.

Kerr, J. W. (1972) Map 1358A Geology: Dobbin Bay, District of Franklin 1:250000, Geological Survey of Canada.

Müller, F. and Iken, A. (1973) Velocity fluctuations and water regime of arctic valley glaciers. *International Association of Hydrological Sciences Publication* **95**, (Symposium on the hydrology of glaciers. Proceedings of the Cambridge Symposium, 7-13 September 1969), 165-182.

Rabus, B.T. and Echelmeyer, K.A. (1997) The flow of a polythermal glacier: McCall Glacier, Alaska, U.S.A. *Journal of Glaciology* **43**, (145), 522-536.

Sharp M.J. (1991) Hydrological inferences from meltwater quality data: the unfulfilled potential. *Proceedings, BHS 3rd National Hydrology Symposium*, Southampton 5.1 - 5.8.

Szilder, K., Lozowski, E.P. and Sharp, M.J. (1997) Glacial lake drainage: a stability analysis. *Annals of Glaciology* **24**, 175-180.

Willis, I.C. (1995) Intra-annual variations in glacier motion: a review. *Progress in Physical Geography,* **19** (1), 61-106.

Table 2.1. Average chemical composition of the eight streams studied. All concentrations are in μeq l^{-1}, except Si (μmol l^{-1}). Values from 1996 are in italics. Concentrations of Ca^{2+}, Mg^{2+}, Na^{+}, K^{+}, HCO_3^{-} and SO_4^{2-} have been corrected for atmospheric input and therefore reflect solute input from crustal sources. n indicates the number of measurements for a particular stream.

		Ca^{2+}		Mg^{2+}		Na^{+}		K^{+}		Si	HCO_3^{-}		SO_4^{2-}		Sum solute		*n*	
	Stream	1994	*1996*	94	*96*	94	*96*	94	*96*	94	94	*96*	94	*96*	94	*96*	94	*96*
Subaerial	Supraglacial	46	*30*	13	*8*	9	*3*	1.9	*0.5*	0.7	52	*60*	7	*4*	137	*117*	75	*15*
streams	Proglacial	259	-	21	-	0	-	0.1	-	1.5	206	-	59	-	524	-	34	-
	West marginal	711	*616*	70	*61*	3	*6*	3.1	*3.1*	1.6	673	*685*	69	*62*	1549	*1439*	57	*15*
	East marginal	662	-	119	-	1	*0*	2.8	-	-	680	-	107	-	1452	-	19	-
Subglacial	**Fountain**	2390	*2618*	246	*635*	60	*193*	9.6	*38.5*	5.1	296	*359*	2399	*3871*	6043	*7193*	7	*1*
streams	**Upwelling**	2210	*1734*	214	*205*	53	*55*	7.4	*13.4*	3.8	306	*385*	2186	*1956*	5013	*4355*	13	*3*
	Subglacial	1701	*1610*	175	*176*	54	*45*	10.7	*9.5*	4.3	262	*374*	1810	*1718*	4031	*3942*	38	*8*
	East subglacial	-	*1160*	-	*119*	-	*28*	-	*6.1*	-	-	*193*	-	-	-	*2741*	-	*1*

Table 2.2. Comparison of characteristics of drainage events in 1994 and 1996. (note PDD – positive degree days)

Drainage Event	Peak Times		PDD between Event peaks		Streams affected by each drainage Event		Hydrograph skewness	
	1994	*1996*	1994	*1996*	1994	*1996*	1994	*1996*
1	190	*192*	91.5	*67*	Fountain Upwelling	*Fountain Upwelling Subglacial West marginal*	+ve	*-ve*
2	204	*200*	57	*23*	Subglacial	*Subglacial East subglacial*	+ve	*-ve*
3	214	-	40	-	Subglacial	-	-ve	-

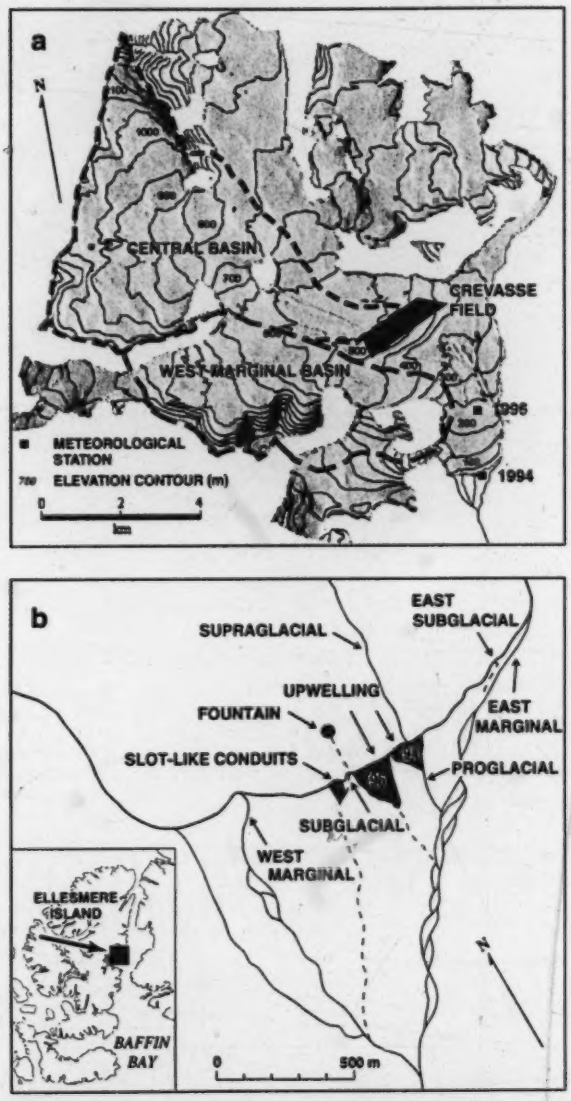

Fig. 2.1 (a) John Evans Glacier. Areas of the west marginal and central basins are outlined,
(b) Configuration of the outflowing streams at the glacier terminus. Areas of subglacial water outflow are shaded dark grey and subglacially-fed streams are represented by dashed lines. Inset: location of John Evans Glacier.

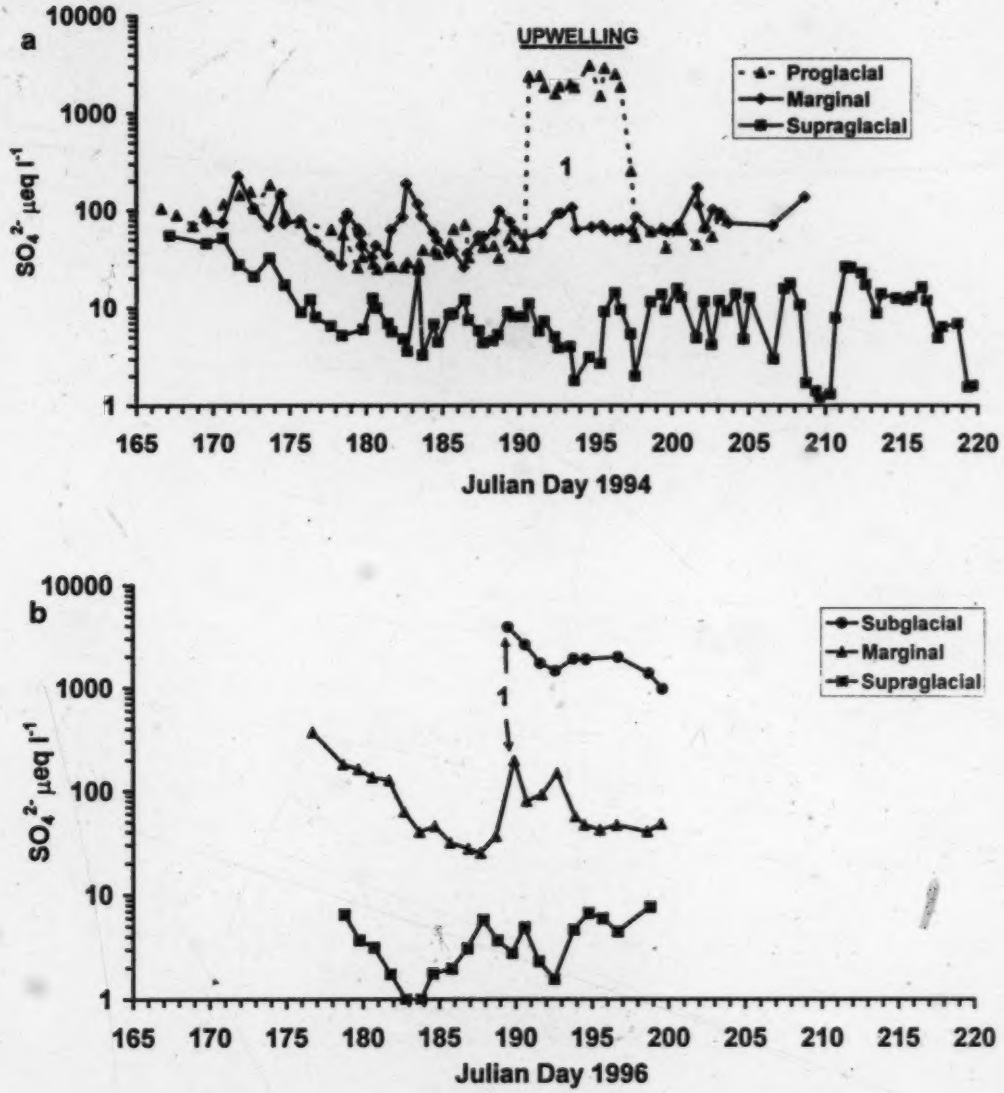

Fig 2.2 (a) SO_4^{2-} concentrations in the supraglacial, proglacial and west marginal streams, 1994; (b) SO_4^{2-} concentrations in the supraglacial, west marginal and subglacial streams, 1996. Drainage event 1 is also noted.

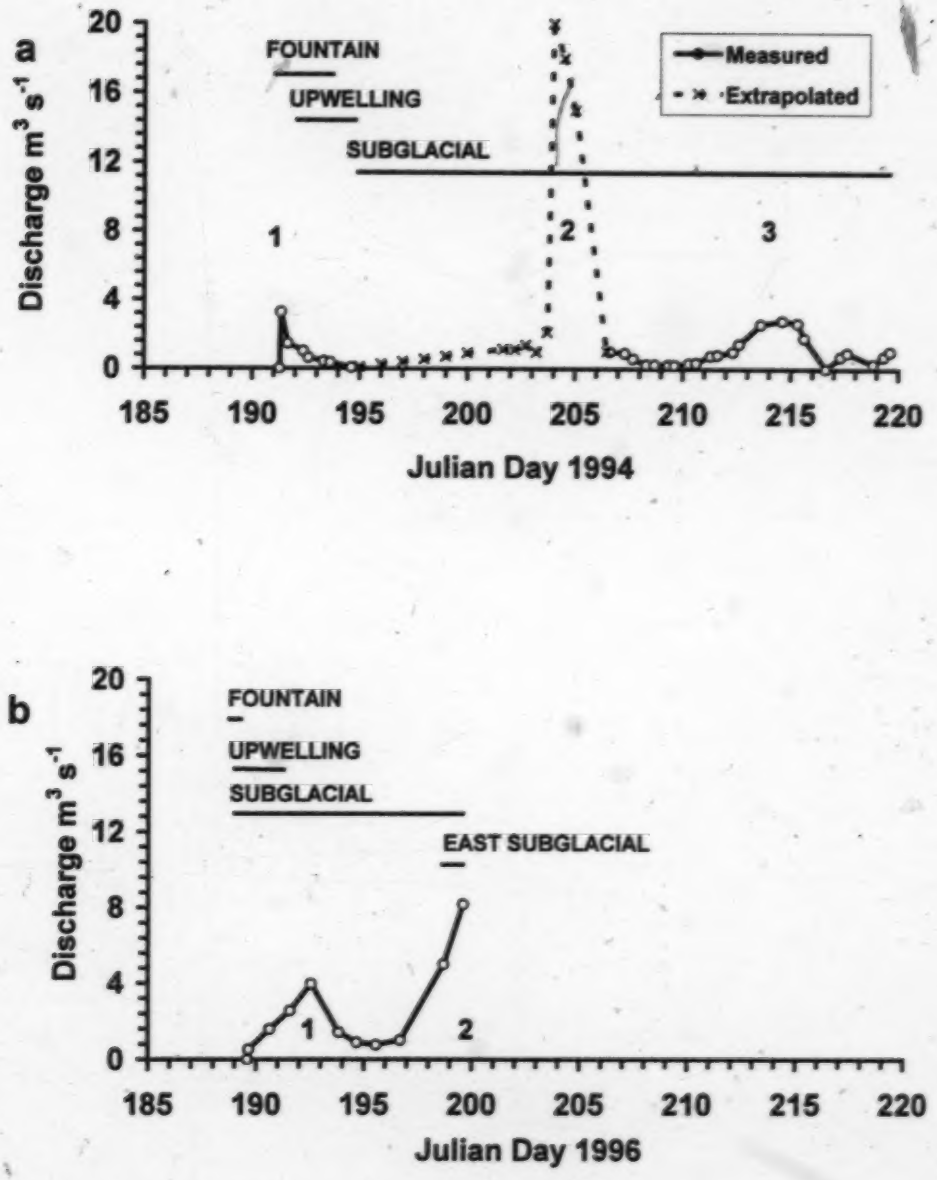

Fig. 2.3 Subglacial discharge hydrographs for (a) 1994 and (b) 1996. Length of horizontal bar indicates the period of discharge from each outlet. Drainage events 1, 2 & 3 are noted on the figures.

Chapter 3. Microbial life beneath a High Arctic Glacier[1]

3.1. INTRODUCTION

Microbial activity has been reported in ice-sediment communities, in the surface layers of perennial and permanent lake ice, at a depth of 2 m (Priscu et al., 1998; Psenner and Sattler, 1998) and in cryoconite holes in shallow (< 3 m deep) meltwater lakes on Arctic ice shelves (Vincent et al., 2000). The lake ice microbial consortia are dependent on photosynthesis to provide energy for growth. In subglacial environments bacterial populations have been reported beneath Alpine glaciers (Sharp et al., 1999), and from subglacially accreted ice above Lake Vostok, Antarctica (Karl et al., 1999; Priscu et al., 1999). However, the biogeochemical function of these populations has not been determined, and it remains to be demonstrated that they are active at *in situ* subglacial temperatures and conditions. Clearly, active subglacial microbial populations would have to be chemotrophic (non-photosynthetic). Demonstrating the viability and geochemical function of subglacial microbial populations has a number of important consequences.

First, viable chemotrophic microbial activity at low temperatures (0 to 4°C) has important implications for global carbon cycling calculations. Traditionally, it has been considered that continental glaciation results in a cessation of geochemical processes beneath the ice (Gibbs and Kump, 1994), and the impact of subglacial microbially mediated weathering has received little consideration. However, during the last glacial maximum, ice sheets covered approximately 20% of the continental northern hemisphere (Holmlund and Fastook, 1995; Ludwig et al., 1999; Marshall and Clarke, 1999) including the area that is currently covered by the boreal forest, the world's largest store of soil carbon, estimated at 330 Pg, (1 Pg = 10^{15} g), (Van Campo et al., 1993). A similar distribution of vegetation is proposed for the last interglacial period (Eemian) as recorded in glacially overridden soils and peat (Dredge et al., 1990; Punkari and Forsstrom, 1995) and paleosols in unglaciated terrain beyond the ice margin (Morozova et al., 1998). These overridden soils and peat

[1] A version of this chapter has been published as **Skidmore, M.**, Foght, J. M. and Sharp, M. J. (2000) Microbial life beneath a high Arctic glacier. ***Applied and Environmental Microbiology*, 66, (8),** 3214-3220.

deposits provide a large source of organic carbon beneath the mid-latitude ice sheets. A number of the current carbon cycle models assume that the carbon accumulated during the Eemian in areas covered by the ice sheets was returned to the atmosphere by the last glacial maximum (Adams et al., 1990; Van Campo et al., 1993; Francois et al., 1999) but with no explanation as to how this was achieved. Ice is an efficient erosive agent (Alley et al., 1997; Hallet et al., 1997) and therefore, it is likely that some of the carbon may be removed by physical transport to the ice sheet margins, either in ice, deforming sediments or meltwater. However, active biogeochemical oxidation or reduction of the remaining carbon beneath warm based sectors of mid-latitude ice sheets may have a significant impact on carbon budget calculations for continental regions during the glacial phase of a glacial/interglacial cycle. Moreover, low temperature respiration and/or fermentation of organic carbon in the subsurface environments of periglacial (Rivkina et al. 1998, Zimov et al., 1993) soils in unglaciated mid-latitude regions and ice marginal zones is potentially an important process hitherto given little consideration on glacial/interglacial timescales.

Second, extreme polar terrestrial environments are being investigated as analogues for viable extra-terrestrial habitats (Andersen et al., 1998; Gilichinsky et al., 1993). Currently, water on Mars has only been observed as ice in the two polar caps (Cantor and James, 1998). Thus, given that all known bacteria on Earth require liquid water to be metabolically active, one of the most likely potential habitats for microbial life on Mars is the polar environments (Skidmore et al., 1998). Moreover, subglacial environments would provide shelter from the harsh conditions at the planet's surface, including large diurnal and seasonal temperature fluctuations and strong UV radiation. Some models suggest that, during times of high obliquity on Mars, surficial melting may have occurred on the north polar ice cap (Pathare and Paige, 1998). Under these conditions, the ice cap may have exhibited polythermal conditions and been more dynamic (Kargel, 1998) and thus capable of basal melting and producing sediment-rich basal ice. Hence, debris-rich ice exposed at the margins of the north polar ice cap or as part of the polar layered deposits may provide a record of dormant or possibly extant microbial life that is relatively accessible.

This study involves a sequence of laboratory experiments conducted between 1996 and 1999 that assess the diversity and viability of microbes from a high Arctic glaciated environment and examine the effects of microbial activity on biogeochemical processes. The experiments also compare microbial population diversity from surficial glacier environments (supraglacial waters and glacier ice which are characterized by low solute (< 10 $\mu S\ cm^{-1}$) and sediment concentrations (< 0.01 $g\ l^{-1}$)) with subglacial environments (subglacial meltwaters and basal ice, which are characterized by high solute (> 100 $\mu S\ cm^{-1}$) and sediment concentrations (> 0.1 $g\ l^{-1}$)).

3.2. MATERIALS AND METHODS

3.2.1. Field site.

The study was performed on samples collected from John Evans Glacier (79° 38'N 74° 23'W), eastern Ellesmere Island, Nunavut, Canada. The local climate is that of a polar desert, with a mean annual air temperature of -14.5°C at the glacier terminus (Arendt, 1997). The glacier has polythermal characteristics, in that cold (sub-freezing) ice at the surface, margins and terminus of the glacier surrounds a core zone where ice at the glacier bed is at the pressure melting point and basal melting occurs. This core zone begins ca. 7 km upglacier from the glacier snout, where the ice is ca. 400 m thick. Between 4 and 7 km from the glacier snout, temperate ice occurs only at the glacier bed, but in the lowest 4 km of the glacier, where ice depths are up to 200 m, there is a layer of temperate basal ice up to 20m thick. (Copland and Sharp, in press). Debris-rich basal ice, up to 0.5 m thick, is widely exposed at the glacier margin. During the summer melt season, meltwaters which have acquired solute from subglacial chemical weathering reactions drain from the glacier at a number of locations (Skidmore and Sharp, 1999).

3.2.2. Definition of ice and water types.

Glacier ice is formed by the processes of firnification or superimposed ice generation (refreezing of percolating waters in near surface snow and firn) at the glacier surface and it has low solute (< 10 μS cm^{-1}) and sediment concentrations (< 0.01 g l^{-1}). Supraglacial meltwaters are generated by melting of snow and ice and flow on the surface of the glacier. They too are characterized by low solute and suspended sediment concentrations. Subglacial waters flow at the bed of the glacier and originate as supraglacial waters which reach the bed through crevasses and moulins, mixed with small amounts of groundwater and basal meltwater generated by frictional and geothermal melting of ice at the glacier base. Subglacial waters interact with the rock and sediments that underlie the ice and hence exhibit high solute (> 100 μS cm^{-1}) and suspended sediment concentrations (> 0.1 g l^{-1}). Basal ice contains significant sediment concentrations and forms at the glacier bed, by a number of mechanisms, that could include folding (Hubbard and Sharp, 1989), regelation of ice into the substrate (Iversen and Semmens, 1995) and basal accretion of super-cooled subglacial water (Lawson et al., 1999). It provides a record of the geochemical and microbiological conditions at the glacier bed and lies stratigraphically unconformably beneath the glacier ice. At John Evans Glacier the basal ice layers were likely formed by either regelation of ice into the substrate or basal accretion of super-cooled water since there is no structural evidence of folding.

3.2.3. Water samples 1996.

The first set of experiments undertaken in 1996 examined the viability of microbes present in glacial meltwaters with different chemical compositions and suspended sediment concentrations, and examined the relationship between suspended sediment concentration and microbiological activity. In July 1996, 4 l samples of subglacial and supraglacial meltwater were collected aseptically from the terminus of John Evans Glacier using twice-autoclaved plastic carboys (Nalgene) with screw-caps fitted with sterile air ports (0.2 μm PTFE filters, Nalge #222). These samples were amended in the field with 10X sterile R2A growth medium lacking agar to a final concentration of tenth-

strength (0.1X) R2A (1X R2A contained, per l of doubly glass-distilled water: 0.5 g yeast extract (Difco); 0.5 g casamino acids (Difco); 0.5 g glucose; 0.5 g soluble starch (Difco); 0.3 g K_2HPO_4; 0.3 g sodium pyrophosphate; 0.25 g BiTek tryptone (Difco); 0.25 g Bacto peptone (Difco); 24 mg $MgSO_4$; adapted from (Atlas, 1995)). Samples were stored on ice and in the dark at ≤ 4°C for up to one month in the field, transported to the laboratory (72 hours) at ≤ 4°C and then incubated stationary in the dark at ≤ 4°C. For comparison, other subglacial and supraglacial water samples were incubated without R2A amendment. The pH and dissolved oxygen concentration of these samples were measured at the time of sampling and seven weeks later using an Orion 290A pH meter fitted with a Ross Sure-flow pH electrode and an Orion dissolved oxygen probe (model 97-08), respectively. H_2S concentrations were analyzed colorimetrically using a Hach H_2S test kit.

In the laboratory, a control was prepared from 3 l heat-sterilized distilled water amended with 30 ml of the R2A stock used in the field. This control flask was incubated in parallel with the water samples. After incubation for two months at 4°C, 100 ml sub-samples of this laboratory control were filtered through 0.2 µm MicroFunnel filtration units (Gelman Sciences) to capture any viable microbes. Each unit was supplemented with an ampoule of R2A broth (Gelman Sciences) and incubated at 22°C or 4°C for one or two months, respectively, to culture recovered microbes. No colonies were observed at either temperature, demonstrating the sterility of the amendment.

After seven weeks incubation at ≤ 4°C, 10 ml sub-samples of the R2A amended and unamended 4 l water samples were inoculated into 50 ml pre-chilled quarter-strength nitrate medium (27) or quarter-strength sulfate medium (Butlin et al., 1949; substituting sodium lactate with sodium acetate and sodium pyruvate) pre-gassed with sterile 10% CO_2/balance N_2 in 125 ml serum bottles fitted with gas-tight septa, and incubated stationary at 4°C in the dark. All manipulations were carried out in a biosafety cabinet under HEPA-filtered airflow. Growth was noted as increasing turbidity and browning of the nitrate medium, or blackening of the sulfate medium from sulfide precipitation, in comparison with parallel uninoculated media. Sub-samples of the same subglacial and supraglacial waters were diluted with cold 3 mM phosphate buffer (pH 7), inoculated

onto pre-chilled quarter-strength plate count agar (Difco) and incubated aerobically at 4°C or 22°C.

3.2.4. Ice samples 1997.

These experiments examined both microbial diversity and rates of biogeochemical activity in thawed samples of glacier ice and basal ice. The chemical and microbiological characteristics of the thawed basal ice also provide information about the nature of subglacial environments. In May 1997, samples of basal ice and glacier ice were collected aseptically from the glacier terminus using ethanol flame-sterilized ice axes. The surface few centimeters of ice were scraped away prior to sampling to avoid atmospheric contamination. Samples were then chipped into flame-sterilized metal collection trays and transferred without handling to sterile plastic bags (Whirl-Pak; Nasco Plastics, ON). Samples remained frozen until used in the experiments. Subsequent manipulations were carried out aseptically in a biosafety cabinet with HEPA-filtered airflow.

3.2.4.1. Anaerobic incubations. Ice was thawed at 4°C in sterile containers and transferred into 168 ml bottles fitted with gas-impermeable septa, containing 50 ml of half-strength growth media as follows: nitrate medium (Mikesell et al., 1993) and sulfate medium (Butlin et al., 1949) pre-gassed with sterile 10% CO_2, balance N_2; R2A medium pre-gassed with sterile 0.5% CO_2, balance N_2. The prepared media bottles were pre-cooled on ice prior to inoculation. For glacier ice samples, the inoculum consisted of 50 ml of meltwater, whereas for basal ice, 5 g of sediment plus 45 ml of associated meltwater were used. Parallel uninoculated controls consisting of 100 ml of each growth medium were prepared. Inoculated, poisoned controls containing 500 μM $HgCl_2$ and 20 mM Na_2MoO_4 (to inhibit potential Hg methylation by sulfate reducing bacteria (Yamamoto-Ikemoto et al., 1994)) were also included to evaluate abiotic contributions to the aqueous geochemistry. Unamended background controls consisting of melted glacier ice (100 ml) or basal ice (10 g sediment plus 90 ml meltwater) were also prepared. All cultures were sealed under the appropriate sterile headspace gases and incubated in the dark at 4°C, stationary, for 90 days. At 14 day intervals, 0.5 ml samples were withdrawn

aseptically through the septa using fine gauge needles and syringes. Basal samples were clarified using a 0.45 μm filter membrane (Millipore) prior to analysis. The concentrations of Cl^-, NO_3^- and SO_4^{2-} in the samples were quantified with a Dionex DX500 ion chromatograph using a Dionex Ionpac AS4 column and an eluent of 1.7 mM Na_2CO_3 and 1.8 mM $NaHCO_3$. Headspace gas concentrations of CO_2 and CH_4 were determined (respectively) on a Hewlett Packard (HP) 5890 Series II gas chromatograph (GC) with a thermal conductivity detector, and a VarianStar 3400 GC or HP 5700A GC fitted with flame ionization detectors. $\delta^{13}C$ values of headspace gases were determined by CF-IRMS using a HP 5890 Series II GC connected to a Finigan Mat 252 mass spectrometer and are reported relative to VPDB.

3.2.4.2. Aerobic incubations: Samples consisting of 100 ml melted glacier ice or 30 ml of melted basal ice were amended with 50 ml half-strength R2A medium. A parallel uninoculated control containing 50 ml of medium was included. All cultures received a 0.2 μm filter-sterilized solution of Na-[2-^{14}C]acetate giving final concentrations of ≤ 50 μM acetate and a total of 98,000 dpm per flask. The culture flasks were sealed with neoprene stoppers under an aerobic headspace and incubated at 8°C in the dark with gyrotory shaking at 200 rpm for 270 days. At intervals, sub-samples of liquid plus headspace were removed aseptically using needle and syringe, acidified, and sparged with N_2 to trap and quantify evolved $^{14}CO_2$ (Fedorak et al., 1982).

3.2.5. 1998 Ice samples.

The 1998/9 experiments recreated *in situ* subglacial conditions as closely as possible in order to establish whether the microbes were viable and active under such conditions. Rates of microbial respiration were measured from both thawed glacier and basal ice at temperatures below and just above 0°C. All manipulations were carried out on ice and the media used were pre-chilled to ensure culture temperatures remained as close to 0°C as possible. Experiments were conducted using fresh samples of basal ice, collected aseptically in July 1998 (as described above) at a site 3 km from the 1997 site, and glacier

ice collected in 1997, which had been stored frozen and undisturbed in the original sterile bags. Samples were melted at 4°C in sterile containers and sub-samples were transferred under HEPA-filtered air flow to sterile 250 ml bottles fitted with gas-tight septa. Unamended samples consisted of 200 ml glacier ice meltwater or 150 g basal ice sediment plus 75 ml associated meltwater. Another set of samples was amended by replacing 20 ml of melted ice with 20 ml of R2A medium (Atlas, 1995) giving a final concentration of 0.1X R2A. Heat-sterilized controls of basal ice containing 100 g twice-autoclaved sediment plus 28 ml of associated meltwater, and glacier ice containing 200 ml meltwater and an uninoculated control containing 200 ml sterile medium were also prepared. Each culture was dosed with a filter sterilized solution of Na-[2-^{14}C]acetate to give a total of 195,000 dpm and acetate concentrations of 50 to 130 μM dependent upon the total volume of the sample, then sealed under an aerobic headspace. One set of unamended samples was incubated at 4°C in the dark. The contents of the remaining bottles were frozen by immersion in glycol at –4.8°C; the bottles were shaken every 15 minutes during freezing to ensure an even distribution of any sediment within the forming ice. These cultures were incubated in the dark, submerged in a refrigerated glycol circulator bath (Cole Parmer Polystat) at -4.8°C for 31 days, then at -1.8°C for 35 days, followed by a further 91 days at +0.3°C. The bath temperature was monitored using a thermistor (Campbell Scientific 107B) coupled to a CR10 datalogger (Campbell Scientific) and remained within ±0.3°C of the desired temperature. After 66 days the frozen samples were melted at +0.3°C and evolved $^{14}CO_2$ was measured by aseptically removing a sub-sample of the liquid and quantifying $^{14}CO_2$ (Fedorak et al., 1982); sediment-laden samples were first clarified by filtration through a 0.2 μm Millipore Millex GS filter unit. The thawed samples were incubated a further 91 days at +0.3°C, with sub-samples withdrawn for $^{14}CO_2$ analysis at intervals. The unfrozen (4°C liquid) cultures were sampled after 97, 122 and 157 days and analyzed for evolved $^{14}CO_2$ as above (Fedorak et al., 1982). Extraction of all sub-samples was performed in a biosafety cabinet and all cultures were kept on ice during the procedure.

3.2.6. Microscopy.

Transmission electron microscopy (TEM) was performed on both cultured and uncultured samples of glacier and basal ice to examine microbial morphology. Drops of melted ice or amended cultures were placed on Formvar-coated copper grids, briefly dried *in vacuuo*, then negatively stained with 0.2 μm filter-sterilized 2 % phosphotungstic acid and examined with a Philips 201 electron microscope.

3.2.7. Organic carbon concentrations.

To examine the availability of organic carbon (OC) in catchment materials, 20 sediment samples were taken from a variety of soil/sediment environments in the proglacial and ice marginal zone. A sub-sample of basal ice was also taken for TOC determination. All sediment samples were dried at 105°C for 24 hours and allowed to cool in a desiccator prior to weighing. The samples were combusted at 550°C for 16 hours and then allowed to cool in a desiccator prior to weighing. The total organic carbon (TOC) content in % weight was determined as 0.4 x organic matter content (the weight loss recorded between the drying stage and the combustion stage) (Bengtsson and Enell, 1986).

Dissolved organic carbon (DOC) concentrations of the basal ice and glacier ice and total organic carbon (TOC) concentration of the glacier ice were determined as follows. All glassware and filters were pre-combusted at 550°C. Ice samples were melted and passed through 0.7 μm Whatman GF/F filters and the filtrate analyzed for DOC. Melted samples were acidified to pH 2 with HCl and sparged with a flow of CO_2-free N_2 gas to remove dissolved inorganic carbon (DIC). A 100 μL sample was dried and flash combusted in a microvolume disposable quartz furnace which was continuously purged with a low flow of He gas. The combustion gases were passed through a series of furnaces containing CuO (850°C), CuO + Ag (450°C), and Cu (680°C) in order to oxidize all CO to CO_2, remove sulfur oxides, and reduce nitrogen oxides to N_2. The gas stream was dried by passage through a nafion dryer, and the purified, dehumidified CO_2 was directed to a

Finigan MAT 252 isotope ratio mass spectrometer for quantification and determination of carbon isotope ratios (Leckrone, 1997). Unfiltered samples of glacier ice were analyzed for TOC, using the same procedure as above (Leckrone, 1997). POC was determined as TOC minus DOC.

3.3. RESULTS

3.3.1. 1996 water samples.

These initial experiments were primarily qualitative, intended to determine whether viable microbes were present in subglacial and/or supraglacial waters. After seven weeks incubation at ≤ 4°C the 4 l subglacial sample amended with 0.1X R2A medium showed depleted dissolved oxygen levels (1.7 ppm v. 10.9 ppm O_2), decreased pH (6.5 v. 7.8), and the presence of H_2S (0.7 ppm v. undetectable) compared to the unamended sample. By contrast, the amended supraglacial sample showed no change in geochemistry. When sub-samples of the R2A-amended subglacial waters were incubated with anaerobic nitrate or sulfate medium at 4°C, the media became brown (nitrate) or black (sulfate) and turbid within six weeks. Sub-samples of the unamended subglacial water were slower to show positive results (four months at 4°C), whereas unamended supraglacial waters did not yield positive results within four months. Parallel bottles inoculated with the laboratory control medium remained sterile, demonstrating that the anaerobes did not arise from the R2A amendment. These subculture experiments were repeated several times with the same results, confirming the observation that viable respiring anaerobes were present in subglacial waters. It was noted that the appearance of turbid cultures was qualitatively proportional to the amount of mineral sediment associated with the water sample.

Aerobic plating of unamended subglacial meltwaters onto quarter-strength plate count agar incubated at 22°C revealed 10^2 colony forming units (cfu) ml^{-1} of water, whereas parallel plates incubated at 4°C yielded $>10^3$ cfu ml^{-1}, many of which were pigmented yellow or orange. Colonies purified from 4°C plates in general were unable to grow when

subcultured at 22°C, suggesting that they are true psychrophiles, whereas those isolated on plates incubated at 22°C were able to grow when cultured at 4°C. R2A amended subglacial waters yielded $>10^6$ cfu ml^{-1} regardless of plate incubation temperature. These were predominantly non-pigmented colonies that could be sub-cultured at either temperature. Further studies are in progress to determine the identity and diversity of these populations. The unamended supraglacial water sample also yielded 10^3 cfu ml^{-1} on plates at 4°C, predominantly pigmented, and 10-fold lower counts on plates at 22°C. The laboratory medium control (0.5 ml of undiluted medium) did not yield any colonies at either temperature within three months incubation.

3.3.2. 1997 ice samples.

The qualitative results from subglacial and supraglacial water samples described above suggested that the subglacial environment harbored viable populations of both aerobes and anaerobes, thus meriting direct study of the ice originating from the glacier base. Experiments with basal ice showed that aerobic and anaerobic microbial activities were detectable at 8°C and 4°C respectively if the sample was amended with low levels of organic carbon (i.e., growth medium) or a terminal electron acceptor such as NO_3^- or SO_4^{2-}. Microbial activity was observed in cultures of the thawed basal ice but not in cultures of the glacier ice, again suggesting an association with the sediment. The absence of microbial activity in the glacier ice confirms the use of suitable aseptic technique to prevent contamination of the samples during sampling and analysis.

Significant depletion of NO_3^- and SO_4^{2-} occurred during anaerobic incubation of amended basal ice (Fig. 3.1). In contrast, the thawed glacier ice samples and uninoculated medium showed no reduction of NO_3^- and SO_4^{2-} within the 90 day incubation period (Fig. 3.1). In the anaerobic cultures of thawed basal ice amended with dilute R2A medium both CO_2 and CH_4 were produced (Table 3.1) at concentrations respectively 10 and 10^4 times higher than in samples of thawed glacier ice or uninoculated medium. The $\delta^{13}C$–CH_4 of the thawed basal ice sample was -73.3‰, clearly demonstrating a microbial origin for the

CH_4. Poisoned controls showed neither depletion of NO_3^- and SO_4^{2-} nor CO_2 and CH_4 production, indicating that abiotic processes were not responsible for the observations. These results indicate that viable, metabolically diverse anaerobic bacteria including nitrate reducers, sulfate reducers and methanogens were present in the basal ice and active in culture at 4°C.

In the aerobic experiment with 1997 ice samples a significant amount of $^{14}CO_2$ was generated from the thawed basal ice amended with ^{14}C-acetate but not from the amended thawed glacier ice or parallel uninoculated control (Fig. 3.2). Again, this implies that microbial activity is associated with the presence of sediment within the ice.

3.3.3. 1998 ice samples.

Whereas the 1997 ice samples were incubated at temperatures higher than those expected in situ and modestly amended with nutrients, the 1998 ice samples were incubated under conditions as close as possible to those found at the at the base of the glacier (temperature ca. 0°C), with minimal organic carbon amendment, sufficient to detect respiration. The experimental temperature was set at 0.3°C in order to ensure that the entire slurry remained in liquid form (> 0°C) due to the tolerances (±0.3°C) on the temperature bath. The experiments were designed to demonstrate not only that viable microbes are present in the basal ice, but also that they are active under simulated *in situ* subglacial conditions. Activity was assessed simply by quantifying aerobic mineralization of radiolabeled acetate to $^{14}CO_2$. ^{14}C-acetate incorporation into biomass and $^{14}CO_2$ depletion by autotrophy were not assessed, nor was oxygen in the sealed headspace replaced during incubation. Thus the measured activity should be considered a conservative estimate of aerobic activity.

Unamended and 0.1X R2A-amended samples were incubated under a sealed aerobic headspace with Na-[2-^{14}C]acetate at progressively higher temperatures, from sub-freezing (-4.8°C and -1.8°C) to just above freezing (+0.3°C). At sub-freezing temperatures no mineralization of the radiolabel was detected after 66 days of incubation (Fig. 3.3) even

though there was likely up to 0.3% liquid water present as brine pockets at the grain boundaries of the ice crystals (Marion and Grant, 1998). $^{14}CO_2$ was produced only when the entire sample was in liquid form. Mineralization of the labeled acetate was observed in both the unamended thawed basal ice and, to a much lesser extent, in the unamended thawed glacier ice. Amendment with 0.1X R2A medium significantly increased acetate mineralization in the glacier ice sample, but had little effect on mineralization rates in the basal ice sample. This implies that microbes in the thawed glacier ice were more nutrient-limited than those in the thawed basal ice. Unamended samples incubated at 4°C produced results similar to those obtained previously at 8°C, with higher rates of acetate mineralization in the thawed basal ice than in the thawed glacier ice (Fig. 3.2).

3.3.4. Microscopy.

Microscopic studies demonstrated the presence of microbes in both freshly thawed uncultured and cultured basal ice samples taken in 1998. Typical prokaryotic cell morphologies, including bacilli, cocci, and cells undergoing division were observed by TEM of both cultured and uncultured basal ice samples (Fig. 3.4). Cells were not exclusively associated with sediment in basal ice samples and were often observed singly rather than in microcolonies or obvious biofilms.

3.3.5. Allochthonous organic carbon.

Uncultured 1998 basal ice samples had sediment concentrations of 2000 g l^{-1}, whereas the glacier ice was free of visible particulates. Particulate organic carbon (POC) concentrations of the basal ice were 0.53 - 0.97 M C compared with 34 μM C in the glacier ice. Basal ice had dissolved organic carbon (DOC) concentrations of 100 μM C compared with 24 μM C in the glacier ice. The average $\delta^{13}C$ of organic carbon (OC) in the basal ice was -23.2 ‰, ($\delta^{13}C$-DOC = -21.0 ‰, $\delta^{13}C$-POC = -28.5 ‰) compared with the average $\delta^{13}C$ of OC in glacier ice of -23.9 ‰, ($\delta^{13}C$-DOC = -24.9 ‰, $\delta^{13}C$-POC = -23.2 ‰). This indicates a much greater source of OC in the basal ice. Sediments sampled in the proglacial and ice marginal zones contained cyanobacterial mats, mosses and plant

remains that comprised 0.3-4.1 weight % OC. This confirms that glacially overridden sediments can provide a source of allochthonous OC to serve as a carbon and energy source in the subglacial environment.

3.4. DISCUSSION

The 1996 experiments clearly demonstrate that viable microbes exist in both the supraglacial and subglacial environments of a polythermal Arctic glacier. Microbial activity was observed to increase with increasing suspended sediment concentration in the water samples, similar to findings from Alpine subglacial environments (Sharp et al., 1999).

The 1997 experiments confirm that there are culturable microbial populations in the debris-rich basal ice. Moreover, the basal ice harbored numerous types of aerobic and anaerobic bacteria, including heterotrophs, nitrate- and sulfate-reducers, and methanogens. It is particularly interesting that methanogens were viable in culture because the samples were not sampled or stored in an anaerobic environment. Moreover, dissolved oxygen was measured at close to 100 % saturation in the subglacial meltwaters (Skidmore, 1995). However, there is considerable variability in the sensitivity of methanogens to oxygen, and viable methanogens have been detected in nominally aerobic environments where anaerobic microenvironments or transient anaerobic conditions occur (Zinder, 1993). The presence of methanogens suggests that although the subglacial meltwaters are essentially aerobic, the underlying thawed subglacial sediments contain anaerobic microenvironments which are retained as the basal ice forms.

The 1998 culture experiments show that aerobic microbial growth is possible in the thawed basal ice under conditions as close to *in situ* as could be achieved in the laboratory, with minimal amendment of organic carbon and without additional nutrients. Addition of 0.1X R2A growth medium had no effect on the respiration rates in the thawed basal ice samples, but produced significant increases in respiration rates in the thawed glacier ice. The latter suggests that microbes are present in the glacier ice but that

they are more nutrient and carbon limited than those in the basal ice, likely due to the low solute content of the thawed glacier ice. Hence, the microbes are not necessarily physically associated with sediment particles. The experiments also show no signs of aerobic respiration at subfreezing temperatures; however, it is likely that longer duration experiments would be required to confirm these observations.

The DOC concentration in the basal ice is at least twice that used for amendment in the culture experiments, and TOC concentrations are orders of magnitude greater. This confirms that there is plentiful OC available in the subglacial sediments to facilitate subglacial microbial metabolism. The source of the organic carbon in the subglacial sediments is most likely from permafrozen soils, over-ridden by the advancing glacier and then finely ground by subglacial abrasion processes. The organic material in present day proglacial and ice marginal sediments, which are likely similar to the source material for the subglacial sediments, consists of cyanobacterial mats, plant material and roots. These types of carbonaceous material are readily biodegradable by microbial activity. OC from cryoconite holes (6 % weight OC) may also be washed into the subglacial environment from the glacier surface.

From the experiments on waters and ice it is evident that there is a clear link between the presence of sediment and the level of microbial activity. The sediment is likely the primary source of the microbes, i.e. that they are present in the soils/sediments that the glacier overrides. From the TEM images (Fig. 3.4 a & d), microbes are clearly associated with the sediment, although perhaps not physically attached. Additionally the sediment provides a source of carbon and weathered sediments produce aqueous nutrients for the subglacial microbial community. Microbes may also be washed into the subglacial environment from the glacier surface; however, it would appear from the culture experiments that it is only in the subglacial environment that the necessary combination of microbes, nutrients and carbon is available to support viable microbial activity. Similarly in the ice-sediment microbial communities in perennial Antarctic lake ice (Priscu et al., 1998) there is a link between the concentration of sediment in the ice and

microbial activity. The sediment provides nutrient enriched microzones to support the microbial community and there is evidence of the bacteria being physically attached to the sediment in these microzones. However, the highest concentrations of bacterial cells and DOC are not directly correlative to high sediment concentrations.

The experimental cultures and DOC/TOC results indicate that there are sufficient nutrients and carbon to support aerobic microbial activity in unfrozen basal sediments beneath John Evans Glacier. Therefore, to maintain the aerobic respiration processes in the subglacial environment a supply of oxygen is clearly required. Potential oxygen sources to the glacier base are from oxygenated surficial waters that reach the bed via crevasses or from subglacial melting of glacier ice. Assuming glacier ice contains 0.09 cm^3 air of standard composition g^{-1} ice (Souchez et al., 1995), and basal melt rates are 12 mm yr^{-1} (6 mm yr^{-1} from geothermal heating and 6 mm yr^{-1} generated from friction assuming that ice slides at 20 m yr^{-1}) (Paterson, 1994), basal melting delivers O_2 to the glacier bed at a rate determined by the product of the basal melt rate (m yr^{-1}) and the O_2 content of the ice (M m^{-3}), giving 1 mM O_2 m^{-2} yr^{-1}. If surficial waters reach the bed the O_2 supply would be significantly higher. If the oxygen supply to the glacier base is completely exhausted then it is evident that there is a diverse population of anaerobic bacteria in the unfrozen sediments. These anaerobic bacteria are viable at 4°C, and it is highly likely that they would also function at 0.3°C, albeit at lower metabolic rates. Hence both aerobic and anaerobic microbial activity in unfrozen sediments beneath a high Arctic polythermal glacier are tenable processes. The implications of these findings are wide ranging and are outlined below.

3.4.1. Glacial/interglacial carbon cycling.

Microbial populations are found in a range of perennially frozen environments (Gilichinsky et al., 1993; Psenner and Sattler, 1998; Priscu et al., 1998; Rivkina et al., 1998), including subglacial environments (Karl et al., 1999; Priscu et al., 1999; Sharp et al., 1999, this study) and sub-zero marine sediments (Sagemann et al., 1998). These environments contain water, nutrients, carbon, and oxygen or a suitable electron acceptor,

thus providing the necessary constituents to support microbial activity. Thus it seems likely that microbial populations were active in the temperate based sectors of the Pleistocene mid-latitude ice sheets, where water and OC (in over-ridden Boreal soils and peat) were present (Dredge et al., 1990; Punkari and Forsstrom, 1995). Viable aerobic and anaerobic bacteria, functionally similar to those cultured from thawed basal ice at John Evans Glacier, have been resuscitated from ancient (≤ 3 million years old) permafrozen Boreal soils from Siberia and cultured at –8°C to 4°C (Gilichinsky et al., 1993; Rivkina et al., 1998). Hence reactivation of microbes during sub-ice sheet thawing of permafrozen soils and peat is a tenable process.

The impact of subglacial microbial activity on carbon cycling models remains unquantified. However, a simple calculation suggests that aerobic respiration of OC, constrained by the supply of oxygen to the ice sheet beds by basal melting alone (1mM O_2 m^{-2} yr^{-1}) could convert 8.1 Pg C to CO_2 over a glacial cycle. Aerobic CO_2 production beneath ice sheets is calculated on the following assumptions: (i) basal melting delivers O_2 to the glacier bed at a rate (mol O_2 m^{-2} yr^{-1}) determined by the product of the basal melt rate (m yr^{-1}) and the O_2 content of the ice (mol m^{-3}); (ii) all the O_2 is converted to CO_2 by microbial processes ($CH_2O + O_2 \rightarrow CO_2 + H_2O$) and (iii) total CO_2 production is calculated as the integral over time of CO_2 production rates in the warm based sectors of ice sheets. The area of warm based ice beneath the Laurentide ice sheet, and its evolution over time, is taken from (Marshall and Clarke, 1999; Marshall and Clark, submitted), and multiplied by 1.13 to account for the area of warm-based ice beneath the Fennoscandian ice sheet based on the difference in areas for the two ice masses (Holmlund and Fastook, 1995).

Higher CO_2 production is likely because the calculation is based on conservative assumptions about basal melt rates and ignores O_2 input from surface waters. In addition, anaerobic decomposition of OC would also contribute to CO_2 evolution under depleted oxygen conditions. Although it is hard to quantify the rate at which this might occur, we note that SO_4^{2-} reduction rates of 0.9-1.2 mM m^{-2} day^{-1} have been reported from Arctic

marine sediments at –1.7 to 0.2°C (Sagemann et al., 1998). Such rates would produce CO_2 at 1000 times the rate calculated from aerobic respiration. Thus, it would be useful to consider the effects of subglacial microbial activity in carbon cycling models on glacial/interglacial timescales.

3.4.2. Ice core gases.

This work has shown the presence of strictly anaerobic methanogenic bacteria in thawed basal ice samples. These bacteria are viable in low temperature cultures suggesting that within the unfrozen basal sediments there are anaerobic microenvironments with the potential to generate methane subglacially. This provides a possible alternative interpretation of the high greenhouse gas load observed in debris-rich basal ice from both the Dye 3 (Souchez et al., 1998) and GRIP (Souchez et al., 1995) ice cores from the Greenland ice sheet (Dye 3 40,000 ppmv and GRIP 130,000 ppmv CO_2; GRIP 6,000 ppmv CH_4). The high greenhouse gas load in the basal ice is interpreted (Souchez et al., 1995; Souchez et al., 1998) to result from the incorporation of ground ice into the glacier ice by glacier flow-induced mixing during ice-sheet build up. Our results suggest that the gases in these ancient samples may include products of *in situ* microbial activity at the base of the ice sheet, such that pre-glacial CH_4 production and subsequent flow mixing may not be required to explain the observed CH_4 values.

3.4.3. Martian polar analogue.

The study has demonstrated that the subglacial environment beneath a polythermal glacier provides a viable habitat for microbial life. There is access to liquid water and sediment (nutrients), and sub-ice microbial communities are protected from diurnal and seasonal temperature fluctuations. Therefore, this environment may provide a model for viable habitats for life on Mars, since similar conditions may exist or have existed in the basal sediments beneath the Martian north polar ice cap (Clifford, 1987).

3.5. REFERENCES

Adams J. M., Faure H., Faure-Denard L., McGlade J. M., and Woodward F. I. (1990) Increases in the terrestrial carbon storage from the Last Glacial Maximum to the present. *Nature* **348**, 711-714.

Alley R. B., Cuffey K. M., Evenson E. B., Strasser J. C., Lawson D. E., and Larson G. J. (1997) How glaciers entrain and transport basal sediment: physical contstraints. *Quaternary Science Reviews* **16**, 1017-1038.

Andersen D. T., Pollard W. H., McKay C. T., and Omelon C. (1998) Perennial springs in the Canadian High Arctic, analogs of past Martian liquid water habitats. *Eos Transactions* **79**(45), 59.

Arendt A. (1997) Mass balance modelling of an Arctic glacier. Unpublished MSc., University of Alberta.

Atlas R. M. (1995) *Handbook of microbiological media for environmental microbiology.* CRC Press. Boca Raton, U.S.A.

Bengtsson L. and M. E. (1986) Chapter 21 : Chemical analysis. In *Handbook of Holocene Palaeoecology and Palaeohydrology.* (ed. B. E. Berglund), pp. 423-451. Wiley-Interscience, Chichester, U.K.

Butlin K. R., Adams M. E., and Thomas M. (1949) The isolation and cultivation of sulfate-reducing bacteria. *Journal of General Microbiology* **3**, 46-59.

Cantor B. A. and James P. B. (1998) Review of the 1990-1997 Hubble space telescope observations of the Martian polar caps. *Proceedings of the 1st International conference on Mars Polar science and exploration. LPI contribution no.* **953**, 5-6.

Clifford S. M. (1987) Polar basal melting on Mars. *Journal of Geophysical Research* **92**(B9), 9135-9152.

Copland L. and Sharp M. J. (in press) Mapping hydrological conditions beneath a polythermal glacier using radio-echo sounding. *Journal of Glaciology.*

Dredge L. A., Morgan A. V., and Nielsen E. (1990) Sangamon and pre-Sangamon interglaciations in the Hudson Bay Lowlands of Manitoba. *Geographie Physique et Quaternaire* **44**(3), 319-336.

Fedorak P. M., Foght J. M., and Westlake D. W. S. (1982) A method for monitoring mineralization of ^{14}C- labeled compounds in aqueous samples. *Water Research* **16**, 1285-1290.

Francois L. M., Godderis Y., Warnant P., Ramstein G., de Noblet N., and Lorenz S. (1999) Carbon stocks and isotopic budgets of the terrestrial biosphere at mid-Holocene and last glacial maximum times. *Chemical Geology* **159**, 163-189.

Gibbs M. T. and Kump L. R. (1994) Global chemical erosion during the last glacial maximum and the present: sensitivity to changes in lithology and hydrology. *Paleoceanography* **9**, 529-543.

Gilichinsky D. A., Soina V. S., and Petrova V. A. (1993) Cryoprotective properties of water in the earth cryolithosphere and its role in exobiology. *Origins of Life and Evolution of the Biosphere* **23**, 65-75.

Hallet B., Hunter L., and Bogen J. (1996) Rates of erosion and sediment evacuation by glaciers: a review of field data and their implications. *Global and Planetary Change* **12**, 213-235.

Holmlund P. and Fastook J. (1995) A time dependent glaciological model of the Weichselian Ice Sheet. *Quaternary International* **27**, 53-58.

Hubbard B. and Sharp M. J. (1989) Basal ice formation and deformation: a review. *Progress in Physical Geography* **13**, 529-558.

Iverson N. R. and Semmens D. J. (1995) Intrusion of ice into porous media by regelation: A mechanism of sediment entrainment by glaciers. *Journal of Geophysical Research* **100**(B7), 10219-10230.

Kargel J. S. (1998) Possible composition of Martian polar caps and controls on ice-cap behaviour. *Proceedings of the 1st International conference on Mars Polar science and exploration LPI contribution no.* **953**, 22-23.

Karl D. M., Bird D. F., Bjorkman K., Houlihan T., Shackelford R., and Tupas L. (1999) Microorganisms in the accreted ice of Lake Vostok, Antarctica. *Science* **286**, 2144-2147.

Lawson D. E., Strasser J. C., Evenson E. B., Alley R. B., Larson G. J., and Arcone S. A. (1999) Glaciohydraulic supercooling: a freeze-on mechanism to create stratified, debris-rich ice. I. Field evidence. *Journal of Glaciology* **44**(148), 547 - 562.

Leckrone K. J. (1997) Continuous flow instrumentation for isotopic analysis of dissolved organic carbon. Unpublished Ph.D. thesis, University of Indiana.

Ludwig W., Amiotte-Suchet P., and Probst J.-L. (1999) Enhanced chemical weathering of rocks during the last glacial maximum: a sink for atmospheric CO_2 ? *Chemical Geology* **159**, 147-161.

Marion G. M. and Grant S. A. (1997) Physical chemistry of geochemical solutions at subzero temperatures. *International symposium on Physics, chemistry and Ecology of Frozen Soils*, 349-356.

Marshall S. J. and Clarke G. K. C. (1999) Modeling North American fresh water runoff through the last glacial cycle. *Quaternary Research.* **52**(3), 300-315.

Marshall, S. J. and Clark P. U. (Submitted) Basal temperature evolution of the Laurentide Ice Sheet and implications for glacial terminations. *Geophysical Research Letters.*

Mikesell M. D., Kukor J. J., and Olsen R. H. (1993) Metabolic diversity of aromatic hydrocarbon-degrading bacteria from a petroleum-contaminated aquifer. *Biodegradation* **4**, 249-259.

Morozova T. D., Velichko A. A., and Dlussky K. G. (1998) Organic carbon content in the late Pleistocene and Holocene fossil soils (reconstruction for Eastern Europe). *Global and Planetary Change* **16-17**, 131-151.

Paterson W. S. B. (1994) *The physics of glaciers*. 3rd ed. Pergamon. Oxford, UK. 480p.

Pathare A. V. and Paige D. A. (1998) Recent liquid water in the polar regions of Mars. *Proceedings of the 1st International conference on Mars Polar science and exploration LPI contribution no.* **953**, 31-32.

Priscu J. C., Adams E. E., Berry Lyons W., Voytek M. A., Mogk D. W., Brown R. L., McKay C. P., Takacs C. D., Welch K. A., Wolf C. F., Kirshtein J. D., and Avci R. (1999) Geomicrobiology of subglacial ice above Lake Vostok, Antarctica. *Science* **286**, 2141-2144.

Priscu J. C., Fritsen C. H., Adams E. E., Giovannoni S. J., Paerl H. W., McKay C. P., Doran P. T., Gordon D. A., Lanoil B. D., and Pinckney J. L. (1998) Perennial Antarctic lake ice: An oasis for life in a polar desert. *Science* **280**, 2095-2098.

Psenner R. and Sattler B. (1998) Life at the freezing point. *Science* **280**, 2073-2074.

Punkari M. and Forsstrom L. (1995) Organic remains in Finnish subglacial sediments. *Quaternary Research* **43**(3), 415-425.

Rivkina E., Gilichinsky D., Wagener S., Tiedje J., and McGrath J. (1998) Biogeochemical activity of anaerobic microorganisms from buried permafrost sediments. *Geomicrobiology* **15**, 187-193.

Sagemann J., Jorgensen B. B., and Greeff O. (1998) Temperature dependence and rates of sulfate reduction in cold sediments of Svalbard, Arctic Ocean. *Geomicrobiology Journal* **15**, 85-100.

Sharp M., Parkes J., Cragg B., Fairchild I. J., Lamb H., and Tranter M. (1999) Widespread bacterial populations at glacier beds and their relationship to rock weathering and carbon cycling. *Geology* **27**(2), 107-110.

Skidmore M. L. (1995) The hydrochemistry of a high Arctic glacier. MSc., University of Alberta.

Skidmore M., Foght J. M., and Sharp M. J. (1998) Microbial experiments on basal ice from John Evans Glacier, eastern Ellesmere Island, N.W.T., Canada. *Proceedings of the 1st International conference on Mars Polar science and exploration. LPI contribution no.* **953**, 34-35.

Skidmore M. L. and Sharp M. J. (1999) Drainage behaviour of a high Arctic polythermal glacier. *Annals of Glaciology* **28**, 209-215.

Souchez R., Bouzette A., Clausen H. B., Johnsen S. J., and Jouzel J. (1998) A stacked mixing sequence at the base of the Dye 3 core, Greenland. *Geophysical Research Letters* **25**(11), 1943-1946.

Souchez R., Lemmens M., and Chappellaz J. (1995) Flow-induced mixing in the GRIP basal ice deduced from the CO_2 and CH_4 records. *Geophysical Research Letters* **22**(1), 41-44.

Van Campo E., Guiot J., and Peng C. (1993) A data-based reappraisal of the terrestrial carbon budget at the last glacial maximum. *Global and Planetary Change* **8**, 189-201.

Vincent W. F., Gibson J. A. E., Pienitz R., Villeneuve V., Broady P. A., Hamilton P. B., Howard-Williams C. Ice shelf microbial ecosystems in the High Arctic and implications for life on Snowball Earth. *Naturwissenschaften* **87**, 137-141.

Yamamoto-Ikemoto R., Matsui S., Komori, T. (1994) Ecological interactions among denitrification, poly-P accumulation, sulfate reduction, and filamentous sulfur bacteria in activated sludge. *Water Science and Technology* **30**, 11, 201–210

Zimov S. A., Zimova G. M., Daviodov S. P., Daviodova A. I., Voropaev Y. V., Voropaeva Z. V., Prosiannikov S. F., Prosiannikova O. V., Semiletova I. V., and Semiletov I. P. (1993) Winter biotic activity and production of CO_2 in Siberian soils: A factor in the greenhouse effect. *Journal of Geophysical Research* **98**(D3), 5017-5023.

Zinder S. H. (1993) Physiological ecology of methanogens. In *Methanogenesis* (ed. J. G. Ferry). Chapman and Hall. New York, U.S.A. p128-206.

TABLE 3.1 Concentration of headspace gases generated during 12 months incubation at 4°C by 1997 thawed ice samples amended with 0.25X R2A medium. Values are means of duplicate analyses.

Sample	CO_2 (ppmv)	CH_4 (ppmv)
Basal ice (debris-rich)	58,000±2700	16,000±100
Glacier ice (debris-poor)	5,500±150	1.7±0.1
Uninoculated medium	8,600±300	1.4±0.2

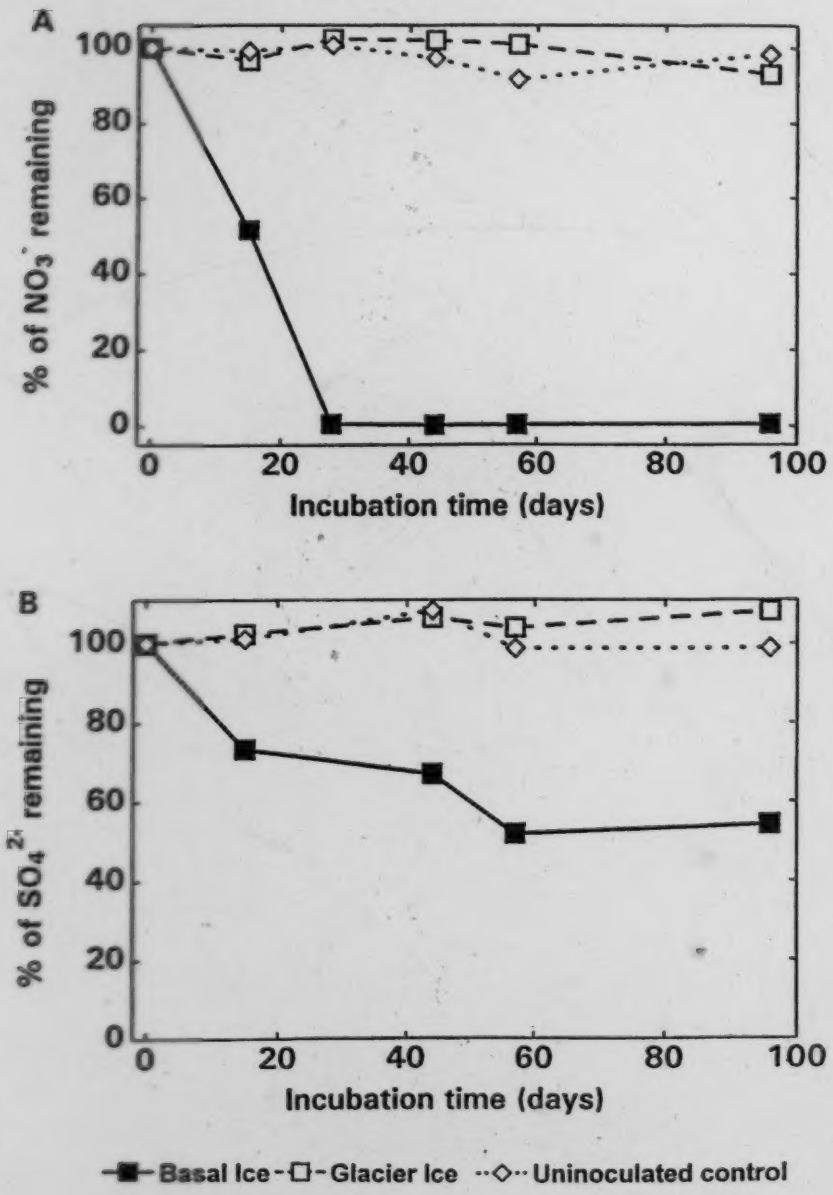

Fig 3.1 Anaerobic incubations of thawed ice at 4°C amended with: (A) dilute nitrate medium (5mM NO_3^-) and (B) dilute sulfate medium (14 mM SO_4^{2-})

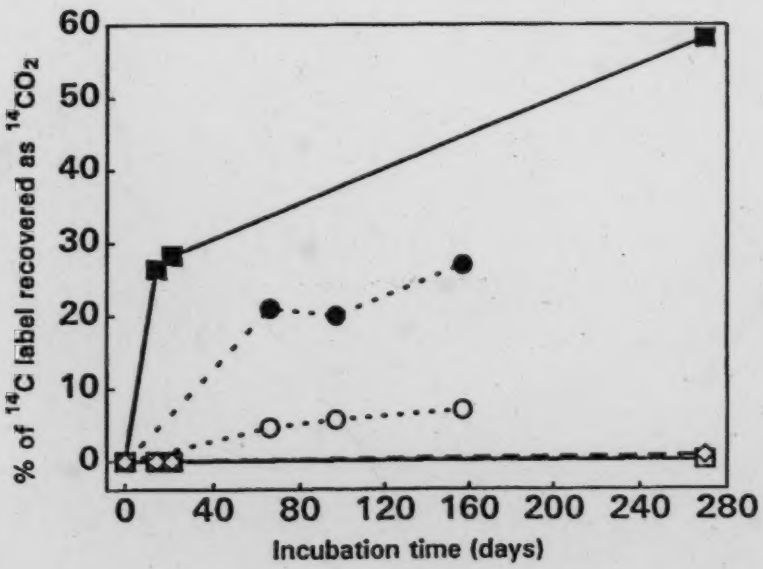

Fig. 3.2 Aerobic incubations of thawed ice samples in the dark. Samples collected in 1997 were supplemented with 98,000 dpm of sodium [2-^{14}C]acetate and incubated at 8°C for 270 days with gyratory shaking at 200 rpm; (■, Basal ice plus dilute R2A medium; □, Glacier ice plus dilute R2A medium; ◇, dilute R2A medium).
1998 samples were supplemented with 195, 000 dpm of sodium [2-^{14}C]acetate and incubated stationary at 4°C for 157 days; (●, Basal ice without R2A medium; ○, Glacier ice without R2A medium).

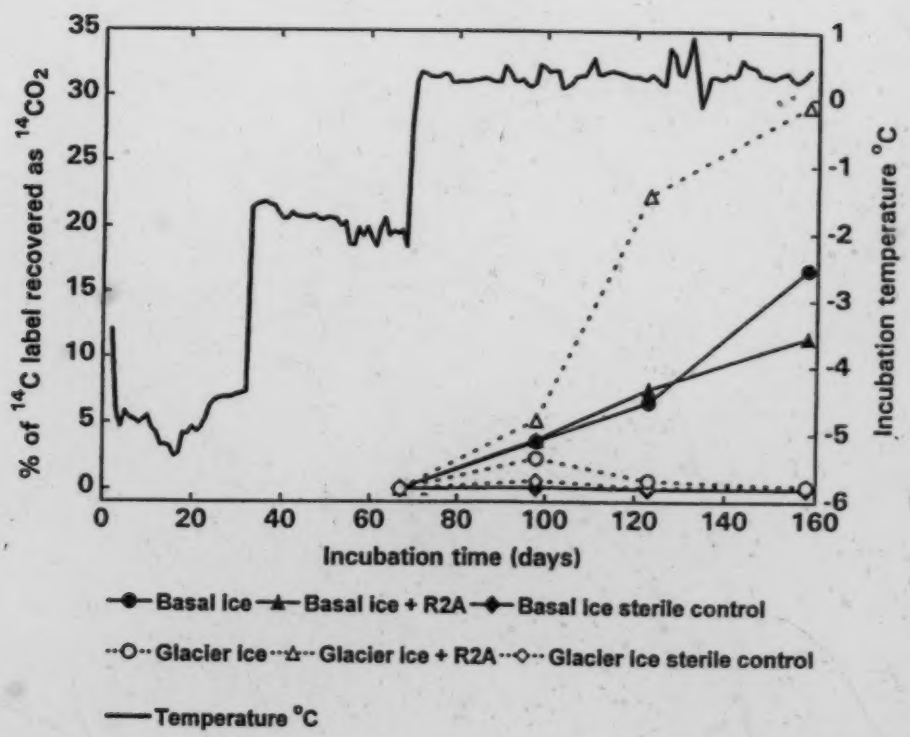

Fig. 3. 3 Aerobic incubation of 1998 ice samples in the dark at increasing temperatures (-4.8°C, -1.8°C and 0.3°C). All samples were supplemented with 195,000 dpm of sodium [2-^{14}C]acetate. Incubation temperatures are also shown.

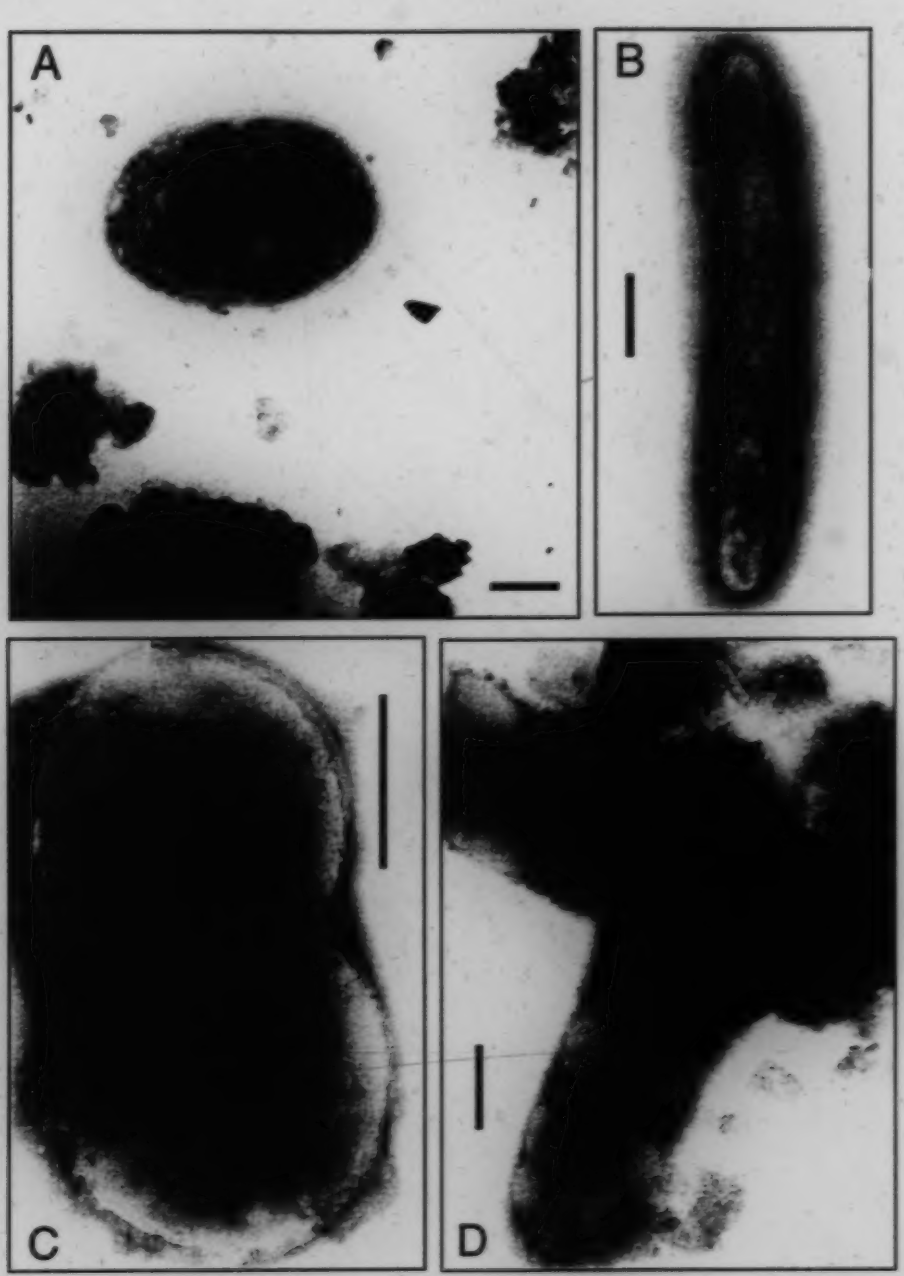

Fig. 3. 4 TEM images of bacteria in meltwater from basal ice samples (scale bars = 0.5 µm). (A) Coccus associated with sediment from uncultured basal ice immediately after thawing. (B) Long thin rod, and (C) actively dividing cocci, both from aerobic stationary culture at 0.3oC without R2A amendment. (D) Short, fat rods, with inclusions, associated with sediment from unamended aerobic culture at 4oC without R2A medium.

Chapter 4. Fractionation of carbon isotopes during the weathering of carbonates in glaciated catchments: Implications for the detection of subglacial microbial activity[1].

4.1. INTRODUCTION

Rates of chemical weathering in glaciated catchments are comparable to those in non-glacial catchments with similar specific runoff (Anderson et al., 1997). However, understanding of the precise mechanisms of subglacial chemical weathering is currently under revision (Tranter et al., in press). It has long been recognised that sulphide oxidation and the dissolution of carbonates are key reactions (Raiswell, 1984; Tranter et al., 1993). However, the source of protons required to dissolve the carbonate, in addition to those derived from sulphide oxidation, is unclear. Earlier research assumed that carbonic acid, derived from dissolution of atmospheric CO_2 was a principal proton source (Reynolds and Johnson, 1972; Raiswell, 1984; Tranter et al., 1993), whereas recent work has suggested that little atmospheric CO_2 may be involved (Tranter et al., in press). Further, Tranter et al., (in press) and Bottrell and Tranter (in press) demonstrate that subglacial conditions may become anoxic, indicating that there is limited access to the atmosphere in some subglacial environments. In addition, microbial populations have been found in association with subglacial sediments from two Swiss glaciers (Sharp et al., 1999) and microbial oxidation of organic C at 0.3°C has been demonstrated using subglacial sediments from John Evans Glacier, Ellesmere Island (Skidmore et al., 2000). This raises the possibility that microbial oxidation of organic carbon is both a cause of anoxia and a source of CO_2 and hence protons at glacier bed. However, direct evidence for *in situ* subglacial microbial activity is limited (Tranter et al., in press).

In unglaciated catchments, $\delta^{13}C$ of dissolved inorganic carbon (DIC) in runoff has been utilised to determine the relative magnitude of microbial (soil) and atmospheric CO_2 sources (Telmer and Veizer, 1999; Amiotte-Suchet et al., 1999). The main potential

[1] This chapter is being split into two papers for submission to *Geochimica et Cosmochimica Acta*

sources of DIC in glacial runoff (carbonate minerals, atmospheric CO_2 and CO_2 from the microbial oxidation of organic carbon) generally have significantly different $\delta^{13}C$ values (Faure, 1986). Hence, $\delta^{13}C$–DIC of glacial runoff has the potential to provide direct evidence of *in situ* subglacial microbial activity. However, glacial weathering processes are dominated by rapid reactions involving trace bedrock components, so kinetic effects might also influence the isotopic composition of DIC.

This paper examines $\delta^{13}C$–DIC data from meltwaters at two glaciers to determine whether $\delta^{13}C$-DIC runoff signatures carry information on CO_2 sources, and allow identification of microbial contributions to DIC. These glaciers were chosen on the basis of their contrasting bedrock lithologies. John Evans Glacier, Ellesmere Island, rests primarily on carbonate bedrock, while Haut Glacier d'Arolla overlies predominantly silicate lithologies. Initial modelling, using standard geochemical models, was undertaken to interpret the field data. These models do not account for the field data unless implausible amounts of microbial CO_2 and extremely negative $\delta^{13}C$-microbial CO_2 values are invoked. Many of the waters are out of chemical equilibrium, indicating that they are likely also out of isotopic equilibrium. Hence, kinetic isotopic fractionation effects may provide an alternative explanation of the data. Weathering experiments, designed to simulate *in situ* conditions, were conducted to determine the occurrence and magnitude of such kinetic effects, which prove to be significant. The kinetic effects were incorporated into the standard geochemical models and provide a more satisfactory explanation of the field data. The field data can then be interpreted in terms of between-glacier differences in lithology and seasonal differences in glacier drainage system properties (such as system structure, discharge and access to supplies of suspended sediment). In some waters it is possible to identify microbial CO_2 input using the new models. However, in others the impact of kinetic isotopic fractionation effects is so dominant that this is not possible. The paper begins with an overview of chemical weathering reactions in glaciated environments, and then examines the likely isotopic fractionations and $\delta^{13}C$-DIC signatures and that may occur as a consequence.

4.1.1. Chemical weathering reactions in glacial environments

The rate of chemical weathering in glaciated terrain was formerly thought to be low and to be controlled by abiotic processes, since temperatures are often at or below freezing, water is in limited supply for much of the year and access to atmospheric CO_2 is limited (Reynolds and Johnson, 1972; Tranter, 1982; Gibbs and Kump, 1994; Kump and Alley, 1994). Recent work has shown that rates of chemical erosion in small glaciated catchments are similar to those in temperate catchments with comparable specific runoff (Anderson et al., 1997). Lithology has an impact on the magnitude of chemical erosion in glaciated catchments (Hodson et al., 2001) that is similar to that observed in temperate catchments (Bluth and Kump, 1994). Generally, basaltic and carbonate bedrock is the most reactive. By contrast, the main geochemical weathering reactions in glacial environments are largely independent of bedrock lithology (e.g. Sharp et al., 1996). Reactive minerals, such as sulphides and carbonates which are often present in trace quantities (< 0.1 %) in the bedrock, have a dominant role in the rock-water interactions which occur, so determining the chemical composition of the meltwaters (Tranter et al., 1993). This assertion is consistent with experimental studies on freshly ground granites, (as would be found in subglacial environments), which demonstrate that calcite weathering predominates over silicate weathering for the first 1000 hours, even when $CaCO_3$ comprises as little as 0.03 % of the bedrock (White et al., 1999).

The dominant chemical weathering reactions in glacial environments are outlined below (following Raiswell, 1984; Raiswell and Thomas, 1984; Tranter et al., 1993; Wadham et al., 1998; Anderson et al., 1999; Tranter et al, in press). Proton sources are primarily from the oxidation of sulphide minerals and carbonation, represented by Equations 1 and 2. Nitric and sulphuric acids stored in the snowpack are usually a minor source, e.g., between 2-11% of the annual total proton supply (Sharp et al., 1995). Finally, oxidation of organic carbon is a potential source of protons (Sharp et al., 1999; Skidmore et al., 2000; Tranter et al., in press), (Equation 3).

The main proton sink is the dissolution of carbonate minerals, calcite and dolomite (Equation 4). A minor proton sink is the (partial) chemical weathering of silicate minerals (Equation 5). Silicate weathering contributes ~ < 12 % of total solute in the most concentrated waters at Haut Glacier d'Arolla with the proportion declining with solute concentration (Tranter et al., in press) and < 1 % of total solute at John Evans Glacier (Skidmore, unpublished data) and is therefore not included in the subsequent analysis. The coupling of sulphide oxidation with carbonate dissolution (Equations 1 and 4) in the subglacial environment has been well documented (e.g. Raiswell and Thomas, 1984; Fairchild et al., 1994; Wadham et al., 1998; Anderson et al., 1999; Tranter et al., in press). Other important reactions are carbonate hydrolysis (Equation 6), which occurs during the initial stages of carbonate weathering and produces significant bedrock DIC without requiring a proton supply, and dissolution of gypsum/anhydrite (Equation 7), which provides an additional SO_4^{2-} source where these minerals are present in the bedrock. Consequently, the primary dissolved species in most glacial meltwaters are Ca^{2+}, HCO_3^- and SO_4^{2-} (Raiswell and Thomas, 1984; Tranter et al., 1993).

The primary chemical weathering reactions in glacial environments perturb DIC equilibria. The "apparent"[2] PCO_2 of glacial meltwaters ranges from $10^{-2.2}$ (this study) - $10^{-5.6}$ atms (Raiswell and Thomas, 1984), indicating that the waters are often out of equilibrium with the atmosphere ($10^{-3.5}$ atms at sea level). The PCO_2 of the waters is controlled both physically (since access to the atmosphere may be restricted in subglacial environments, preventing both ingassing and outgassing of CO_2) and kinetically (since rapid initial chemical weathering processes produce disequilibrium PCO_2 conditions; Tranter et al., 1993). These factors in turn are largely controlled by the nature of the glacial hydrological system, which determines water:rock ratios, water residence times and whether the channels/cavities are water full (Sharp, 1991).

[2] PCO_2 values reflect the partial pressure of CO_2 in a hypothetical atmosphere with which the waters would be in equilibrium.

Proton sources.

Sulphide Oxidation (SO)

$4FeS_{2\,(s)} + 15O_{2\,(aq)} + 14H_2O_{(l)} \rightarrow 16H^+_{(aq)} + 8SO_4^{2-}{}_{(aq)} + 4Fe(OH)_{3\,(s)}$ (1)

pyrite — ferric oxyhydroxides

Carbonation (CB)

$CO_{2\,(g)} + H_2O_{(l)} \leftrightarrow H_2CO_{3\,(aq)} \leftrightarrow H^+_{(aq)} + HCO_3^-{}_{(aq)}$ (2)

Atmospheric

Microbial respiration (MR)

$C_{(s)} + O_{2\,(aq)} + H_2O_{(l)} \quad H_2CO_{3\,(aq)} \leftrightarrow H^+_{(aq)} + HCO_3^-{}_{(aq)}$ (3)

Organic

Proton sinks.

Carbonate dissolution (CD)

$CaCO_{3\,(s)} + H^+_{(aq)} \leftrightarrow Ca^{2+}{}_{(aq)} + HCO_3^-{}_{(aq)}$ (4)

Calcite

Silicate weathering (SW)

$CaAl_2Si_2O_{8\,(s)} + 2H^+_{(aq)} \leftrightarrow Ca^{2+}{}_{(aq)} + H_2Al_2Si_2O_{8\,(s)}$ (5)

Anorthite (Ca-feldspar) — weathered feldspar surfaces

Other weathering reactions.

Carbonate hydrolysis (CH)

$CaCO_{3\,(s)} + H_2O_{(l)} \rightarrow Ca^{2+}{}_{(aq)} + HCO_3^-{}_{(aq)} + OH^-_{(aq)}$ (6)

Calcite

Gypsum dissolution (GD)

$CaSO_4.2H_2O_{(s)} + H_2O_{(l)} \leftrightarrow Ca^{2+}{}_{(aq)} + SO_4^{2-}{}_{(aq)} + 3H_2O_{(l)}$ (7)

Gypsum

Frequently, the PCO_2 of glacial meltwaters indicates that chemical equilibration of DIC with the atmosphere has not been achieved, and physical barriers may limit CO_2 exchange with the atmosphere. Isotopic exchange of $^{13}CO_2$ and $^{12}CO_2$ commences concurrently with CO_2 exchange. However, once chemical equilibrium is achieved, isotopic equilibrium may not have been achieved (Szaran, 1997). So, it is reasonable to

infer that glacial meltwaters that are not in chemical equilibrium with atmospheric PCO_2 may not be in isotopic equilibrium with the atmosphere. It follows that an understanding of reaction rates in the DIC-carbonate system and the associated kinetic and equilibrium isotopic fractionations is important to interpret the $\delta^{13}C$-DIC of glacial meltwaters.

4.1.2. Isotopic fractionation and carbonate equilibria.

4.1.2.1. Chemical equilibria in the carbonate system

Carbonate equilibria can be described using the following Equations (Stumm and Morgan, 1996)

$$CO_{2\,(g)} \leftrightarrow CO_{2\,(aq)} \quad \text{(a)}$$

$$CO_{2\,(aq)} + H_2O_{\,(l)} \leftrightarrow H_2CO_3{}^*{}_{(aq)} \quad \text{(b)}$$

$$H_2CO_3{}^*{}_{(aq)} \leftrightarrow H^+{}_{(aq)} + HCO_3{}^-{}_{(aq)} \quad \text{(c)}$$

$$HCO_3{}^-{}_{(aq)} \leftrightarrow H^+{}_{(aq)} + CO_3{}^{2-}{}_{(aq)} \quad \text{(d)}$$

where $H_2CO_3{}^*$ represents both dissolved CO_2 and undissociated H_2CO_3

The slowest component of this set of reactions is the gas transfer reaction (a). This reaction is frequently slower than other reactions that produce or consume CO_2 in the aqueous phase, such as calcite dissolution and precipitation (Stumm and Morgan, 1996). Reaction (b) is reported to equilibrate on the order of 20-200 seconds (following Mills and Urey, 1940) in stirred solutions. Where solutions are not stirred the rate of hydration is calculated to be two orders of magnitude slower, and hence full hydration equilibria may take up to 5 hours (Szaran, 1997). Reactions (c and d) are reported to equilibrate on the order of seconds (Stumm and Morgan, 1996).

4.1.2.2. Equilibrium isotope fractionations in the carbonate system

If glacial waters are in chemical equilibrium, as indicated by a PCO_2 of $10^{-3.5}$ atm. (a situation that is not frequently observed in glacial environments), then they may be approaching or at isotopic equilibrium with the atmosphere. Equilibrium isotopic fractionations occur during all stages of the dissolution and dissociation of CO_2 in solution. Equilibrium constants relating the $\delta^{13}C$ fractionations for the reactions $CO_{2\,(g)}$ - $CO_{2\,(aq)}$, $CO_{2\,(g)}$ - $HCO_3^-{}_{(aq)}$ and $CO_{2\,(g)}$ – $CO_3^{2-}{}_{(aq)}$ have been determined experimentally (e.g. Deines et al., 1974). These fractionation factors are temperature dependent, being greatest at 0°C, which is the likely temperature for geochemical reactions in subglacial environments. The majority of DIC at the pH of glacial waters, (typically 6-9; e.g. Raiswell and Thomas, 1984), is as HCO_3^- and thus the fractionation between $CO_{2\,(g)}$ and HCO_3^- ($\varepsilon_{HCO3\text{-}g}$) is of greatest interest to this study. Fractionation occurs during the hydration stage of the reaction (Zhang et al., 1995) and has been determined experimentally by numerous workers, (Deuser and Degens, 1967; Wendt, 1968; Mook et al., 1974; Zhang et al., 1995 and Szaran, 1997) yielding values for ($\varepsilon_{HCO3\text{-}g}$) at 0°C in the range of + 9.2 to + 10.78 ‰. Theoretical calculations (Wigley et al., 1978) yield an equilibrium fractionation between CO_2 and DIC species (predominantly HCO_3^-) of + 10 ‰ at T = 0°C and pH ~7.5 - 9.0. This coincides with the median value in the range outlined above and this value is used in all subsequent calculations.

4.1.2.3. Kinetic fractionations in the carbonate system

Before isotopic equilibrium is achieved in the DIC system, kinetic fractionation processes occur, for which kinetic fractionation factors have been determined experimentally. Vogel et al., (1970) and Zhang et al., (1995) demonstrate a kinetic fractionation of CO_2 (ε_k), in the initial stages of CO_2 transfer across the gas-water interface. At 5°C, (ε_k) is – 1.0 ‰. This is in addition to the equilibrium fractionation factor ($\varepsilon_{g\text{-}s}$) and presumably will be carried through to the HCO_3^- phase during CO_2 hydration. Szaran (1997) reveals another kinetic fractionation effect. In the initial stages of the equilibration between $CO_{2\,(g)}$ and $HCO_3^-{}_{(aq)}$, the fractionation factor ($\varepsilon_{HCO3\text{-}g}$) is significantly reduced from the

equilibrium value (e.g. after 1 hour it is 2 ‰ compared to 9.9 ‰ at equilibrium). Through time, ($\varepsilon_{HCO3\text{-}g}$) increases rapidly at first, slowing as it approaches the equilibrium value. For unstirred solutions at 7°C and low total system pressures (0.25 atm), it takes ~ 20 hours for isotopic equilibrium to be achieved. Higher total system pressures, (> 0.25 atm) as are common in subglacial environments, lead to slower isotopic equilibration. A pressure increase to ~ 1 atm results in a 4 fold increase in equilibration time. Conversely, stirring of the solutions results in a 7 fold reduction in equilibration time (Szaran, 1997). However, in subglacial environments temperatures would be lower (0°C) and longer equilibration times would be expected due to the lower energy of the molecules in the cooler solutions. From this experimental work, it seems reasonable to anticipate that in the initial stages of chemical weathering in subglacial environments $\varepsilon_{HCO3\text{-}g}$ will be lower than the equilibrium value.

2. STUDY AREAS

4.2.1. John Evans Glacier

4.2.1.1. Site description

John Evans Glacier is a large valley glacier located at 79° 40' N; 74° 00' W, on eastern Ellesmere Island, Nunavut, Canada (Fig. 4.1 a). The main arm of the glacier occupies the western part of a 220 km^2 catchment, of which ~ 75% is glaciated. The glacier spans an elevation range from 100-1500 m, and is up to 400 m thick. Below an altitude of 700 m, ice at the glacier bed is temperate and basal melting and subglacial drainage occur (Copland and Sharp, in press). The glacier is underlain by an Ordovician/Silurian carbonate/evaporite sequence with a minor clastic component (Kerr, 1972; Fig. 4.1 a). The main minerals in the bedrock are calcite, dolomite, gypsum and quartz. Subglacial sediments also contain trace quantities of pyrite, sanidine, anorthoclase, muscovite and clinochlore. Meltwater runoff from the glacier occurs primarily via two ice-marginal streams and a subglacial stream. Only the west marginal stream, hereafter termed the "marginal" stream, and the subglacial stream were studied.

4.2.1.2. Hydrology and access to atmospheric gases

The nature of the glacial hydrological system is a major determinant on PCO_2 (see Section 1.1.). The marginal stream, draining the west marginal basin (Fig. 1a), has free access to the atmosphere throughout most of its routing, so atmospheric CO_2 exchange is not physically limited. Thus, the PCO_2 of marginal waters is determined primarily by kinetic processes associated with carbonate weathering. Waters flowing in the subglacial drainage system originate mainly from the glacier surface in the central basin (Fig. 4.1 a), where they have free access to the atmosphere. Recent work (K. Heppenstall, personal communication) indicates that some of these surficial waters have undergone a degree of carbonate weathering in ice marginal environments that drain to ice marginal lakes that in turn overflow into the supraglacial system. These waters have lower than atmospheric PCO_2 values. The supraglacial waters drain to the glacier bed in a crevasse field ~4 km from the glacier terminus (Fig. 4.1 a). In the subglacial environment, the drainage system may be pressurised to levels greater than atmospheric as indicated by the artesian fountains of subglacial water which emerge on the glacier surface near the glacier terminus. Hence, except under recession flow conditions, there is probably limited access to atmospheric CO_2 in this environment (Skidmore and Sharp, 1999). Thus, both physical and kinetic processes affect the PCO_2 of subglacial waters.

4.2.2. Haut Glacier d'Arolla

4.2.2.1. Site description

The Haut Glacier d'Arolla is located at the head of Val d'Hérens, Switzerland, and has an area of ~ 6.3 km^2 (Fig. 4.1 b). The main ice tongue descends to the snout at ~2560 m, and is fed from a compound basin of maximum elevation 3838 m. The glacier is temperate and has been in retreat during recent years. It has a maximum ice thickness of 180 m (Sharp et al., 1993). The catchment is underlain by schists, gneisses, schistose granites and gabbro of the Arolla series, and by amphibolite (Mazurek, 1986). The bedrock contains trace quantities of geochemically reactive minerals such as carbonates and

sulphides (Brown, 1991). Albite, anorthite, microcline and sanidine are the main feldspars and no evidence of gypsum is found (D. Webb, personal communication).

4.2.2.2. Hydrology and access to atmospheric gases

Two different types of drainage system underly the glacier. Distributed subglacial drainage systems are spatially extensive, transmit relatively small fluxes of water and are essentially physically closed to atmospheric CO_2, since they are normally water full. By contrast, channelised drainage systems are localised, transmit relatively high fluxes of water and are potentially open to atmospheric CO_2, particularly during low flows (Hooke, 1989; Paterson, 1994). At the onset of the melt season in May, subglacial drainage is largely via the distributed system (Nienow et al., 1998). During the meltseason, the channelised subglacial system expands up glacier, following the pattern of snowline retreat, and by August an arborescent system of basal channels is established beneath the glacier (Nienow et al., 1998). A residual distributed drainage system co-exists with the channelised system and there is exchange of water and sediment between the two systems (Hubbard et al., 1995). The distributed drainage system is fed by snowmelt and basal icemelt and makes a proportionally greater contribution to runoff at low seasonal and diurnal discharges. The channelised system is fed by icemelt from the glacier surface and therefore dominates at high seasonal and diurnal discharges. Water residence times in the distributed system are ~ > 10 hours compared to 0.5 - 2 hours in the channelised system (Richards et al., 1996). Channels within 500 m of the terminus are usually open to the atmosphere, whereas further upglacier, they are often full and therefore closed to the atmosphere (Richards et al., 1996).

4.3. METHODS

4.3.1. John Evans Glacier

4.3.1.1. Water sampling

In 1998, water samples were taken every other day from the supraglacial, marginal and subglacial streams, c. 20 m from the glacier terminus, from 2nd July - 22nd July (Julian Day, hereafter JD, 183-203). The samples were vacuum filtered through 0.45 μm cellulose nitrate filter membranes. The pH of the filtrate was measured immediately after filtration using an Orion 290A pH meter fitted with a Ross Sure-flow pH electrode, calibrated using Orion low ionic strength buffers. Total alkalinity was determined colorimetrically by titration of a 100 ml sample with 0.16N H_2SO_4 using a Hach digital titrator to an endpoint of pH 4.5. Two 20 ml samples were retained for analysis of major anion and cation concentrations by ion chromatography (see Skidmore and Sharp, 1999 for full details). Precision of SO_4^{2-} determinations was < ± 1.6 % at concentrations > 50 μeq l^{-1} and ± 50 % at concentrations < 2 μeq l^{-1}. Parallel 250 ml or 125 ml aliquots of glacial meltwater taken from the marginal and subglacial streams and were vacuum filtered using sterile 0.2 μm cellulose nitrate filter units and transferred to autoclaved 250 ml septum closure amber glass bottles or autoclaved 45 ml amber glass EPA vials for $\delta^{13}C$–DIC analysis. All samples were kept at c. ≤ 8°C in the dark in the field and stored in a refrigerator at 4°C prior to analysis.

4.3.1.2. $\delta^{13}C$-DIC analysis

All water samples were withdrawn from the collection vessels using needles and syringes, displacing the water with He gas. The sample was injected into pre-evacuated reaction vessels containing between 1-5 ml 100% H_3PO_4, depending on sample size. Injection volumes of water varied from 7-125 ml, depending on the concentration of DIC. The evolved headspace gas from the reaction vessel was injected into an HP series II 5890 Gas Chromatograph for gas separation and passed through a Mat Combustion Interface. The purified and dehumidified CO_2 was directed to a Finigan Mat 252 Mass

Spectrometer for isotope ratio measurement. The majority of samples were injected at least twice to check sample reproducibility. Internal precision was ± 0.5 ‰.

4.3.1.3. Isotopic analysis of rock and sediment samples

Samples of the local limestone and dolostone bedrock were taken from the proglacial area of John Evans Glacier. Samples of recent subglacially-derived sediment were collected in the proglacial area from overbank deposits from active subglacial stream outlets. The rock samples were crushed, and fresh unweathered chips were powdered. XRD analysis confirmed that the limestones were pure, revealing only calcite (with minor ankerite), and that the dolostone was a mixture of calcite and dolomite (with minor quartz). The glacially derived suspended sediment contained a mixture of, calcite, dolomite, gypsum and quartz (with minor sanidine).

The $\delta^{13}C$ of carbonate in rock and sediment samples and the $CaCO_3$ (Fisher Chemicals) used in the weathering experiments (see Section 4.3.3.) was also determined. Weighed, powdered samples were reacted under vacuum with 100% H_3PO_4 to liberate CO_2 from any carbonate minerals present in the sample (McCrea, 1950). The isotope ratio of the CO_2 was determined on a Finigan Mat 252 Mass Spectrometer and values are reported relative to V-PDB. Duplicate analyses were undertaken for all samples, following the full analytical procedure using separate reaction vessels for each aliquot. The range between duplicates was 0.2 ‰.

4.3.1.4. $\delta^{34}S$ analysis

0.25 l – 10 l samples were taken from supraglacial, marginal and subglacial streams in 1998 and vacuum filtered through 0.45 μm cellulose nitrate filter membranes into opaque polyethylene bottles and stored at 4°C. In the laboratory, the samples were passed through anion exchange resin (Bio-Rad AG-1-X8) to trap the SO_4^{2-}. It was necessary in some cases to combine 2-4 daily samples to provide sufficient SO_4^{2-} to obtain a $\delta^{34}S$-SO_4 analysis. Samples of gypsum, both as bedrock nodules and reprecipitated salts, were powdered for isotopic analysis. XRD analysis confirmed the samples to be pure gypsum.

Unweathered pyrite chips were hand picked from crushed shale. Extraction of the SO_4^{2-} from the ion exchange columns and all isotopic analysis of the waters and rock powders for $\delta^{34}S$ were performed at the Environmental Isotope Laboratory, University of Waterloo, (for full details of methods see Heemskerk (1993)).

4.3.2. Haut Glacier d'Arolla

4.3.2.1. Water sampling

Discharge is monitored continuously during May through September at a weir operated by Grande Dixence (GDSA), some 1 km from the glacier terminus (Fig. 4.1 b). The precision and accuracy of these measurements is ~ 5%. Bulk meltwater runoff was sampled during 1994 on May 21st (JD 141), May 23rd (JD 143), July 24th (JD 205) and August 18th (JD 230) at least four times each day, c. 200m from the glacier terminus (Fig. 4.1 b). In total, some 3 l of bulk runoff was collected on each occasion. 100 ml was vacuum filtered through 0.45 µm membrane filters and stored in 2 x 50 ml PVC bottles, one for anion analysis and the other for alkalinity titration. 1.8 l of meltwater was syringe filtered through a 0.45 µm filter membrane into a graduated HDPE gas-seal bottle, to which 200 ml of 4 g l^{-1} NaOH, saturated with $Sr(OH)_2$ by addition of $SrCl_2$ (400 g l^{-1} as Sr), stabilising solution was added. This sample was used for $\delta^{13}C$-DIC determination. Individual aliquots of 100 ml were collected by drawing water into the syringe, and the total time required for filtration was ~ 1 hour. Hence the samples collected for anion analyses were not exactly coincident with the $\delta^{13}C$-DIC sample.

Alkalinity (HCO_3^-) was determined by titration to endpoint 4.5 using 0.01 M HCl and BDH 4.5 indicator. The precision of measurement is dependent on titre volume, and is typically ± 1% for the values reported herein. The HCO_3^- concentration was determined from the alkalinity after correcting for the H^+ needed to acidify the combined sample and titre volume to pH 4.5. A Dionex 4000i was used for determination of SO_4^{2-} by ion chromatography. Detection limits were ~ 0.1 µeq l^{-1}, and precision of determinations was ± 3 % at concentrations > 50 µeq l^{-1}.

In situ subglacial meltwaters were sampled from the base of boreholes (see Fig. 1b) on August 16th and 19th, 1994 (JD 228 and 231 respectively), from Hole 74 (JD 228 and 231) and 68 (JD 231). Full details of borehole sampling can be found in Lamb et al., (1995) and Tranter et al., (in press). Subglacial meltwaters were treated as above.

4.3.2.2. Rock samples

Twelve samples of different rock types were collected from the western, median and eastern moraines, and the proglacial plain. These include amphibolite, calc silicate, felspathic and amphibolitic gneisses and mica-schist (see Appendix 4.1).

4.3.2.3. δ^{13}C-DIC and rock samples

The δ^{13}C-DIC, largely $HCO_{3\,(aq)}^-$, was determined as follows. The 2 l of stabilised solution was added to a 2.1 l spherical glass vessel that contained 20 ml of 100 % phosphoric acid and had been otherwise evacuated. The vessel was attached to a vacuum preparation line and the CO_2 was separated from the water during distillation of the whole sample. The CO_2 gas was cryogenically purified and frozen into a cold finger of accurately known volume, and the yield was determined using a capacitance manometer. The δ^{13}C of carbonate in rock samples was determined using the same methods as for the John Evans Glacier rock samples.

All CO_2 gases produced were analysed isotopically on a VG SIRA 10® Isotope Ratio Mass Spectrometer. Standard correction procedures were used (Craig, 1957) and the results are reported relative to the V-PDB standard. Precision was ± 0.5 ‰ for the water and ± 0.1 ‰ for the rock analyses.

4.3.3. Laboratory free drift weathering experiments

A series of free drift weathering experiments was undertaken to investigate whether kinetic isotopic fractionation was occurring during CH (Equation 6) or CD (Equation 4) driven by CB (Equation 2). The experiments were carried out using pure, powdered $CaCO_3$ and subglacially derived sediments, under both closed and open system conditions. Open system experiments had free access to the atmosphere throughout. Closed system experiments were conducted in water filled sealed bottles, preventing exchange with the atmosphere. Effectively, the closed system conditions provide a measure of the isotopic fractionation associated with CH, whereas the open system conditions provide a measure of that associated with CH, CD and CB.

Initial experiments using $CaCO_3$ powders with concentrations in the range (0.01 – 10 g l^{-1}) demonstrated that the solutions remained in chemical equilibrium with the overlying atmosphere at concentrations < 0.1 g l^{-1} (Sharp, unpublished data). At concentrations > 0.1 g l^{-1}, the solutions initially exhibited low PCO_2 values, returning to equilibrium on a time scale of days. At concentrations > 0.5 g l^{-1}, the variability in SI_{cc} and PCO_2 through time was independent of sediment concentration. Hence, sediment concentrations of 0.01 g l^{-1} and 5 g l^{-1} were chosen to examine the isotopic behaviour of carbonate dissolution in systems with both equilibrium and disequilibrium PCO_2 values. These values also cover the range of suspended sediment concentrations observed in the field at John Evans Glacier (Skidmore, 1995) and Haut Glacier d'Arolla (Brown et al., 1994).

Three sets of weathering experiments were undertaken, using glacially derived suspended sediment from John Evans Glacier at concentrations of 5 g l^{-1} under both open and closed system conditions, and 0.01 g l^{-1} under open system conditions only. Three parallel sets of experiments were performed under the same conditions using powdered $CaCO_3$ instead of glacial suspended sediment. Ten bottles were prepared for each set of experiments, one for each time step, (1, 2, 5, 10, 20, 60, 120, 360, 1440 and 10040 minutes). Grain size analysis of the < 300 μm fraction of sediment derived from debris-rich basal ice using a Sedigraph (Micromeritics 2000) revealed only grains < 50 μm. The

< 63 μm fraction of $CaCO_3$ and glacial sediment was therefore used in weathering experiments to simulate conditions analogous to those at the glacier bed. To remove any organic carbon and to sterilise the samples, all powders were combusted overnight at 550°C. Prior to the experiment, the polypropylene bottles were triple rinsed with 0.2 μm filtered deionised water and filled brim full (c. 300 ml), capped and placed in the fridge to cool to ambient temperature, ~5°C. For the experiments that were open to the atmosphere, 100 ml of water was decanted prior to addition of the sediment to minimise spillage during subsequent shaking. The sediment was added to the bottles and placed in a gyratory shaker at 200 rpm in the fridge. After the requisite time had elapsed, the samples were immediately vacuum filtered through 0.45 μm cellulose nitrate filter membranes. pH was determined as above and samples for $\delta^{13}C$ analysis were transferred to either autoclaved 45 ml EPA vials or autoclaved 120 ml serum bottles and stored at 4°C prior to analysis. $\delta^{13}C$ – DIC was determined using the same methodology as for John Evans Glacier waters, (Section 4.3.1.2.). Major anion and cation concentrations were determined by ion chromatography (Skidmore and Sharp, 1999). Alkalinity was determined by charge balance from the ion chromatography results, and DIC speciation and PCO_2 values for the water analyses were computed using PHREEQC (Parkhurst and Appelo, 1999).

4.3.4. $\delta^{13}C$-DIC geochemical and biogeochemical models

Discussion of the results obtained from both the field and the laboratory experiments requires the calculation of a range of theoretical values for $\delta^{13}C$ - DIC based on current understanding of the chemical weathering mechanisms and likely isotope fractionation factors. Disagreement between the calculated and measured values may indicate that either the isotope fractionation factors or understanding of the chemical weathering mechanisms are incorrect. The following sections (4.3.4.1.- 4.3.4.7) outline the weathering reactions involved in the geochemical models, including specific model assumptions.

4.3.4.1. Weathering processes and $\delta^{13}C$ - DIC

The averaged $\delta^{13}C$ value of atmospheric CO_2 for the period 1990-1993 is -7.8 ‰ (Trolier et al., 1995). Therefore, with a ~ +10 ‰ equilibrium fractionation ($\varepsilon_{HCO3\text{-}g}$) at 0°C, the $\delta^{13}C$ of DIC in glacial meltwaters will gradually approach a value of ~ +2.2 ‰ on full chemical and isotopic re-equilibration with the atmosphere, irrespective of the original carbon source. The following discussion assumes that re-equilibration with the atmosphere is limited. This assertion is supported by data showing that glacial meltwaters are typically out of equilibrium with respect to atmospheric CO_2 (Raiswell and Thomas, 1984; Tranter et al., 1993; Fairchild et al., 1994; Skidmore, 1995; Anderson et al., 1999), and therefore must carry some information about DIC sources and the fractionations associated with weathering processes. SO, CH, CB and CD have been identified as the major weathering reactions in glacial environments (see Section 4.1.1.). By estimating the proportion of solute that arises from each of these reactions, it is possible to calculate theoretical values for $\delta^{13}C$ – DIC in the meltwaters.

4.3.4.2. Carbonate hydrolysis and carbonation of carbonates.

The dissolution of carbonates occurs in two stages. The first stage is CH, (Equation 6) which occurs without acid input, followed by CD which is driven by protons derived from either carbonic acid (Equation 4) or SO (Equation 1). CO_2 required to form carbonic acid is derived either from atmospheric (CB), (Equation 2) or microbial sources, (MR), (Equation 3). In glacial systems, especially subglacial environments, re-equilibration with the atmosphere following CH may be physically and kinetically limited, as indicated by non-equilibrium PCO_2 values in glacial runoff. Moreover, CD in subglacial environments may be limited to that driven by SO, unless there is a large microbial CO_2 source, since access to the atmosphere is restricted. The geochemistry of subglacial borehole waters from Haut Glacier d'Arolla suggests that little atmospheric CO_2 is used in subglacial chemical weathering, and that CH and SO-CD are the dominant weathering processes (Tranter et al., in press). This finding is partially supported by the PCO_2 data in this study (Fig. 3b) which indicate that the subglacial waters have PCO_2 values greater than

atmospheric. This suggests that evolution of subglacial waters occurred under "closed system" (as defined by Tranter et al., 1993) conditions. In the subsequent model simulations, a scenario for this "closed system" at Haut Glacier d'Arolla is included. (Section 3.4.5.).

4.3.4.3. Contribution of protons via sulphide oxidation (SO)

There are two potential sources for dissolved SO_4^{2-}, the atmosphere and weathered catchment minerals. At Haut Glacier d'Arolla, the majority of the SO_4^{2-} is derived from sulphide oxidation (Sharp et al., 1995). SO is coupled to CD (Equations 1 and 4) such that an equal amount of DIC in μeq l^{-1} is produced from CD for every μeq l^{-1} SO_4^{2-} from SO. The DIC produced is assumed to have a bedrock carbonate $\delta^{13}C$ value.

At John Evans Glacier, there is an additional SO_4^{2-} source from anhydrite/gypsum. The proportion of SO_4^{2-} from sulphide oxidation in the marginal and subglacial streams is calculated as follows, after correcting for the atmospheric component using isotope mass balance (Equation 8). The SO_4^{2-} concentrations in supraglacial streams in 1998 were low (< 7 μeq l^{-1}) and $\delta^{34}S$ was 21.7 ‰. This SO_4^{2-} input is assumed to be derived from atmospheric sources. Hence, the daily values for the marginal and subglacial stream waters were corrected for atmospheric SO_4^{2-} input by subtracting the product of the supraglacial SO_4^{2-} value measured on that day and the $\delta^{34}S$ value (Equation 8). Partitioning the SO_4^{2-} between the two remaining sources, GD (Equation 7) and SO (Equation 1) is also accomplished by simple isotope mass balance (Equation 8).

$$\delta_{(aq)}[SO_4^{2-}{}_{(aq)}] - \delta_{(atm)}[SO_4^{2-}{}_{(atm)}] = \delta_{so}[SO_4^{2-}{}_{so}] + \delta_{gyp}[SO_4^{2-}{}_{gyp}] \quad (8)$$

where square brackets denote concentration in μeq l^{-1}, the subscript $_{aq}$ denotes the value measured in either the marginal or subglacial stream, and the subscripts $_{atm}$, $_{so}$ and $_{gyp}$ denote an atmospheric, sulphide or gypsum source, assuming that $\delta_{(atm)} = 21.7$ ‰ (n = 1), $\delta_{so} = -5.2$ ‰ (n=2) and δ_{gyp} is +31 ‰ (n=5) and that SO_4^{2-} is not utilised by microbial activity. The gypsum value is within the range reported for Ordovician gypsum (+27 – 31

‰) (Clark and Fritz, 1997). Solution of Equation 8 suggests that SO produced 6.4 – 9.6 % of the SO_4^{2-} in the subglacial stream and 26 - 38 % in the marginal stream.

4.3.4.4. Subglacial carbonate precipitation

In glacial catchments, the majority of solute acquisition occurs in subglacial environments. These are generally characterised by high water:rock ratios and relatively long water-rock contact times. In certain cases mineral precipitation may occur subglacially, either due to freezing of the waters (e.g. Hallet, 1976) or possibly through mixing of waters of different chemical compositions (Skidmore, unpublished data). The potential effect of subglacial precipitation on δ^{13}C-DIC of the outflowing waters is discussed below. Supraglacial meltwaters are generally dilute since there is limited water rock interaction and suspended sediment concentrations are low (< 0.01 g l^{-1}). However, at John Evans Glacier, some supraglacial streams are fed by ice-marginal lakes that are in turn fed by ice-marginal channels draining across carbonate bedrock. These streams typically have a higher solute content than those that are fed solely by supraglacial runoff (K. Heppenstall, personal communication). Hence the waters that flow into the subglacial environment are a mixture of solute rich and solute poor waters. The more solute-rich inflowing waters have PCO_2 values below atmospheric (K. Heppenstall, personal communication) and a geochemistry similar to the more dilute marginal stream waters, reflecting CH and CB-CD as the main solute acquisition processes. Therefore, supraglacial δ^{13}C-DIC values are likely to be similar to dilute marginal stream waters (Fig. 4.2).

Major ion chemistry indicates that significant quantities of dolomite and gypsum are dissolved in the subglacial environment (Skidmore 1995, Skidmore and Sharp 1999). These reactions, predominantly dolomite dissolution, both drive down the PCO_2 and, through the common ion effect, drive $SI_{cc} > 0$, presumably resulting in calcite precipitation in the subglacial environment. This limits the amount of DIC in subglacial waters (Skidmore, 1995). Experimental work indicates that at isotopic equilibrium, calcite precipitation produces δ^{13}C values that are 0.6 ‰ heavier than δ^{13}C-DIC at 0°C

(Mook et al., 1974). However, the fractionation approaches 0 ‰ under non-equilibrium conditions (Dandurand et al., 1982). Therefore, the δ^{13}C-DIC in the outflow will be unchanged or lighter than the inflowing solution as a result of precipitation processes.

4.3.4.5. Bedrock carbonate $\delta^{13}C$ variability

Mean values for the δ^{13}C of carbonate bedrock in the John Evans Glacier catchment are –0.2 ± 0.05 ‰ and +0.7 ± 0.05 ‰ for calcite and dolomite respectively. By contrast, the δ^{13}C value of carbonates in the < 63 μm fraction of the subglacially derived suspended sediment is –1.6 ± 0.05 ‰ and –2.7 ± 0.05 ‰ for calcite and dolomite respectively. In 1998, the Ca:Mg ratios in the marginal and subglacial streams were 15:1 and 4:1 respectively (after correction for Ca derived from gypsum dissolution), indicating the dominance of calcite weathering. In the following calculations for John Evans Glacier, we assume that the carbonate being chemically weathered at John Evans Glacier has a δ^{13}C value of -0.9 ‰, (the mean of the two calcite values). This assumption may be in error by ~ ±1.6 ‰.

The amount of $CaCO_3$ in the different rock types in the Arolla catchment is variable, ranging from < 0.005 – 0.58 wt %, 12 samples. Isotopic determinations were possible at concentrations > 0.08 wt %, and the δ^{13}C of the $CaCO_3$ ranges from -0.9 to -6.6 ‰ (Appendix 1). The modal value is in the range of -2.4 ‰ to -2.7 ‰, and the mass weighted mean δ^{13}C value is -2.4 ‰. The latter value is used in subsequent calculations for Haut Glacier d'Arolla.

4.3.4.6. Model assumptions

The reactions included in models 1-5 are tabulated below.

Model	Reactions
1	SO-CD + CB-CD
2	SO-CD + MR-CD
3	CH + SO-CD + MR-CD
4	CH + SO+CD + MR-CD relative to M3
5	SO-CD + x(MR-CD) + (1-x) (CB-CD) where $0 < x < 1$

and indicate increases and decreases in the proportion of DIC from an individual weathering reaction.

The following assumptions apply to the geochemical model (M1; Equation 9), biogeochemical model (M2; Equation 10), and carbonate hydrolysis biogeochemical model, (M3; Equation 11 Haut Glacier d'Arolla only);

- bedrock carbonate ($\delta^{13}C$ = -0.9 ‰ for John Evans Glacier or $\delta^{13}C$ = -2.4 ‰ for Haut Glacier d'Arolla),
- atmospheric CO_2 ($\delta^{13}C$ = -7.8 ‰ – the averaged atmospheric value for 1990-1993; Trolier et al., 1995),
- microbial CO_2 ($\delta^{13}C$ = -25 ‰ an average value for photosynthetic algae (Hoefs, 1980), which is similar to the average $\delta^{13}C$ value of two analyses of OC from basal ice at John Evans Glacier (-23.2 ‰)).
- ε_k = -1 ‰ (Zhang et al., 1995).
- Initially, no equilibrium fractionation is assumed and $\varepsilon_{HCO3\text{-}g}$ is set as 0 ‰ to derive the lowest possible $\delta^{13}C$-DIC values.

M1-3 assume that for each equivalent of SO_4^{2-} derived from sulphide oxidation, $(SO_4^{2-})_{so}$, 1 equivalent of HCO_3^- is released from the dissolution of carbonate (Equations 1 and 3) with a $\delta^{13}C$ of the bedrock carbonate ($r\delta^{13}C$). Of the remaining HCO_3^-, half comes from the bedrock carbonate ($r\delta^{13}C$) and half comes from the atmosphere (M1) or microbial oxidation of organic matter (M2) (Equation 2). In M3, the initial 190 μeq l^{-1} DIC are

from CH (as predicted by PHREEQC), with a $\delta^{13}C$ of the bedrock carbonate ($r\delta^{13}C$). Half of the remaining DIC comes from bedrock carbonate ($r\delta^{13}C$) and half from microbial oxidation of organic matter.

Initially, the CO_2 that diffuses into solution (M1) will probably only exhibit kinetic isotopic fractionation (ε_k -1 ‰) and hence is likely to have an "atmospheric" $\delta^{13}C$ value of - 8.8 ‰ (M1-atmospheric source) and – 26 ‰ (M2-microbial source). These modelled values provide end member scenarios, which produce the lightest feasible $\delta^{13}C$–DIC values, assuming that, initially, there is insufficient time for isotopic equilibration between HCO_3^- and atmospheric CO_2 (i.e. $\varepsilon_{HCO3\text{-}g} = 0$). Over time and with free contact with the atmosphere, equilibration will occur and $\varepsilon_{HCO3\text{-}g}$ will increase to the equilibrium value, + 10 ‰, producing $\delta^{13}C$ –DIC values heavier than those modelled.

Modified biogeochemical models (M4) (Equation 12) and (M5) (Equation 13) are used to predict the observed $\delta^{13}C$–DIC values using isotope mass balance. In M4, the proportion of DIC from CH is reduced from 190 μeq l^{-1} and the proportion from MR-CD is increased commensurately. In M5, a proportion of the non-bedrock DIC is from a microbial source and the remainder from an atmospheric source.

4.3.4.7. Physical environments represented by models 1-5

The different hydrological environments at Haut Glacier d'Arolla and John Evans Glacier represent a range of physical environments in which $\delta^{13}C$-DIC may be affected by varying degrees of contact between water and atmospheric gases (sections 4.2.1.2. and 4.2.2.2.). Hence, there is unlikely to be one single model that describes all environments. Although modelled environments are unlikely to be exactly analogous to glacial environments, it is however possible to identify the closest analogues. Both M1 and M2 are "end member" scenarios since they assume chemical equilibrium conditions, which are apparently infrequent in glacial systems. M1 assumes free access to atmospheric CO_2, and represents marginal stream conditions (at John Evans Glacier). M2 represents conditions in a "closed system" subglacial environment from which atmospheric CO_2 is

excluded and only microbial CO_2 is available. M3 represents a "closed system" subglacial environment similar to M2. However M3 assumes staged chemical evolution of waters; CH occurs initially, followed by SO-CD, and finally by MR-CD. M4 is a model intermediate between M2 and M3, where the magnitude of CH is reduced and the component of MR-CD is increased commensurately in order to match the predicted $\delta^{13}C$–DIC with the measured $\delta^{13}C$–DIC value. M5 is similar to M2, but it simulates conditions under which "closed system" subglacial waters are exposed to the atmosphere and additional DIC is generated by CB-CD from the influx of atmospheric CO_2.

Model 1, Geochemical model

$$\delta^{13}C\text{-DIC} = \frac{r\delta^{13}C(S) + [(r\delta^{13}C - 8.8)/2][DIC\text{-}S]}{DIC} \quad (9)$$

Model 2, Biogeochemical model

$$\delta^{13}C\text{-DIC} = \frac{r\delta^{13}C(S) + [(r\delta^{13}C - 26)/2][DIC\text{-}S]}{DIC} \quad (10)$$

Model 3, CH biogeochemical model

$$\delta^{13}C\text{-DIC} = \frac{r\delta^{13}C(CH) + r\delta^{13}C(S) + [(r\delta^{13}C - 26)/2][DIC\text{-}(S+CH)]}{DIC} \quad (11)$$

Model 4, Modified CH biogeochemical model

$$\delta^{13}C\text{-}DIC = \frac{r\delta^{13}C(CH) + r\delta^{13}C(S) + (1-a)[(r\delta^{13}C-26)/2][DIC\text{-}S] + a(r\delta^{13}C)[DIC\text{-}S]}{DIC} \quad (12)$$

Where $0 < a < 1$

Model 5, Modified biogeochemical model

$$\delta^{13}C\text{-}DIC = \frac{r\delta^{13}C(S) + x[(r\delta^{13}C-26)/2][DIC\text{-}S] + (1-x)[(r\delta^{13}C-8.8)/2][DIC\text{-}S]}{DIC} \quad (13)$$

Where $r\delta^{13}C$ is the $\delta^{13}C$ value of the bedrock carbonate, S is the concentration of DIC derived from SO-CD, CH is the concentration of DIC derived from CH and x is the fraction of microbial CO_2 required to simulate the measured $\delta^{13}C$–DIC values.

4.4. RESULTS

4.4.1. Field data

4.4.1.1. John Evans Glacier

Fig. 2 shows the $\delta^{13}C$-DIC time series for John Evans Glacier. Both the marginal and subglacial $\delta^{13}C$-DIC values are significantly lighter than bedrock $\delta^{13}C$ values and, to a lesser degree, lighter than atmospheric CO_2. Marginal stream values are relatively constant at around – 9 ‰. By contrast, subglacial waters are lighter (average = -13.5 ‰ range -12 to – 15.7 ‰) early in the season, with an almost stepwise change to heavier values after JD 193 (average =-10.8 ‰ range -8.5 to –13 ‰). The change to heavier values correlates with an increase in DIC of the subglacial waters (Table 4.1).

4.4.1.2. Haut Glacier d'Arolla

Fig. 4.3 a shows the association between discharge and δ^{13}C-DIC in the runoff for each sampling day during the meltseason. The range in discharge is from 0.14 m^3 s^{-1} in May (JD 141), when discharge is almost constant and dominated by snowmelt, to 5.1 m^3 s^{-1} in July (JD 205), when discharge increases by ~2 m^3 s^{-1} during the day and is dominated by ice melt. δ^{13}C-DIC values range from -4.0 to -7.5 ‰ during May, from -4.0 to -8.2 ‰ during July and from –2.6 to -3.8 ‰ in August. In all cases there is a trend to lighter δ^{13}C-DIC values later in the day. For JD 143, 205 and 230, this isotopic trend can be clearly linked to increasing discharge. The diurnal range in both discharge and δ^{13}C-DIC is smaller on JD 143 than on JD 205. However, it is difficult to generalise that δ^{13}C–DIC changes are related to discharge changes from only these two diurnal surveys. The bulk meltwater δ^{13}C-DIC values range mainly between the bedrock value –2.4 ‰ and the atmospheric CO_2 value –7.8 ‰ (-8.8 ‰, if ε_k = -1 ‰). However, the borehole water δ^{13}C-DIC values (Table 4.1) are either close to, or lighter than the atmospheric δ^{13}C-CO_2 value.

4.4.2. δ^{13}C–DIC values predicted using geochemical/biogeochemical models

The range of δ^{13}C-DIC values measured in the glacial meltwaters is summarised in Table 1. For comparison, Table 1 also shows the range of δ^{13}C-DIC values predicted using Models 1-5. The predicted values are compared with the observed values to identify those models that most accurately simulate the observed data. If the predicted values are within 0.5 ‰ (the analytical error in δ^{13}C-DIC determination) of the measured values then a particular model is assumed to provide a plausible, but not necessarily unique, explanation of the observation. All measured values are lighter than the full chemical and isotopic equilibrium value of 2.2 ‰. Hence, if the measured δ^{13}C-DIC value is heavier than the predicted value for a particular model, it is possible that the model could describe the chemical weathering processes that have occurred so long as a degree of isotopic equilibration (i.e. $\varepsilon_{HCO3\text{-}g} > 0$) has occurred.

4.4.2.1. John Evans Glacier

For John Evans Glacier, M1 produces δ^{13}C-DIC values that are significantly heavier (average = - 4.7 ‰) than the measured values in both the marginal (average = - 8.8 ‰) and subglacial waters (average = - 12.0 ‰). This indicates that M1 cannot be used to account for the measured values. For the marginal stream, M2 produces values that are all lighter than the measured values, whereas M5 implies that for marginal stream waters 32-63 % of the non-bedrock C has to be derived from microbially produced CO_2. For subglacial waters, M2 produces values that are heavier than measured values for early melt season waters. In these cases, M5 predicts that 100 % of the non-bedrock C has to be derived from microbially produced CO_2, but to achieve isotope mass balance, δ^{13}C-microbial CO_2 values as light as –55 ‰ are required. Such light isotopic values could only realistically be produced by the oxidation of CH_4. Later in the season, M5 predicts that 50-100 % of the non-bedrock C has to be derived from microbially produced CO_2 ($\delta^{13}C$ = –26 ‰). M3 assumes closed system evolution of waters without atmospheric input and therefore, was only applied to the subglacial waters, producing a wide range of δ^{13}C-DIC values. Generally, predicted values are lower than measured, especially early in the meltseason. Only on JD 193 is the predicted value lighter than measured and therefore, M4 is applied to the JD 193 case to achieve isotope mass balance.

4.4.2.2. Haut Glacier d'Arolla

M1 predicts δ^{13}C-DIC values that are generally heavier than the measured values, though the difference is less than for John Evans Glacier. M2 predicts values that are lighter than those measured. M3 accurately predicts morning values for each of the sampling days during the meltseason. However the predicted afternoon values do not decline sufficiently to match the observed values. M4 predicts increased microbial CO_2 as a proportion of DIC later in the day, and in some cases the afternoon values are greater than double the morning values. Using M5, the amount of microbially produced CO_2 required is, on average, greater earlier in the season, and it shows some systematic diurnal variability, increasing later in the day. The late season (August) waters provide the only case in either

the John Evans Glacier or Arolla datasets where the observed δ^{13}C-DIC values are heavier than the M1 predictions. M5 suggests that all borehole waters require a significant proportion of microbially produced CO_2, and in one case, the requisite δ^{13}C of the microbial CO_2 (–28.7 ‰) is lighter than –26 ‰.

4.4.2.3. Interpretation of δ^{13}-DIC data based on Bio- and geochemical models

Clearly neither M1 nor M2 simulate realistic δ^{13}C–DIC values for the glacial meltwaters at either John Evans Glacier or Haut Glacier d'Arolla. At Haut Glacier d'Arolla M3 is the most realistic model based on the geochemical data and it produces plausible δ^{13}C-DIC values for the morning samples. In these cases ~ 12 % of DIC is from microbial CO_2 early in the season and ~ 4 % later in the season. Such proportions of microbial CO_2 do not seem unreasonable at low diurnal discharges. However, the doubling of microbial CO_2 input later in the day that is required to achieve isotope mass balance, as simulated in M4, would require more than a four-fold increase in the microbial CO_2 flux due to the accompanying rise in discharge.

From first principles, M3 seems the most appropriate model for simulating the geochemical evolution of the subglacial waters at John Evans Glacier. However, the simulated δ^{13}C–DIC values are generally significantly lower than the measured values. Where applicable, M4 and M5 both indicate that a substantial amount of microbially-derived CO_2 is required to produce the observed δ^{13}C–DIC values in both the marginal and subglacial streams at John Evans Glacier. Similarly, at Haut Glacier d'Arolla, the model results suggest that microbial CO_2 may be an important component of the DIC budget for the borehole waters. The seasonal trend for bulk meltwaters indicates that the microbial input may be greater early in the melt season. Throughout the meltseason at Haut Glacier d'Arolla there is also a diurnal trend, where afternoon waters, usually associated with increased discharges, require increased microbial CO_2 input. It is, however, difficult to explain the microbial CO_2 input required by M4 or M5 for the following reasons.

1. At John Evans Glacier there is a significant mismatch between M3, M4 and M5 isotopic predictions and the geochemical data. The average subglacial water chemistry data (DIC ~ 250 μeq l^{-1} and $PCO_2 = 10^{-5}$ to 10^{-4}) indicates that CH is the dominant weathering process. Therefore, from first principles M3, which assumes CH, SO-CD and MR-CD as the sequence of weathering reactions is the most appropriate geochemical model, however, the simulated $\delta^{13}C$–DIC values are often far from the measured values. M5 produces an isotopic mass balance, however, the weathering reaction sequence SO-CD, MR-CD and CB-CD and no CH seems physically untenable in the subglacial environment at John Evans Glacier. The bedrock underlying the glacier is dominated by carbonate and as is common in subglacial environments, finely comminuted bedrock carbonate is likely present. The kinetics for CH are extremely rapid relative to the other weathering mechanisms and it seems unlikely that no CH will occur in the subglacial environment where freshly ground carbonate is likely abundant, as demonstrated by suspended sediment concentrations of ~ 1 g l^{-1} in subglacial runoff, which is predominantly carbonate.

2. At Haut Glacier d'Arolla, the trend to lighter values at higher discharges later in the day is hard to account for by microbial means. Theoretically, it is possible to account for the observations either by either increased rates of microbial CO_2 production or via flushing of a microbial CO_2 rich reservoir.

   Later in the day, a greater proportion of the water in the bulk meltwaters is ice melt routed through major channels (residence times < ~ 0.5-2 hrs). Thus, extremely rapid rates of microbially mediated weathering would be required to produce a fourfold increase in the microbial CO_2 flux in the quickflow waters. Significant bacterial populations 10^6 ml^{-1} have been observed in Haut Glacier d'Arolla bulk meltwaters and subglacial borehole waters, of which 5-24 % are dividing (Sharp et al., 1999). It is inferred (Sharp et al., 1999) that these bacteria are active at the glacier bed, however, no data exist on rates of microbial CO_2 production in these environments. To produce the modelled increase in microbial CO_2 input of 22 μM, required to balance the $\delta^{13}C$-DIC values, a rate of 5.5 μM CO_2 g^{-1} hr^{-1} is necessary (assuming a sediment concentration of 5 g l^{-1}). Experimental work using subglacial sediments has

demonstrated rates of microbial CO_2 production of 100 μM CO_2 kg^{-1} yr^{-1} at 0.3°C, which translates to a rate of 0.00001μM CO_2 g^{-1} hr^{-1} (Skidmore et al., 2000). Therefore, the required rates at Haut Glacier d'Arolla are 5 orders of magnitude higher than have been measured at similar ambient temperatures, which is a key factor determining microbial CO_2 production rates in cold environments (e.g. Sagemann et al., 1998; Rivkina et al., 2000). It is acknowledged that there are differences in the boundary conditions in the laboratory experiments relative to the field situation, in terms of sediment concentration and composition and the turbulent nature of the field environment. However, these are unlikely to account for the 5 orders of magnitude difference in rates.

The distributed system is believed to provide the most viable subglacial microbial habitat, due to the low water flow rates and high rock:water ratios, which facilitates high chemical weathering rates and thus microbial nutrient supply (Tranter et al., in press). The flushing of high microbial CO_2 waters from the distributed system may theoretically provide a mechanism for the increased CO_2 flux, however, it is unclear whether a large enough subglacial CO_2 reservoir exists. Furthermore, at maximum discharges it has been demonstrated that the hydraulic gradient forces water from the channelised system into the distributed system rather than vice versa (Hubbard et al., 1995). Thus, flushing of microbial CO_2 from a reservoir in the distributed system under high discharge conditions seems unlikely.

3. The simulations all assume that $\varepsilon_{HCO3\text{-}g}$ is zero, i.e. that no isotopic equilibration with the atmosphere has occurred. However, the John Evans Glacier waters all have PCO_2 values in the range 10^{-5} to 10^{-4} atm, an order of magnitude higher than those generated by CH, indicating that partial chemical re-equilibration has likely occurred. Szaran, (1997) demonstrated experimentally that isotopic equilibration begins simultaneously with chemical equilibration. Therefore, a degree of isotopic equilibration in natural systems may be expected, especially since the rate of isotopic equilibration is initially rapid, slowing as equilibrium is approached (Szaran, 1997). If partial isotopic equilibration has occurred in conjunction with chemical equilibration, then with all other variables held constant, the amount of isotopically light CO_2

required to produce the measured values would have to be increased. Unfortunately, it is not possible to quantify the degree of isotopic equilibration, and therefore the increases in microbial CO_2 necessary to balance this process.

4.4.2.4. Summary

Generally, all the models fail to explain adequately the light isotopic values that are measured in the field. Hence, it appears that either the geochemical model of weathering in glacial environments or the assumptions about the major processes determining the $\delta^{13}C$ values are incorrect or incomplete. The basic geochemical model has been applied successfully to glacial meltwaters draining a variety of bedrock lithologies, yielding similar interpretations of the weathering processes (Raiswell, 1984; Raiswell and Thomas, 1984; Tranter et al. 1993; in press; Anderson, 1999; Sharp et al., submitted). Therefore, it seems more likely that the assumptions (section 4.3.4.6) about the processes controlling the $\delta^{13}C$ values are incorrect or incomplete.

In addition to microbial CO_2, it seems likely that there may be other geochemical processes that produce isotopically light $\delta^{13}C$-DIC. At Haut Glacier d'Arolla, light isotopic values are observed when discharge is high and subglacial water residence times are short. This suggests that light $\delta^{13}C$-DIC values are associated with rapid processes of solute acquisition. Since the PCO_2 of these waters indicate that they are significantly out of chemical equilibrium, there may be kinetic isotopic effects that are not included in the models, but which could be important for interpretation of the $\delta^{13}C$ data. A series of weathering experiments was undertaken to investigate the possible effects of these processes on $\delta^{13}C$–DIC (see Section 4.4.3.3. for experimental methods).

4.4.3. Free drift weathering experiments

4.4.3.1. Alkalinity variations

The ~ 220 to 260 μeq l^{-1} of alkalinity produced in the first minute of all the 5 g l^{-1} experiments demonstrate CH as the initial weathering reaction (Fig 4.4 a). In the closed system $CaCO_3$ experiment no additional alkalinity is produced after the first minute, indicating that only calcite hydrolysis occurred. In the 5 g l^{-1} closed system sediment experiment, alkalinity increased from 1-5 minutes, but remained reasonably constant thereafter. This suggests that both calcite and dolomite hydrolysis occurred initially and then no further weathering occurs. In the open system 5 g l^{-1} experiments, the increases in alkalinity following CH reflect CB-CD as the main weathering process. In the $CaCO_3$ experiment alkalinity concentrations reached a plateau at ~1300 μeq l^{-1} after 6 hours when solutions were close to calcite saturation. However, in the sediment experiment, alkalinity continued to rise beyond the 6 hour $CaCO_3$ experiment plateau. This reflects dolomite dissolution, since solutions were close to saturation with respect to calcite. Similarly in the 0.01 g l^{-1} open system experiments, CH was followed by CB-CD, with greater alkalinity concentrations produced by the sediment relative to the $CaCO_3$.

4.4.3.2. Chemical and isotope equilibrium

Fig. 4.4 b shows the temporal variation in PCO_2 during the weathering experiments. Both the closed system 5 g l^{-1} weathering experiments showed low PCO_2 values ($< 10^{-6}$ atm) for all time steps. The PCO_2 values were significantly lower for the sediment experiments than for the $CaCO_3$. The open system 5 g l^{-1} experiments initially showed low PCO_2 values similar to the closed system experiments. However, the values returned to equilibrium after 2 hours ($CaCO_3$) and 24 hours (sediment). The 0.01 g l^{-1} experiments for both $CaCO_3$ and sediment were essentially in chemical equilibrium with the atmosphere throughout.

Fig. 4.4 c, d and e show the temporal variations in δ^{13}C-DIC. The closed system experiments both showed significant negative departures from the isotopic equilibrium

value of -3.4 ‰, for all time steps (Fig. 4.4 c). The open system 5 g l^{-1} $CaCO_3$ experiment was close to chemical equilibrium after only 1 hour and equilibrium was attained after 2 hours (Fig. 4.4 b), but isotope equilibrium took > 6 hours and was achieved by 24 hours (Fig. 4.4 d). The 5 g l^{-1} sediment experiment was approaching chemical equilibrium after 6 hours, but isotope equilibrium took > 6 hours and was achieved by 24 hours (Fig. 4.4 d). Isotope equilibrium was achieved after 24 hours in the 0.01 g l^{-1} $CaCO_3$ experiment, (Fig. 4.4 e) but did not appear to be attained in the 0.01 g l^{-1} sediment experiment. These results confirm that isotope equilibrium significantly lagged chemical equilibrium in the open system experiments. Moreover, the 0.01 g l^{-1} experiments demonstrate that significant departures from isotope equilibrium can occur even when there is no departure from chemical equilibrium.

4.4.3.3. Isotopic fractionation.

In all experiments, regardless of sediment concentration and open/closed system characteristics, there was an initial marked decrease in $\delta^{13}C$-DIC values relative to the bulk carbonate ($CaCO_3$ $\delta^{13}C$ = -3.3 ‰, sediment $\delta^{13}C$ = -2.15 ‰) (Fig. 4.4 c, d, e). Thereafter, the open system 0.01 g l^{-1} and 5 g l^{-1} experiments all showed similar patterns of change in $\delta^{13}C$-DIC (Fig. 4.4 d and e). After the initial rapid decrease in the first minute, values became increasingly negative over the subsequent 5 - 60 minutes. They then slowly became more positive until isotopic equilibrium was reached after ~24 hours. In the 5 g l^{-1} experiments, the pattern of isotopic change through time was broadly similar for both the sediment and the $CaCO_3$. For the 0.01 g l^{-1} experiments, the secondary negative $\delta^{13}C$ shift was less prolonged and less pronounced than for the 5 g l^{-1} experiments. The $\delta^{13}C$ shift was greater for the sediment than for the $CaCO_3$ in all cases where sediment concentrations were the same.

The 5 g l^{-1} $CaCO_3$ experiment was the only one that clearly showed attainment of isotopic equilibrium after 24 hours. The equilibrium fractionation factor $\varepsilon_{HCO3\text{-}g}$, - the difference between the $\delta^{13}C$ of the fridge air (-13.8 ‰) and the equilibrium (24 hour) $\delta^{13}C$ value (-3.4 ‰) - for this experiment was 10.4 ‰, which is close to that (10.2 ‰) determined by

Mook et al. (1974) and Zhang et al. (1995) at 5°C. The 5 g l^{-1} sediment experiment was approaching isotopic equilibrium after 24 hours, but the continued addition of DIC from the dissolution of dolomite (Fig. 4a) with a $\delta^{13}C$ value of –2.7 ‰ likely accounts for the heavier than equilibrium value (~ -3.4‰).

4.4.3.4. $\delta^{13}C$ variations in relation to weathering reactions

4.4.3.4.1. Carbonate hydrolysis. It is evident from the PCO_2 and DIC data that the initial $\delta^{13}C$ departure is associated with the hydrolysis phase of carbonate dissolution, which occurs during the first minute of each experiment. These data also indicate that the sediment is initially more reactive than the $CaCO_3$, especially in the 5 g l^{-1} experiments. The greater reactivity of the sediment is likely due to smaller grain sizes in the glacial flour and/or abrasion features, such as strained/shattered crystal lattices caused by subglacial grinding of the sediments. The kinetic fractionation factor associated with hydrolysis of the carbonate (hereafter, ε_b) is –5.4 ‰ for $CaCO_3$ and –10.6 ‰ for the sediment. This kinetic bedrock fractionation (KBF) probably arises because $Ca^{12}CO_3$ weathers preferentially with respect to $Ca^{13}CO_3$, since less energy is required to break the molecular bonds of $Ca^{12}CO_3$. The larger negative fractionation for the sediment is likely due to the fact that the sediment is initially more reactive than the $CaCO_3$. It may also be due in part to the effect of dolomite hydrolysis. However, from the data it is not possible to determine individual fractionation (ε_b) values for calcite and dolomite hydrolysis.

4.4.3.4.2. Carbonation of carbonates. In both the 0.01 and 5 g l^{-1} open system experiments, $\delta^{13}C$-DIC values declined after one minute as the process of CB-CD began. The following analysis evaluates (a) whether this is due to a negative fractionation associated with CB-CD that is additional to the KBF identified above (see section 4.4.3.4.1.), and (b) if so, whether it is more likely associated with the bedrock carbonate or the influxing CO_2. To assess (a) the $\delta^{13}C$–DIC was predicted for the time steps from 5 – 360 minutes assuming that all bedrock DIC produced from both CH and CB-CD has a $\delta^{13}C$ value equal to the 1 minute (CH) $\delta^{13}C$ value (-12.8 ‰ for the sediment and – 8.7 ‰ for the $CaCO_3$). Following the stoichiometry of Equation 3, for every 2 moles of HCO_3^-

added to the DIC, one is from the atmosphere and one is from the bedrock carbonate. However, CH results in waters that have low PCO_2 values, high pH and thus a proportion of alkalinity exists as OH^- and CO_3^{2-}. A small portion of the influxing atmospheric CO_2 will serve to lower pH and change the alkalinity and thus DIC speciation, rather than to dissolve carbonate directly. DIC speciation for each time step (CO_3^{2-}, HCO_3^-, $CO_{2(aq)}$) and OH^- was determined using PHREEQC (Appelo and Parkhurst, 1999). The relative contributions of atmospheric CO_2 and bedrock carbonate to DIC were calculated by comparing the concentration of CO_3^{2-}, HCO_3^-, $CO_{2(aq)}$ and OH^- in successive time steps. After 1 minute, OH^- and CO_3^{2-} decreased, reflecting the dissolution of atmospheric CO_2, which lowered pH and increased PCO_2. This component of the DIC was assigned a $\delta^{13}C$–atmospheric CO_2 value. The remaining change in DIC was assumed to be from coupled CB-CD. $\delta^{13}C$-DIC values for the waters were predicted using the following isotope mass balance Equation (14) (Fig. 4.4 d).

$$\delta_{DIC}\,[DIC] = \delta_{ch}\,[DICch] + \delta_{atm}\,[DICatm] + \delta_{carb}\,[DICcarb] \qquad (14)$$

where [DICch] is DIC from CH, [DICatm] is DIC from equilibration of PCO_2, [DICcarb] is DIC from CB-CD. δ_{ch} is the $\delta^{13}C$-DIC value measured after one minute, reflecting DIC generated by CH and represents that of the bedrock carbonate. The atmospheric CO_2 in the fridge has a $\delta^{13}C$ of –13.8 ‰. Assuming there is a –1 ‰ kinetic fractionation (Zhang et al., 1995), the $\delta^{13}C$ of the CO_2 dissolving into solution (δ_{atm}) is initially -14.8 ‰. δ_{carb} is the $\delta^{13}C$ value of DIC arising from the CB-CD, where equal proportions of DIC come from the bedrock and the atmosphere ($(\delta_{ch} + \delta_{atm})/2$). It is assumed that $\varepsilon_{HCO3\text{-}g}$ is 0 ‰.

DIC changes for successive time steps in the 0.01 g l^{-1} experiments were extremely small and the associated error terms are thus too large to permit accurate analysis. Hence, the analysis focuses on the 5 g l^{-1} experiments where DIC changes are larger and the effects of CB-CD on $\delta^{13}C$-DIC can be more precisely understood. The $\delta^{13}C$-DIC values predicted using Equation 14 are shown on Fig. 4.4 d. The predicted values are heavier than the measured values for both the sediment and the $CaCO_3$. This indicates that in

addition to the negative fractionation associated with hydrolysis, there is also an additional negative fractionation associated with the carbonation reaction. However, it is difficult to assess whether this negative fractionation is associated with atmospheric CO_2 and/or the bedrock carbonate. Whatever the process, it appears that it occurs in a similar manner for both $CaCO_3$ and for the glacial sediment, given the similar shape of the $\delta^{13}C$-DIC evolution curves (Fig. 4.4 d). To achieve isotope mass balance for the time period 5 – 360 minutes, two end member scenarios are possible: -

Scenario 1. During carbonation of carbonates, the bedrock $\delta^{13}C$ value is fixed at the 1-minute value and the atmospheric $\delta^{13}C$-CO_2 value is allowed to vary to achieve isotope mass balance. Hence, values of ε_k more negative than -1 ‰ are required.

Scenario 2. The atmospheric $\delta^{13}C$-CO_2 value is fixed at –14.8 ‰ ($\delta^{13}C$ of fridge air and ε_k = -1 ‰) and the bedrock fractionation value, ε_b is allowed to vary to achieve isotope mass balance. Hence, values of ε_b lower than the 1 minute value are required.

The two scenarios were evaluated for both the $CaCO_3$ and the sediment experiments. However, the discussion focuses on the $CaCO_3$ experiment, since it deals with a simpler system. The sediment experiment is more complex to interpret since there are additional complicating factors (e.g. greater heterogeneity in the sediment mineralogy) making it difficult to isolate the effect of individual processes.

Fig. 4.5 shows the ε_k and ε_b values required for each time step in the 5 g l^{-1} $CaCO_3$ experiment, given Scenarios 1 and 2 respectively. It is evident that the patterns of variation in ε_k and ε_b required by the 2 scenarios are similar. In this case ε_b is the fractionation of the carbonate bedrock from dissolution due to carbonation. However, it is difficult to explain the variations in ε_b required by Scenario 2, since there is no obvious reason why, following the initial negative shift of –5.4 ‰ associated with CH there should subsequently be a large negative shift of up to –25 ‰ as rates of carbonate dissolution are significantly reduced after 1 minute (see Fig. 4.4 a). In fact, the converse

may be expected. If the initial kinetic fractionation is a surface area effect, then, as the carbonate is more completely dissolved during carbonation, it is more likely that ε_b would decrease, resulting in values closer to the bulk carbonate $\delta^{13}C$.

Scenario 1 provides a better physical explanation of how isotopic mass balance may be achieved. Following CH, rates of CO_2 draw down are initially high, but they decline as PCO_2 moves towards equilibrium with the atmosphere (Fig. 4.6). Fig. 4.7 demonstrates that there is an association between ε_k and the rate of CO_2 draw down. ε_k is most negative when draw down rates are rapid. As the rate of CO_2 draw down decreases, ε_k approaches zero. This suggests that rapid influx of CO_2 into solution favours the lighter isotope, $^{12}CO_2$, with the bias decreasing through time as the rate of CO_2 draw down decreases. However, if ε_b is more positive than the 1 minute, (CH) value during CB-CD due to "whole mineral" dissolution, then ε_k values would have to be commensurately lighter than the modelled values with the increase in ε_b. The current data set does not allow this possible change in ε_b to be quantified.

4.4.3.5. Effect of carbonate concentration on ε_b and ε_k

The experiments highlight that there are two negative kinetic isotope fractionation processes, both of which are abiotic. The first is associated with CH and is primarily controlled by the physical properties of the sediment, (e.g. grain size, fracture properties, mineralogy). The second fractionation is most likely associated with the rate at which CO_2 diffuses into solution. The carbonate concentration of the sediment that is weathering is also a key variable in determining $\delta^{13}C$ variations. The magnitude of ε_b is initially the same regardless of carbonate concentration (Fig. 4.4 d and e). However, at low sediment (and carbonate) concentrations (0.01 g l^{-1}), the kinetic bedrock fractionation (ε_b) dominates over ε_k and its effect on $\delta^{13}C$–DIC is short lived (cf. Fig. 4.4 d and e). First, PCO_2 equilibrium is only slightly perturbed in the 0.01 g l^{-1} experiment since the amount of DIC generated by CH is limited. Hence the rate at which CO_2 dissolves into solution to restore PCO_2 equilibrium is significantly lower than at higher carbonate concentrations, therefore (ε_k) is likely small. Second, if kinetic bedrock fractionation

(KBF) is primarily a surface-area effect then this can only persist for a short time at low sediment concentrations since "whole rock" dissolution will dominate more quickly than at higher concentrations, producing $\delta^{13}C$ values similar to the bulk rock value. This is evident in Fig. 4.4e where the return to isotopic equilibrium following CH occurs earlier than in the equivalent 5 g l^{-1} experiment (Fig. 4.4 d).

The effect of carbonate concentration is likely important for interpretation of the field data. Where carbonate concentrations are low, KBF will dominate, but its impact on $\delta^{13}C$–DIC may only be detectable where water residence times are extremely short (< 20 minutes) and the processes of whole mineral dissolution have not yet become effective. At higher carbonate concentrations KBF will persist for longer, generating proportionately more light $\delta^{13}C$-DIC. In open systems kinetic fractionation of CO_2 (KFC) will also have a greater impact in generating light $\delta^{13}C$–DIC at higher carbonate concentrations due to increased drawdown rates. It is not possible to determine from the weathering experiments whether KBF occurs during the initial stage of carbonate weathering from protons derived by SO. However, it seems reasonable to expect that fractionation of the bedrock carbonate may occur during SO/CD, if the reaction kinetics are rapid enough. As for CH, carbonate concentration will also affect the impact of KBF from coupled SO/CD on $\delta^{13}C$-DIC, since that will control the magnitude of "selective" relative to "whole" rock dissolution.

4.5. INTERPRETATION OF FIELD DATA

Previously (Section 4.4.2.4.), it has been demonstrated that standard biogeochemical and geochemical models do not adequately account for the $\delta^{13}C$-DIC field data. The experimental work demonstrates that kinetic fractionation processes can impart large negative isotopic fractionations during carbonate weathering. Hence, the kinetic fractionation processes need to be incorporated into the geochemical and biogeochemical models to interpret the field data.

4.5.1. John Evans Glacier

Fig. 4.8 a and Fig. 4.9 show the association between δ^{13}C-DIC and DIC and δ^{13}C-DIC and PCO_2 respectively. The John Evans Glacier data show an increasing trend in both DIC and PCO_2 between subglacial and marginal stream waters. These increases are accompanied by an increase in δ^{13}C-DIC.

4.5.1.1 Subglacial stream water geochemistry

The subglacial waters have an average composition of 250 μeq l^{-1} DIC, PCO_2 $<10^{-4}$ atm and δ^{13}C-DIC = –12.8 ‰ (Fig. 4.8 a and Fig. 4.9). These subglacial waters are similar geochemically and isotopically to the 1-minute waters from the 5 g l^{-1} weathering experiments (cf. Figs. 4.4 c and e). However, the PCO_2 values are closer to equilibrium than the experimental values. The 1 minute waters in the weathering experiments are generated by CH and therefore, by analogy, one could interpret the John Evans Glacier subglacial waters as also being the product of CH. In reality, the field situation is likely more complicated than this, since other weathering processes, including GD and possibly SO-CD are involved, and there is also the possibility of subglacial carbonate precipitation (see Section 4.3.4.6.). The evidence suggests that the subglacial hydrological environment is predominantly water-filled and that subglacial waters have limited contact with the atmosphere. Therefore, it seems reasonable to assume that CH is the dominant process in determining subglacial δ^{13}C–DIC and that there is little atmospheric CO_2 input. It is possible to calculate average ε_b values for the field data assuming all the DIC is from CH. For a bedrock δ^{13}C carbonate of –0.9 ‰, the average ε_b value is –11.9 ‰. For the sediment δ^{13}C of –2.15 ‰, ε_b is -10.65 ‰, which is closer to the experimentally derived ε_b for the 5 g l^{-1} experiment of –10.7 ‰. The PCO_2 values indicate that some re-equilibration with the atmosphere may have occurred, so some of the light δ^{13}C-DIC values may also reflect KFC processes. However, it is not possible to determine the magnitude of ε_k for the subglacial waters from the field data.

4.5.1.2. Marginal stream water geochemistry

Marginal stream waters are on average isotopically heavier than subglacial waters, (–8.8 ‰ cf. –12.8 ‰), contain ~200 μeq l^{-1} more DIC (Fig. 4.8 a) and have PCO_2 values at or closer to atmospheric values ($10^{-3.5}$ atm) (Fig. 4.9). From the water chemistry data (Table 4.1), it is reasonable to argue that CH and CB-CD are the main chemical weathering processes in these waters. Hence, it is likely that CH in the marginal stream waters initially results in waters that are isotopically and geochemically similar to subglacial waters. The influx of atmospheric CO_2 to both increase PCO_2 and dissolve further bedrock carbonate is reflected in the evolutionary trend shown as Pathway 1 in Fig. 4.8 a and Pathway 3, Fig. 4.9. The field data reflect evolutionary $\delta^{13}C$–DIC processes similar to those observed in the open system (5 g l^{-1} sediment) weathering experiments. In these experiments CB-CD produced waters on average 2 ‰ lighter in $\delta^{13}C$–DIC than the CH (1 minute) value, whereas the marginal stream waters are 4 ‰ heavier than the CH $\delta^{13}C$–DIC (subglacial) value. In the field, atmospheric $\delta^{13}C$–CO_2 is –8.8 ‰, which is 6 ‰ heavier than the fridge CO_2, -14.8 ‰. This accounts for the 6 ‰ difference in the $\delta^{13}C$–DIC values between the field and laboratory experiments, and indicates that the average ε_k value in the field is likely of a similar magnitude to that observed in the experimental work. Therefore, the KBF and KFC processes observed in the laboratory experiments apparently occur in the field as well. Moreover, ε_b and ε_k are remarkably similar for the experimental and field data. It is not possible to discount the possibility of microbial CO_2 input to the $\delta^{13}C$-DIC of either the marginal or subglacial streams from analysis of the field data. However, it would be difficult to distinguish this component from the bulk $\delta^{13}C$–DIC value due to large impact of kinetic fractionation processes.

4.5.1.3. Seasonal changes in subglacial $\delta^{13}C$–DIC

The anomalous subglacial data point located within the marginal stream field (Fig. 4.8 a and Fig. 4.9) reflects an abrupt change in subglacial stream chemistry. This change occurs on JD 193 with a rapid increase in DIC (Table 4.1) and accompanying heavier $\delta^{13}C$–DIC (Fig. 4.2). Field observations indicate that discharge was very low on JD 193

due to cooler air temperatures that reduced melt input to the subglacial system. As the melt input is reduced water flow velocities decrease and the subglacial system may not be water filled throughout. Therefore, following CH, it is possible that there was increased atmospheric input to the waters allowing both partial re-equilibration with the atmosphere and increased levels of CB-CD. Hence, the subglacial waters, have $\delta^{13}C$–DIC and PCO_2 values similar to the marginal stream waters, which have free access to the atmosphere. Moreover, $SO_4^{2-}{}_{(so)}$ levels in the subglacial stream remain constant, or lower than the preceding days (Table 4.1) so increased SO-CD does not appear to be the cause of the increase in DIC. The gradual decrease over JD 195 and 197 in both DIC concentrations and $\delta^{13}C$-DIC from the JD 193 value most likely reflect a decrease in atmospheric CO_2 input. This is in agreement with the observation that supraglacial inputs were higher on JD 195 and 197, likely resulting in increased water flow velocities and a water-full subglacial drainage system with less contact between the waters and the atmosphere.

4.5.2. Haut Glacier d'Arolla

In contrast to the John Evans Glacier data, the Haut Glacier d'Arolla waters show considerably more diurnal and seasonal variability in $\delta^{13}C$-DIC and DIC concentrations. However, the waters cluster into three distinct groups based on time of year and the sampling location. In the early season (May), the bulk waters are clustered, around an average DIC value of ~ 600 μeq l^{-1} and an average $\delta^{13}C$-DIC of ~ -6 ‰ (Fig. 4.8 b). The later season bulk waters (July and August) have much lower (~ 300 μeq l^{-1}) DIC and a wider range in $\delta^{13}C$-DIC values than the early season waters. Within the late season data there is a marked trend to heavier $\delta^{13}C$-DIC values with only small accompanying increases in DIC. One of the borehole waters has a DIC significantly higher than the bulk meltwaters and both have $\delta^{13}C$-DIC values lighter than the majority of bulk meltwaters.

The Haut Glacier d'Arolla waters all have PCO_2 values above the atmospheric value of $10^{-3.5}$ (Fig. 4.9). There is evidence of a diurnal trend throughout the season to PCO_2 values closer to that of the atmosphere at times of higher discharge (Fig. 4.3 b and Pathways 3 and 4, Fig. 4.9).

4.5.2.1. Distributed and channelised system δ^{13}C-DIC.

The nature of the subglacial hydrological system at Haut Glacier d'Arolla is important in determining geochemical variability of bulk meltwaters on both a diurnal and seasonal basis (see section 4.2.2.2.). The hydrochemical model for Haut Glacier d'Arolla (Richards et al., (1996); Brown et al., (1996)) suggests the chemical composition of the bulk meltwaters results from (a) chemical evolution of waters in the distributed system, which is closed with respect to atmospheric CO_2 (Tranter et al., in press; Bottrell and Tranter, in press), (b) dilution of distributed system waters by mixing with ice and snowmelt in the channelised system, where there is greater access to the atmosphere (at least at diurnal minimum discharges) and (c) post mixing reactions (PMR) (largely carbonate hydrolysis) with suspended sediment in the channel environment. Concentrated waters from the distributed system make a proportionally greater contribution to bulk meltwaters at low seasonal and diurnal discharges (Richards et al., 1996). By contrast, dilution within the channelised system is proportionally greater at higher seasonal and diurnal discharges (Brown et al., 1996). PMR make the greatest contribution to bulk runoff when suspended sediment concentrations are highest, during high diurnal discharges late in the melt season (Brown et al., 1996). PMR largely produce DIC via CH and therefore, from the experimental work it seems likely that KBF may affect the δ^{13}C–DIC from PMR. If so, the effect of KBF on bulk meltwater δ^{13}C–DIC will be related to the relative contribution of PMR to total DIC.

4.5.2.1.1. Distributed system δ^{13}C –DIC

To interpret the δ^{13}C–DIC data using the hydrochemical model of Brown et al., (1996), outlined above, (section 4.5.2.1.), it is first necessary to establish the isotopic and geochemical composition of the distributed system waters and their variability during the meltseason. M3 simulates solute acquisition in a "closed" system subglacial environment where solute acquisition occurs via CH, SO-CD and MR-CD. The δ^{13}C-DIC values simulated by M3 closely match the measured values a) in bulk meltwaters at low

discharges throughout the melt season b) in concentrated borehole waters, and to a lesser extent c) all early season bulk meltwaters (Table 2). These waters all have PCO_2 values > -2.8 atm. (Fig. 4.9) indicating that they have not had significant contact with the atmosphere, supporting the validity of M3 as a simulation model. The simplest interpretation of these data is that they have evolved in the distributed system, without significant dilution or input from PMR. Water types A, B and C represent "end member" water types for each data subset (Fig 4.8 a) that have evolved under closed system conditions, as would be found in the distributed drainage system. Type A water reflects late season distributed system waters, B early season distributed system waters and C borehole distributed system waters.

Negligible amounts of microbial CO_2 (~3%) are required to account for the measured $\delta^{13}C$–DIC of Type A waters using M3. Thus this component could realistically be zero given the analytical uncertainties in the $\delta^{13}C$ determinations. Therefore, type A waters may be produced by CH and SO-CD alone. However, type B and C waters contain DIC in excess of that generated by CH and SO-CD. This can be accounted for by MR-CD. Predicted microbial CO_2 inputs rise to 10-14 % of DIC in type B waters and to 20 % of DIC in type C waters (Table 4.2). Pathway 2 represents a possible evolutionary pathway for the distributed system waters reflecting initially only DIC from CH+SO-CD (type A) with increasing contributions from SO-CD and MR-CD in type B and C waters (Fig. 4.8 b). Water flow velocities in the distributed system increase during the meltseason, reducing water:rock contact times and thus the chemical evolution of the waters. This most likely accounts for the difference between the late season water A and early season water B. Water type C is a 'pure' distributed system subglacial water since it was sampled from a borehole that did not initially have a direct connection to the channelised subglacial drainage system. Water B could be generated by a 1.5 fold dilution of water C. This could occur in the early melt season if pure type C water from the distributed system was diluted by mixing with snowmelt in the residual channel system underlying the lower 500 m of the glacier. Water flow velocities are low at this stage of the season, when discharge is ~ 0.1 m^3 s^{-1} and entrain little sediment. Therefore PMR do not occur and mixing of the waters results in simple dilution.

Pathway 2, Fig. 4.8 b, identifies a trend towards lighter δ^{13}C-DIC values with increasing DIC concentrations, likely due to increased microbial CO_2 input. In each data subset there is a trend to light isotopic values with decreasing DIC concentrations as indicated by lines a, b and c. In the bulk meltwater data there is a diurnal trend to lighter δ^{13}C-DIC values later in the day which occurs throughout the melt season. These trends may be related to dilution of distributed waters by ice/snowmelt and DIC acquisition from PMR, which may be affected by KBF.

4.5.2.1.2. Channelised system δ^{13}C-DIC

The hydrochemical model of Brown et al., (1996) is applied to the bulk meltwater analyses for JD 205 (when diurnal variation in δ^{13}C-DIC is greatest) to determine the amount of DIC generated by PMR and its δ^{13}C-DIC signature. M3 (section 4.3.4.6.) accurately predicts the measured δ^{13}C-DIC for 1000 hrs on JD 205 and therefore, these waters are assumed to represent flow from the distributed system only. In the following mixing models (Equations 15 and 16) the base flow component is the 1000 hrs value for discharge, chemical and isotopic composition, and is assumed to be constant throughout the day. As discharge rises during the day the channelised component of bulk runoff increases, relative to the distributed component. The rise in discharge is accompanied by a decrease in SO_4 and DIC concentrations and in PCO_2, with values moving closer to atmospheric (Table 4.2, Fig. 4.3 b). A simple mass balance equation (Equation 15) is used to estimate the proportions of baseflow from the distributed system and quickflow through the channelised system. It follows that the chemical and isotopic composition of the channelised component can be determined using Equation 16.

$$Q\ \text{Quickflow}\ (Q_q) = Q\ \text{Total}\ (Q_t) - Q\ \text{Baseflow}\ (Q_b) \quad (15)$$

$$\text{and}\ Q_q C i_q = Q_t C i_t - (Q_b) C i_b \quad (16)$$

where C is the concentration of an individual chemical species, *i*.

The predicted chemical composition of the quickflow component and its variation over JD 205 are shown in Table 4.2. Quickflow waters have two solute sources, a supraglacial component from the atmospheric aerosol, on average ~ 5 μeq l^{-1} SO_4^{2-} (Tranter et al., in press) and 23 μeq l^{-1} DIC as $CO_{2\,(aq)}$ if the waters are in equilibrium with atmospheric CO_2; and a PMR component derived from weathering of suspended sediment. O_2 concentrations in supraglacial waters at Haut Glacier d'Arolla are undersaturated with respect to the atmosphere, (30-90 % saturated), indicating that gas-water equilibrium has not been achieved (Brown et al., 1994b). Hence, undersaturation with respect to atmospheric CO_2 may also be expected. Using O_2 saturation levels as a guide, DIC levels in supraglacial waters are assumed to range from 7-21 μeq l^{-1}. Solute acquisition in the channelised system is via PMR mainly producing DIC by CH, however, up to ~ 10 μeq l^{-1} SO_4^{2-} from SO may also be generated (Brown at al., 1996). The predicted SO_4^{2-} concentration for the quickflow component from the combination of supraglacial sources (~ 5 μeq l^{-1}) and PMR (~10 μeq l^{-1}) (Brown et al. 1996) is ~ 15 μeq l^{-1}, which is similar to the values modelled for the JD 205 data using Equation 16 (Table 2).

DIC in the quickflow component is comprised of DIC from dissolution of atmospheric CO_2 in the supraglacial environment and DIC from CH and SO-CD due to PMR in the subglacial channelised environment. Bedrock DIC generated from both CH and SO-CD in the quickflow component is assumed to have the same isotopic composition due to the rapid weathering rates. The $\delta^{13}C$–DIC of the bedrock component of the quickflow is derived using Equation 17.

$$\delta_{bedrock} = \delta^{13}C\text{-}DIC_q - \delta_{atm}DIC_{atm} \,/\, DIC_{bedrock} \qquad (17)$$

where δ_{atm} = -8.8 ‰ and DIC_{atm} = 21 μeq l^{-1}. This scenario produces the lowest $DIC_{bedrock}$ concentrations and hence, the lowest possible $\delta^{13}C\text{-}DIC_{bedrock}$ values, in the range –7.1 to –16.5 ‰ (Table 2). Subtracting the bedrock carbonate value of –2.4 ‰

from the $\delta^{13}C\text{-}DIC_{bedrock}$ produces values of ε_b as large as –14.1 ‰. This is slightly more negative than the value for John Evans Glacier sediment of -11.9 ‰.

Incorporating KBF into the hydrochemical model of Brown et al., (1996) provides a plausible explanation for the $\delta^{13}C$-DIC trend (a) in the late season meltwaters, reflecting dilution of distributed system waters and addition of isotopically light DIC from PMR (Fig. 4.8 b). Similarly lines (b) and (c) represent the evolution of Type B and C waters respectively following dilution and DIC addition from PMR. Pure dilution of the distributed system waters would result in a simple movement to the left on (Fig. 4.8 b) from water type A, B or C, whereas the curves reflect the combined processes of dilution and PMR. The lines a, b and c, have a common endpoint, representing 100 % dilution of the distributed system waters and 100 % of DIC generated by in the quickflow system, mainly from PMR. The lines are generated using a simple mixing model with end members A and Q, B and Q, and C and Q respectively. The maximum DIC concentration of the quickflow component (Q) following PMR is likely to be ~221 $\mu eq\ l^{-1}$, comprising 21 $\mu eq\ l^{-1}$ DIC as atmospheric CO_2, 190 $\mu eq\ l^{-1}$ DIC from CH and 10 $\mu eq\ l^{-1}$ from SO-CD. The $\delta^{13}C$-DIC of the Q waters is -15.7 ‰, using the DIC concentrations outlined above and values of –16.5 ‰ for $\delta^{13}C\text{-}DIC_{bedrock}$ and –8.8 ‰ for $DIC_{atm.}$ Increased movement along lines a, b and c away from the end member water reflects increasing dilution and an increasing fraction of DIC from PMR.

In the early season, (May) there is little movement along (b) away from type B water, which reflects limited dilution of distributed system waters by surficial snowmelt and minimal DIC input from PMR due to limited mobilisation of suspended sediment. By contrast, the significant movement along line (a) in July and August indicates both increased dilution due to greater volumes of surficial icemelt and significant DIC input from PMR. The data point on line (c) is more difficult to explain using the model since it requires a reasonably large dilution of the concentrated borehole water (type C) and input of DIC from PMR. Both borehole water samples were taken from the base of the same borehole, but the more dilute water was sampled 3 days after the concentrated one. However, Lamb (1997) noted that between JD 228 and 231, there was an influx of dilute

meltwater (~10 μS cm^{-1}) into the borehole from an englacial connection, leaving the borehole stratified with low conductivity waters overlying concentrated basal waters. The borehole then began to drain, presumably mixing the overlying dilute waters with basal waters as basal drainage occurred. The chemical and isotopic composition of the englacial component is unknown and it may be possible that these waters have acquired some isotopically light DIC through CH (englacially) prior to entering the hole. Hence, the resulting "bulk" borehole water sampled on JD 231 may simply reflect mixing and dilution of the concentrated basal waters, but without significant PMR.

4.5.2.2. Comparison of field and laboratory ε_b values

The JD 205 data indicate that at higher discharges and presumably higher SSC[3] the contribution of DIC from CH increases. This agrees with the experimental work of Brown et al., (1994) using Haut Glacier d'Arolla sediment, which demonstrates that DIC production increases with sediment concentration. Brown et al., (1994) also argue that the rate of dissolution is faster in meltwater with higher SSC, although the mechanisms for this are not outlined. Presumably, it is due to an increase in carbonate reaction sites at higher SSC. On JD 205, as DIC concentrations from CH increased, ε_b became increasingly negative. This suggests that at Haut Glacier d'Arolla the magnitude of ε_b may be linked to SSC, (more specifically the concentration of suspended carbonate). By contrast in the laboratory experiments ε_b was similar in both the 0.01 g l^{-1} and 5 g l^{-1} experiments. This indicates that the concentrations and the reactivity of the sediment (< 63 μm fraction) in the laboratory experiment result in sufficient reaction sites for full kinetic fractionation to occur. In contrast at Haut Glacier d'Arolla, sediments contain on average only 0.15 wt % carbonate (the average value for catchment bedrock). Thus, with sediment concentrations in the range 1 - 5 g l^{-1}, carbonate concentrations are 0.0015 - 0.0075 g l^{-1}, (which are lower than the weathering experiment value of 0.01 g l^{-1}), and a range of size fractions including those > 63 μm there will be significantly fewer carbonate reaction sites in the field environment.

[3] Suspended sediment concentration (SSC) data are not available for JD 205. However, it is has been well documented that there is a positive correlation between SSC and discharge (e.g. Gurnell, 1987), and therefore, it is reasonable to assume that SSC rises as discharge increases during the day.

Hence, the difference in ε_b values between the early afternoon and late afternoon waters on JD 205 (Table 4.2), most likely relates to availability of carbonate reaction sites and water:rock contact time. Later in the afternoon, discharge and probably also water velocity are higher, reducing water:rock contact times. SSC's are also higher, increasing the number of reaction sites relative to the early afternoon (for simplicity it is assumed that the carbonate content, size fraction and freshness of the mineral surfaces of suspended sediment are invariant). Therefore, CH in late afternoon waters involves extremely rapid reactions at carbonate mineral surfaces allowing maximum kinetic fractionation.

4.5.2.3. PCO_2 v δ^{13}C-DIC relationships

The same nomenclature for water types and evolution lines is used in Fig. 4.9 as in Fig. 4.8 b and the evolution of the Haut Glacier d'Arolla waters reflects the two component model. (see Section 4.5.2.1.2) The lines a, b, and c reflect mixing in a "closed system" environment, i.e. that there is no re-equilibration with the atmosphere, which appears to be a reasonable simulation for the borehole data (Line c, Fig. 4.9). However, the curvilinear mixing lines a and b do not reflect the linear trends in the bulk meltwater data as shown by Pathways 3 and 4. Pathway 3, for the early season waters shows the greater departure from the evolution line (b). A possible explanation for the PCO_2 trends is that in addition to mixing of distributed and channelised waters there is degassing of the waters as atmospheric re-equilibration occurs, thus driving the waters towards atmospheric equilibrium. This seems possible given that the subglacial channels are not always water full especially close to the glacier terminus.

4.5.3. Summary

Overall, KBF has a less pronounced effect on the δ^{13}C–DIC of meltwaters at Haut Glacier d'Arolla than at John Evans Glacier. However, KBF is important at Haut Glacier d'Arolla, especially later in the season, when the channelised component of bulk runoff increases. In the distributed drainage system at Haut Glacier d'Arolla, where water flow

rates are low and water:rock contact times long it appears that weathering by CH does not produce significant isotopic fractionation. This does not mean that there is no kinetic fractionation during the initial dissolution phase, rather that if the whole mineral is eventually dissolved then to retain isotope mass balance, subsequent DIC fractions must be isotopically heavy, resulting in total DIC which reflects the bulk mineral $\delta^{13}C$ value. By contrast in channelised environments at Haut Glacier d'Arolla where water:rock contact times are considerably shorter, CH causes kinetic fractionations due to selective dissolution of $Ca^{12}CO_3$. At John Evans Glacier, where carbonate concentrations are higher, CH causes significant kinetic fractionations in both the marginal and subglacial streams.

At Haut Glacier d'Arolla there is clear evidence of microbial CO_2 input to borehole waters and bulk runoff that is composed primarily of distributed system waters. These water contain DIC in excess of that produced by CH and SO-CD. Here, as the amount of "excess" DIC increases as a proportion of DIC the $\delta^{13}C$-DIC becomes increasingly negative, as would be expected if the additional DIC had a microbial source (-26 ‰). An atmospheric source for the "excess DIC" is unlikely because a) the distributed waters are physically isolated from the atmosphere b) the PCO_2 of the these waters indicates that they are up to an order of magnitude higher than that of the atmosphere, and thus degassing rather than draw down of CO_2 is likely if an atmospheric connection is made and c) the $\delta^{13}C$ of atmospheric CO_2 would have to have be –26 ‰ to achieve isotopic mass balance. Such negative atmospheric CO_2 values have only been inferred in the very early stages of CB-CD in weathering experiments when PCO_2 values are low (10^{-6}), (some 3-4 orders of magnitude lower than the measured waters) and CO_2 drawdown rates high, so this seems unlikely. Microbial CO_2 therefore, probably accounts for between 10-20% of DIC in the distributed system waters at Haut Glacier d'Arolla.

By incorporating kinetic fractionation factors into the geochemical model it is possible to identify waters containing isotopically light DIC that is the result of kinetic fractionation processes. At Haut Glacier d'Arolla these are bulk waters, where decreases in DIC concentration (from an "end member" water) are associated with increasingly negative

δ^{13}C-DIC. At John Evans Glacier all marginal and subglacial stream waters show evidence of kinetic fractionation where the dominant weathering processes are CH and CB-CD. In these kinetically affected waters there is no clear evidence of microbial CO_2 input. However, the impact of kinetic processes (KBF and KFC) on δ^{13}C–DIC is so dominant that it would be difficult to identify microbial CO_2 signatures at the low levels (10-20 % of total DIC) found in the concentrated Haut Glacier d'Arolla waters.

4.6. CONCLUSIONS

1. The weathering experiments demonstrate previously undiscovered kinetic fractionation processes, kinetic bedrock fractionation (KBF) and kinetic fractionation of atmospheric CO_2 (KFC) that occur during carbonate weathering. KBF occurs during CH and KFC is of importance during coupled CB-CD. Both of these kinetic fractionation processes result in δ^{13}C-DIC values that are significantly depleted relative to the bedrock carbonate. From the field data, the magnitude of KBF appears to be related to the $CaCO_3$ concentration, being more negative at high $CaCO_3$ concentrations. KFC appears to be more significant at higher $CaCO_3$ concentrations. John Evans Glacier field data and weathering experiments on John Evans Glacier sediments show remarkably similar fractionation factors, and for KBF (ε_b = -11.6 ‰ and –10.7 ‰) and KFC (ε_k, = -6 ‰ and –6 ‰) processes respectively.

2. The current equilibrium geochemical and biogeochemical models cannot account for the range of δ^{13}C–DIC values measured in the field.

3. Incorporation of KBF and KFC processes into the geochemical models is necessary to fully account for the field δ^{13}C–DIC values. It is possible to clearly identify environments where light δ^{13}C-DIC is a result of kinetic processes and where it is indicative of *in situ* subglacial microbial activity using this combined approach. The field data reflect the experimental findings that kinetic fractionation processes have a greater overall impact on δ^{13}C-DIC where bedrock carbonate concentrations are higher. δ^{13}C–DIC values at John Evans Glacier are significantly lighter on average

than the Haut Glacier d'Arolla values, even though the bedrock carbonate values for John Evans Glacier are ~ 1.5 ‰ heavier.

4. The effects of KBF on the δ^{13}C-DIC are strong where (a) carbonate hydrolysis (CH) occurs shortly before waters emerge from glacier (e.g. via post-mixing reactions in high discharge bulkwaters in July at Haut Glacier d'Arolla), and (b) carbonate weathering does not proceed beyond the hydrolysis phase, because saturation with respect to calcite/dolomite is reached and access to atmospheric CO_2 source is limited (e.g. subglacial waters at John Evans Glacier, where the drainage system is water filled). At John Evans Glacier the subglacial drainage system has only a single supraglacial input location, which prevents continued mixing with new inputs of dilute supraglacial water as waters move downstream to the outlet at the terminus. KBF effects are less apparent where (a) CH and coupled sulphide oxidation and carbonate dissolution (SO-CD) occur in a closed-system, low-flow environment (e.g. Haut Glacier d'Arolla undiluted distributed system waters), such that "whole mineral" dissolution occurs and δ^{13}C-DIC largely reflects the bedrock value), and (b) waters have extended contact with atmospheric CO_2 after CH has occurred, allowing re-equilibration with the atmosphere and DIC production from carbonation of carbonates with atmospheric CO_2 (CB-CD), driving δ^{13}C-DIC towards the bedrock value (e.g. marginal and low-flow subglacial waters at John Evans Glacier).

5. Subglacial chemical weathering processes are dominated by CH, SO-CD and MR-CD. Thus, at both John Evans Glacier and Haut Glacier d'Arolla, they involve minimal consumption of atmospheric CO_2. This contrasts with the conclusions drawn by Sharp et al., (1995) and Hodson et al., (2000), whose analyses neglected CH as a weathering process in subglacial environments. It also contradicts the assertion of Kump and Alley, (1994) that weathering in subglacial environments is limited because of a lack of access to an atmospheric CO_2 source.

6. PCO_2 equilibrium occurs significantly faster than isotopic equilibrium and thus PCO_2 values may be only a coarse guide to the isotopic equilibrium conditions. High

carbonate concentrations lead to rapid weathering (CH) which results in rapid CO_2 draw down rates via CB-CD. This appears to prevent the process of isotopic fractionation $\varepsilon_{HCO3\text{-}g}$ from occurring during at least the first 2-6 hours of the carbonation reaction, and demonstrates that $\varepsilon_{HCO3\text{-}g}$ can be zero for up to 6 hours after the start of the reaction. This is considerably longer than previously reported, e.g. by Szaran (1997), albeit under different initial experimental conditions.

4.7. REFERENCES

Amiotte-Suchet P., Aubert D., Probst J. L., Gauthier-Lafaye F., Probst A., Andreux F., and Viville D. (1999) $\delta^{13}C$ pattern of dissolved inorganic carbon in a small granitic catchment: the Strengbach case study (Vosges mountains, France). *Chemical Geology* **159**, 129-145.

Anderson S. P., Drever J. I., and Humphrey N. F. (1997) Chemical weathering in glacial environments. *Geology* **25**, 399-402.

Bluth G. J. S. and Kump L. R. (1994) Lithologic and climatologic controls of river chemistry. *Geochimica Cosmochimica Acta* **58** (10), 2341-2359.

Bottrell, S. H. and Tranter, M. (in press) Sulphide oxidation under partially anoxic conditions at the bed of the Haut Glacier d'Arolla, Switzerland. *Hydrological Processes.*

Brown G. H. (1991) Solute provenance and transport pathways in Alpine glacial environments. Ph.D., Southampton.

Brown G. H., Sharp M. J., Tranter M., Gurnell A. M., and Nienow P. W. (1994a) Impact of post-mixing reactions on the major ion chemistry of bulk meltwaters draining the Haut Glacier d'Arolla, Valais, Switzerland. *Hydrological Processes* **8**, 465-480.

Brown G. H., Tranter M., and Sharp M. J. (1996) Experimental investigations of the weathering of suspended sediment by alpine glacial meltwater. *Hydrological Processes* **10**, 579-597.

Brown G. H., Tranter M., Sharp M. J., Davies T. D., and Tsiouris S. (1994b) Dissolved oxygen variations in alpine glacial meltwaters. *Earth Surface Processes and Landforms* **19**, 247-253.

Clark I. D. and Lauriol B. (1992) Kinetic enrichment of stable isotopes in cryogenic calcites. *Chemical Geology (Isotope Geoscience Section)* **102**, 217-228.

Clark P. (1997) *Environmental Isotopes in Hydrogeology*.

Copland L. and Sharp M. J. (in press) Mapping thermal and hydrological conditions beneath a polythermal glacier with radio-echo sounding. *Journal of Glaciology*.

Craig H. (1957) Isotopic standards for carbon and oxygen and correction factors for mass spectrometric analysis of carbon dioxide. *Geochimica et Cosmochimica Acta* **12**, 133-149.

Dandurand J. L., Gout R., Hoefs J., Menschel G., Schott J., and Usdowski E. (1982) Kinetically controlled variations of major components and carbon and oxygen isotopes in a calcite-precipitating spring. *Chemical Geology* **36** (299-315).

Deuser W. G. and Degens E. T. (1967) Carbon isotope fractionation in the system CO_2 (gas) - CO_2 (aqueous) - HCO_3 (aqueous). *Nature* **215**, 1033-1035.

Fairchild I. J., Bradby L., Sharp M., and Tison J.-L. (1994) Hydrochemistry of carbonate terrains in alpine glacial settings. *Earth Surface Processes and Landforms* **19**, 33-54.

Faure G. (1986) *Principles of isotope geology*. Wiley.

Gibbs M. T. and Kump L. R. (1994) Global chemical erosion during the last glacial maximum and the present: sensitivity to changes in lithology and hydrology. *Paleoceanography* **9**, 529-543.

Gurnell A. (1987) Suspended sediment. In *Glaciofluvial sediment transfer: An alpine perspective* (ed. A. M. Gurnell and M. J. Clark), pp. 305-354. Wiley and Sons.

Hallet, B. (1976) Deposits formed by subglacial precipitation of $CaCO_3$. *Bulletin of the Geological Society of America* **87**, 1003-15.

Heemskerk R. (1993) Sulphur 34/32 determination. *Environmental Isotope Laboratory, Department of Earth Sciences, University of Waterloo*. Technical Procedure 26, 7.

Hodson A., Tranter M., and Vatne G. (2000) Contemporary rates of chemical denudation and atmospheric CO_2 sequestration in glacier basins: an Arctic perspective. *Earth Surface Processes and Landforms* **25**, 1447-1471.

Hoefs J. (1980) *Stable Isotope Geochemistry*. Springer Verlag.

Hooke R. L. B. (1989) Englacial and subglacial hydrology: a qualitative review. *Arctic and Alpine Research* **21**, 221-233.

Hubbard B. P., Sharp M. J., Willis I. C., Nielsen M. K., and Smart C. C. (1995) Borehole water-pressure variations and the structure of the subglacial hydrological system of the Haut Glacier d'Arolla, Valais, Switzerland. *Journal of Glaciology* **41**, 572-583.

Kerr J. W. (1972) Map 1358A Geology: Dobbin Bay, District of Franklin. Geological Survey of Canada.

Kump, L.R. and Alley, R.B., 1994. Global chemical weathering on glacial time scales. In: Usselman, T.M. and Hay, W.W. (eds.), Material Fluxes on the Surface of the Earth, National Research Council, Washington, DC, pp. 46-60.

Lamb H. R., Tranter M., Brown G. H., Hubbard B. P., Sharp M. J., Smart C. C., Willis I. C., and Nielsen M. K. (1995) The composition of subglacial meltwaters sampled from boreholes at the Haut Glacier d'Arolla, Switzerland. *International Association of Hydrological Sciences Publications* **228**, 395-403.

Mazurek M. (1986) Structural evolution and metamorphism of the Dent Blanche nappe and the Combin zone west of Zermatt. *Ecologae Geologische Helvetica* **79**, 41-56.

McCrea J. M. (1950) On the isotope chemistry of carbonates and a paleotemperature scale. *Journal of Chemical Physics* **18**, 849-857.

Mills G. A. and Urey H. C. (1940) The kinetics of isotope exchange between carbon dioxide, bicarbonate ion, carbonate ion and water. *Journal of the American Chemical Society* **62**, 1019-1026.

Mook W. G., Bommerson J. C., and Staverman W. H. (1974) Carbon isotope fractionation between dissolved bicarbonate and gaeous carbon dioxide. *Earth and Planetary Science Letters* **22**, 169-176.

Nienow P., Sharp M., and Willis I. (1998) Seasonal changes in the morphology of the subglacial drainage system, Haut Glacier d'Arolla, Switzerland. *Earth Surface Processes and Landforms* **23**, 825-843.

Parkhurst D. L. and Appelo C. A. J. (1999) User's guide to PHREEQC (Version 2)--a computer program for speciation, batch-reaction, one-dimensional transport, and inverse geochemical calculations, pp. 312. U. S. Geological Survey.

Paterson W. S. B. (1994) *The physics of glaciers*. Pergamon.

Raiswell R. (1984) Chemical Models of solute acquisition in glacial melt waters. *Journal of Glaciology* **30** (104), 49-57.

Raiswell R. and Thomas A. G. (1984) Solute aquisition in glacial melt waters. I Fjallsjokull (south-east Iceland): Bulk melt waters with closed system characteristics. *Journal of Glaciology* **30** (104), 35-42.

Reynolds R. C. and Johnson N. M. (1972) Chemical weathering in the temperate glacial environment of the Northern Cascade Mountains. *Geochimica Cosmochimica Acta* **36**, 537-554.

Richards K., Sharp M. J., Arnold N., Gurnell A., Clark M., Tranter M., Nienow P., Brown G., Willis I., and Lawson W. (1996) An integrated approach to modelling hydrology and water quality in glacierized catchments. *Hydrological Processes* **10**, 479-508.

Rivkina E. M., Friedmann E. I., McKay C. P., and Gilichinsky D. A. (2000) Metabolic activity of permafrost bacteria below the freezing point. *Applied and Environmental Microbiology* **66** (8), 3230 - 3233.

Sagemann, J., Jorgensen B. B. and Greeff O. 1998. Temperature dependence and rates of sulfate reduction in cold sediments of Svalbard, Arctic Ocean. *Geomicrobiology Journal* **15**:85-100.

Sharp M. (1991) Hydrological inferences from meltwater water quality data: the unfulfilled potential. *BHS 3rd National Hydrology Symposium*, 5.1- 5.7.

Sharp M. (1996) Weathering pathways in glacial environments: hydrological and lithological controls. *Fourth International Symposium on the Geochemistry of the Earth's Surface*, 652-655.

Sharp M., Parkes J., Cragg B., Fairchild I. J., Lamb H., and Tranter M. (1999) Widespread bacterial populations at glacier beds and their relationship to rock weathering and carbon cycling. *Geology* **27** (2), 107-110.

Sharp M. J., Creaser R. A., and Skidmore M. (submitted) Strontium isotope composition of runoff from a glacierised carbonate terrain. *Geochimica Cosmochimica Acta.*

Sharp M. J., Richards K. S., Willis I., Arnold N., Nienow P., Lawson W., and Tison J.-L. (1993) Geometry, bed topography and drainage system structure of the Haut Glacier d'Arolla, Switzerland. *Earth Surface Processes and Landforms* **18**, 557-571.

Sharp M. J., Tranter M., Brown G. H., and Skidmore M. (1995) Rates of chemical denudation and CO_2 drawdown in a glacier-covered alpine catchment. *Geology* **23**, 61-64.

Skidmore M., Foght J., and Sharp M. (2000) Microbial life beneath a high Arctic glacier. *Applied and Environmental Microbiology* **66** (8), 3214-3220.

Skidmore M. L. (1995) The hydrochemistry of a high Arctic glacier. MSc., University of Alberta.

Skidmore M. L. and Sharp M. J. (1999) Drainage behaviour of a high Arctic polythermal glacier. *Annals of Glaciology* **28**, 209-215.

Stumm W. and Morgan J. J. (1996) *Aquatic chemistry: Chemical equilibria and rates in natural waters*. Wiley-Interscience.

Szaran J. (1997) Achievement of carbon isotope equilibrium in the system HCO_3 (solution) - CO_2 (gas). *Chemical Geology* **142**, 79-86.

Telmer K. and Veizer J. (1999) Carbon fluxes, pCO2 and substrate weathering in a large northern river basin, Canada: carbon isotope perspectives. *Chemical Geology* **159**, 61-86.

Tranter M. (1982) Controls on the chemical composition of Alpine glacial meltwaters. Ph.D., East Anglia.

Tranter M., Brown G. H., Raiswell R., Sharp M. J., and Gurnell A. M. (1993) A conceptual model of solute acquisition by Alpine glacial meltwaters. *Journal of Glaciology* **39**, 573-581.

Tranter M., Sharp M. J., Lamb H. R., Brown G. H., Hubbard B. P., and Willis I. C. (in press) Chemical weathering at the bed of Haut Glacier d'Arolla, Switzerland - a new model. *Hydrological Processes*.

Trolier M., White J. W. C., Tans P. P., Masarie K. A., and Gemery P. A. (1996) Monitoring the isotopic composition of atmospheric CO_2: Measurements from the NOAA global air sampling network. *Journal of Geophysical Research* **101**(D20), 25,897-25-916.

Vogel J. C., Grootes P. M., and Mook W. G. (1970) Isotopic fractionation between gaseous and dissolved carbon dioxide. *Zeitschrift fur Physik* **230**, 225-238.

Wadham J. L., Hodson A. J., Tranter M., and Dowdeswell J. A. (1998) The hydrochemistry of meltwaters draining a polythermal-based, high Arctic glacier, south Svalbard: I The ablation season. *Hydrological Processes* **12**, 1825-1849.

Wendt I. (1968) Fractionation of carbon isotopes and its temperature dependence in the system CO_2-Gas-CO_2 in soluton and HCO_3-CO_2 in solution. *Earth and Planetary Science Letters* **4**, 64-68.

White A. F., Bullen T. D., Vivit D. V., Schulz M. S., and Clow D. W. (1999) The role of disseminated calcite in the chemical weathering of granitoid rocks. *Geochimica Cosmochimica Acta* **63** (13/14), 1939-1953.

Wigley T. M. L., Plummer L. N., and Pearson F. J. (1978) Mass transfer and carbon isotope evolution in natural water systems. *Geochimica Cosmochimica Acta* **42**, 1117-1139.

Zhang J., Quay P. D., and Wilbur D. O. (1995) Carbon isotope fractionation during gas-water exchange and dissolution of CO_2. *Geochimica Cosmochimica Acta* 59 (1), 107-114.

Table 4.1 Geochemical and isotopic field data and output from Models 1-5

	Julian Day	$SO_4^{2-}{}_{(xs)}$ µeq l^{-1}	DIC µeq l^{-1}	Measured $\delta^{13}C$	M1 $\delta^{13}C$	M2 $\delta^{13}C$	M3 $\delta^{13}C$	M4 Micro CO_2 as % of DIC	M5 Micro CO_2 %	M5 Atm CO_2 %	M5 Micro CO_2 $\delta^{13}C$
John Evans Glacier											
Marginal	183.7	9	450	-10.1	-4.8	-13.2		28	62	38	
Stream	185.5	7	540	-8.4	-4.8	-13.3		15	41	59	
	187.6	16	566	-8.8	-4.7	-13.1		17	47	53	
	189.7	13	494	-8.4	-4.7	-13.1		16	42	58	
	191.6	16	392	-8.2	-4.7	-12.9		21	41	59	
	193.5	18	344	-7.4	-4.6	-12.8		20	32	68	
	195.7	18	354	-8.0	-4.7	-12.8		22	39	61	
	197.6	13	296	-9.5	-4.7	-12.9		31	57	43	
	199.6	11	316	-9.7	-4.7	-13.0		34	59	41	
	201.6	13	312	-10.0	-4.7	-12.9		35	63	37	
	203.5	11	312	-8.5	-4.7	-13.0		28	44	56	
Subglacial	183.6	100	222	-13.5	-3.1	-7.8	-0.9		100	0	-47.0
Stream	185.4	81	216	-13.0	-3.4	-8.8	-0.9		100	0	-39.4
	187.4	53	230	-12.0	-3.9	-10.6	-0.9		100	0	-29.8
	189.7	37	204	-13.2	-4.1	-11.2	-0.9		100	0	-31.0
	191.5	107	230	-15.7	-3.0	-7.6	-0.9		100	0	-56.4
	193.5	38	420	-8.5	-4.5	-12.3	-12.4	23	49	51	
	195.6	59	302	-10.7	-4.1	-11.0	-5.3		96	4	
	197.5	27	304	-10.8	-4.5	-12.3	-8.1		80	20	
	199.6	25	266	-11.2	-4.5	-12.3	-5.7		86	14	
	201.6	28	246	-13.0	-4.4	-12.0	-3.7		100	0	-28.5
	203.5	0	236	-10.8	-4.9	-13.5	-5.8		69	31	
Haut Glacier d'Arolla											
Bulk	141.5	286	588	-4.3	-4.0	-8.5	-4.8	10	8	92	
Meltwaters	141.6	282	568	-5.3	-4.0	-8.3	-4.4	12	35	65	
	141.6	287	588	-6.0	-4.0	-8.4	-4.6	15	51	49	
	141.7	290	608	-6.6	-4.1	-8.6	-4.9	18	62	38	
	141.7	283	608	-5.9	-4.1	-8.7	-5.0	15	41	59	
	143.4	221	568	-5.6	-4.4	-9.6	-5.6	14	17	83	
	143.5	221	568	-6.4	-4.4	-9.6	-5.6	17	32	68	
	143.6	221	528	-7.3	-4.3	-9.3	-5.0	21	59	41	
	143.7	207	488	-6.8	-4.2	-9.2	-4.6	19	49	51	
	205.4	105	320	-3.5	-4.5	-10.3	-3.3	5	0	100	
	205.5	95	308	-4.4	-4.6	-10.6	-3.2	9	0	100	
	205.6	79	296	-6.1	-4.8	-11.1	-3.5	11	5	95	
	205.8	78	284	-8.3	-4.7	-11.0	-3.0	8	43	57	
	230.4	134	342	-2.6	-4.3	-9.6	-3.0	3	0	100	
	230.5	152	317	-3.8	-4.1	-8.5	-2.3	6	0	100	
Borehole	228.0	404	890	-7.2	-4.1	-8.8	-6.3	20	67	33	
Waters	231.0	169	430	-10.5	-4.3	-9.6	-4.3	30	100	0	-28.7

Table 4.2. Predicted quickflow (Q_q) geochemistry for JD 205 at Haut Glacier d'Arolla

	Measured Q_t and Q_s geochemistry						Predicted Q_q geochemistry					
JD	SO_4^{2-} µeq l^{-1}	DIC µeq l^{-1}	log PCO_2 atm	Measured $\delta^{14}C$ per mille	Discharge (Q) $m^3 s^{-1}$	Q_q % of total Q	SO_4^{2-} µeq l^{-1}	DIC µeq l^{-1}	log PCO_2 atm	$\delta^{14}C$-DIC	rock $\delta^{14}C$	ε_b
205.4	105	320	-2.4	-3.5	2.83	-	-	-	-	-	-	-
205.5	95	308	-2.6	-4.4	3.60	22	13	57	-	-7.8	-7.2	-4.8
205.6	79	296	-2.8	-6.1	4.87	42	18	110	4.11	-9.6	-9.8	-7.4
205.8	78	284	-2.9	-8.3	4.91	43	17	100	4.19	-14.9	-16.5	-14.1

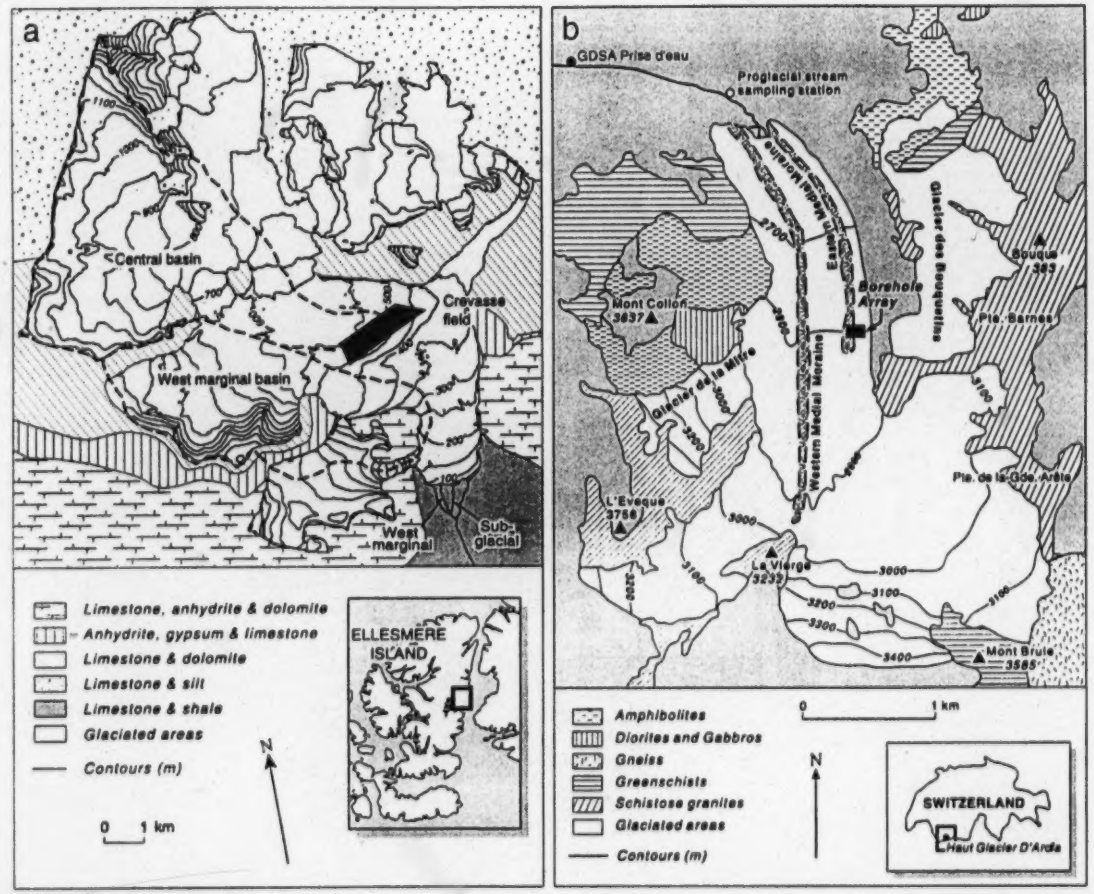

Fig 4.1 Location maps and bedrock geology of (a) John Evans Glacier and (b) Haut Glacier d'Arolla

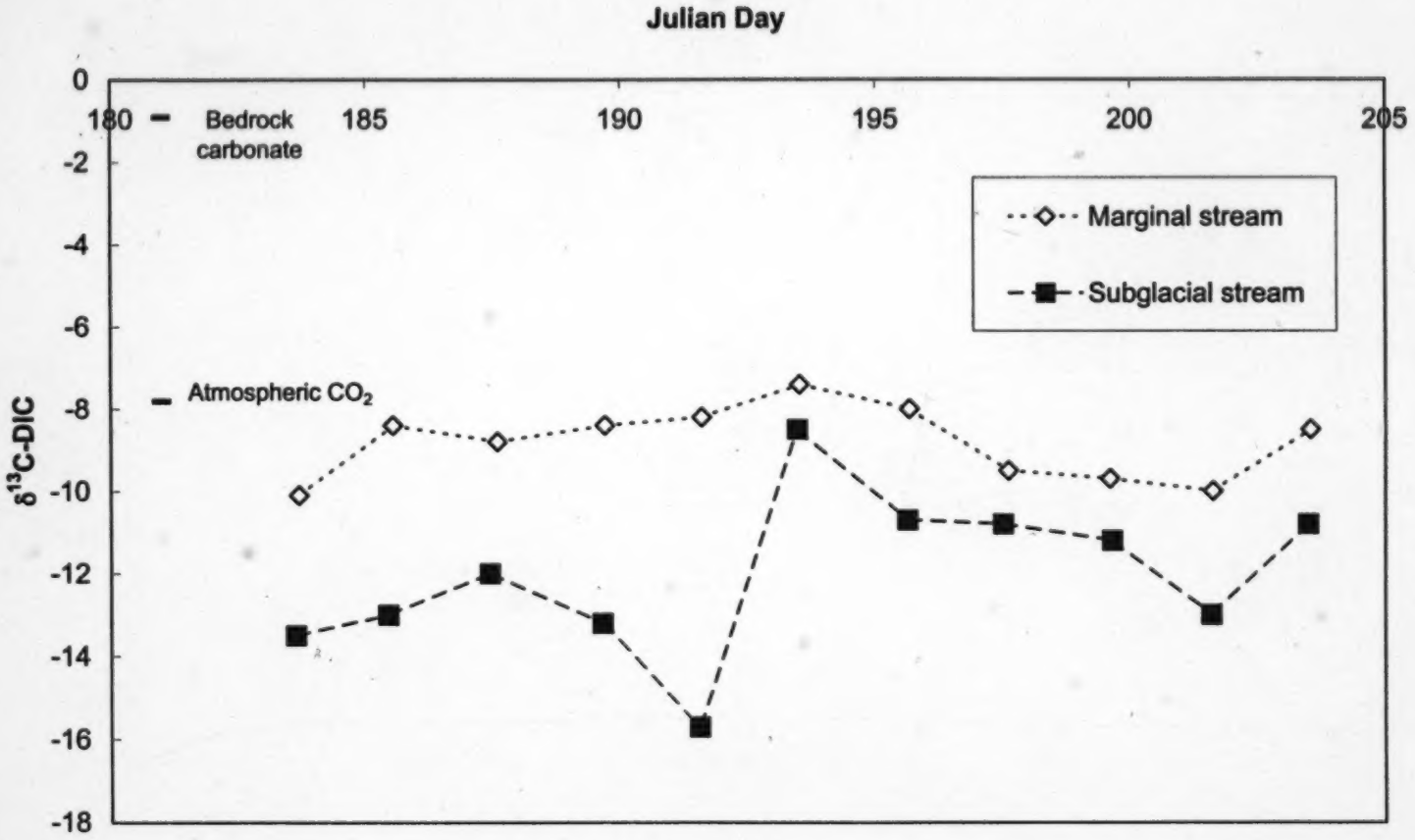

Fig. 4.2 John Evans Glacier δ^{13}C-DIC time series

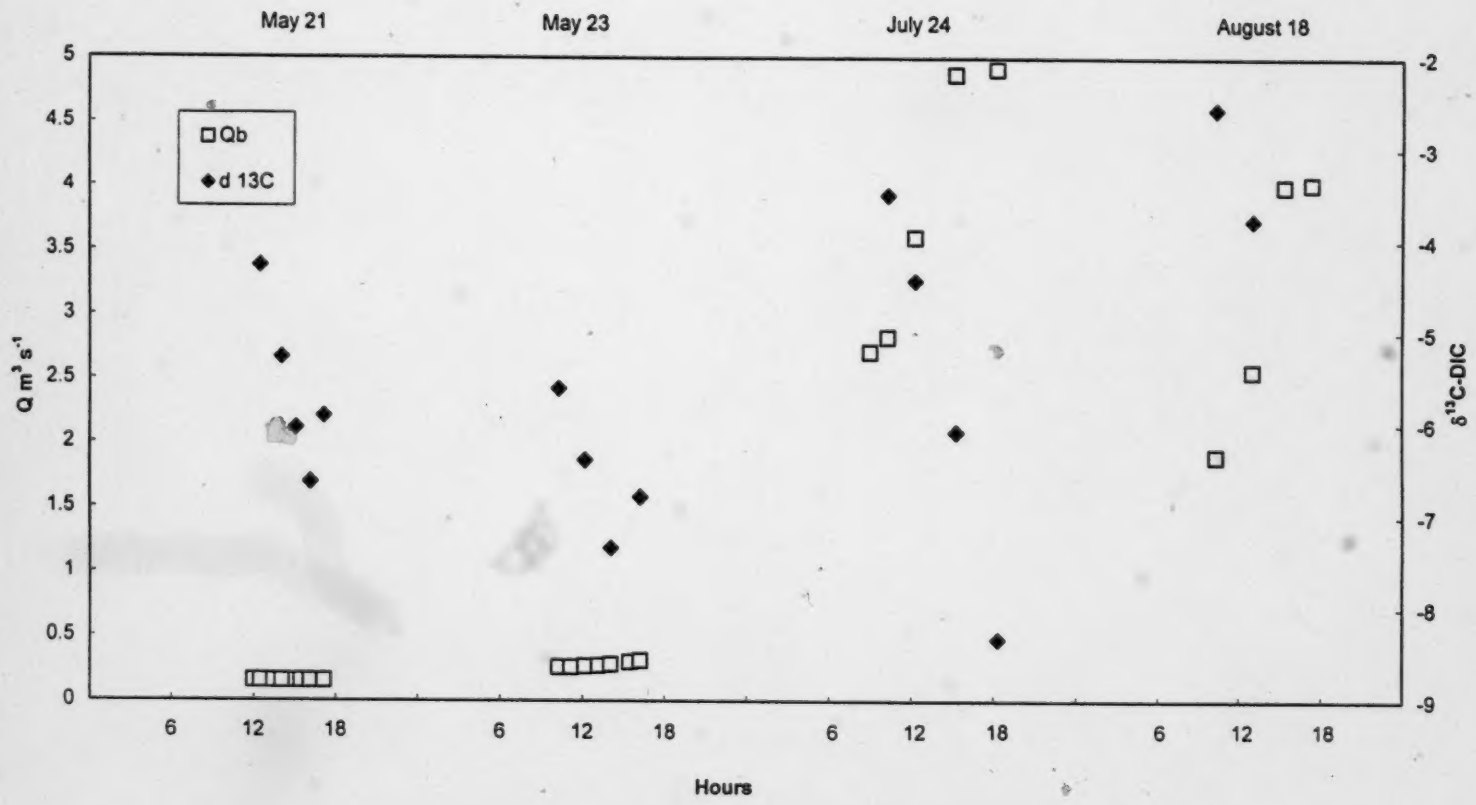

Fig. 4.3 a Haut Glacier d'Arolla diurnal Q and δ^{13}C-DIC variations

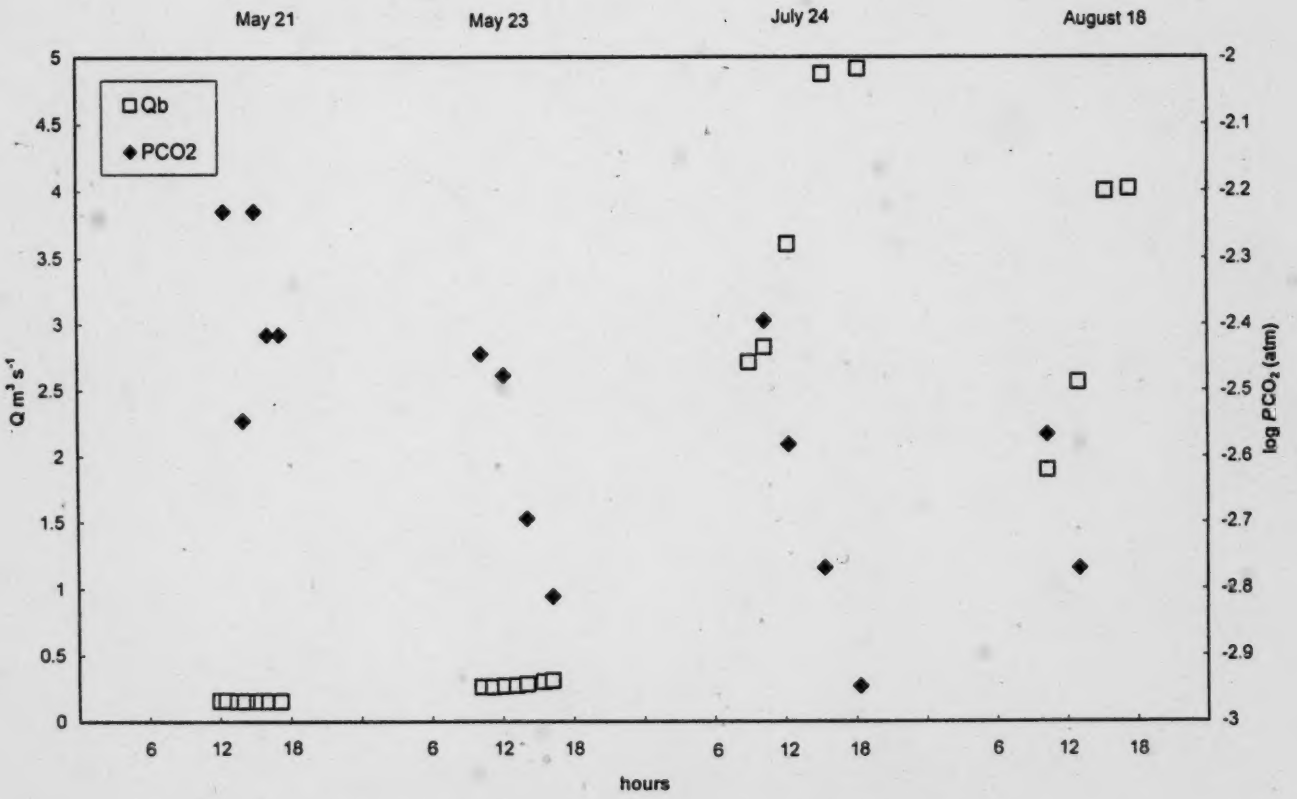

Fig. 4.3 b Haut Glacier d'Arolla diurnal Q and log $P\,CO_2$ variations

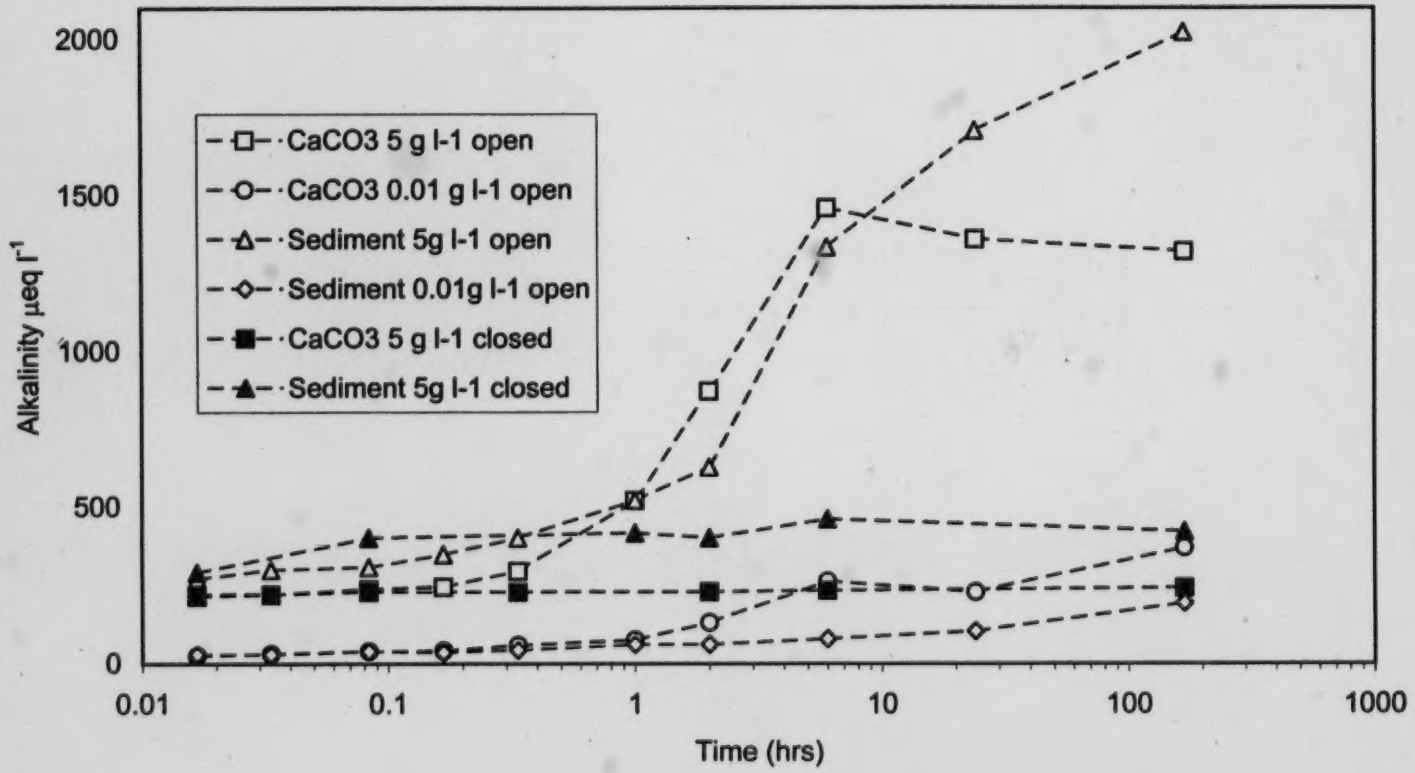

Fig. 4.4 a Weathering experiment alkalinity v time

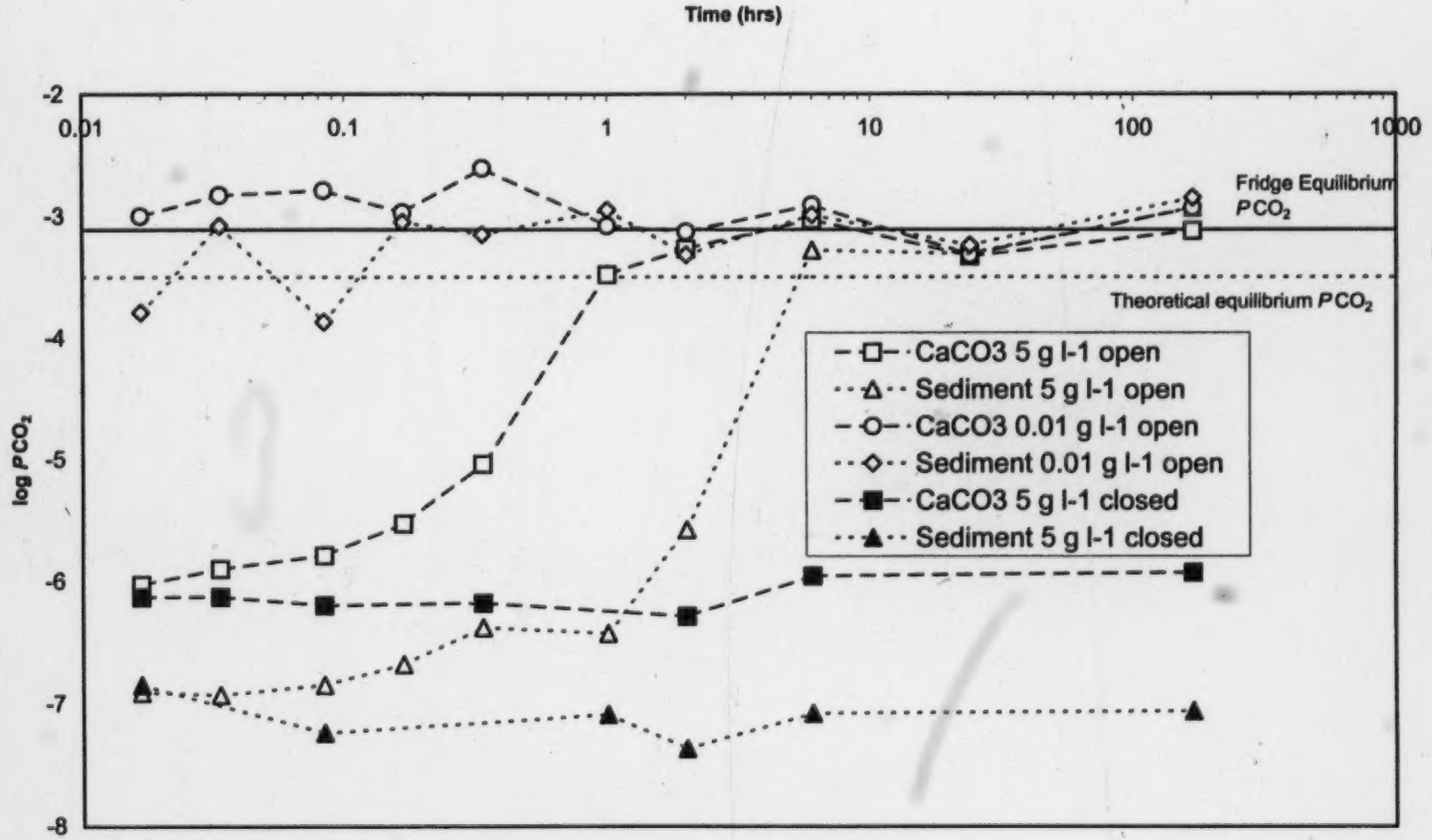

Fig. 4.4 b Weathering experiments PCO_2

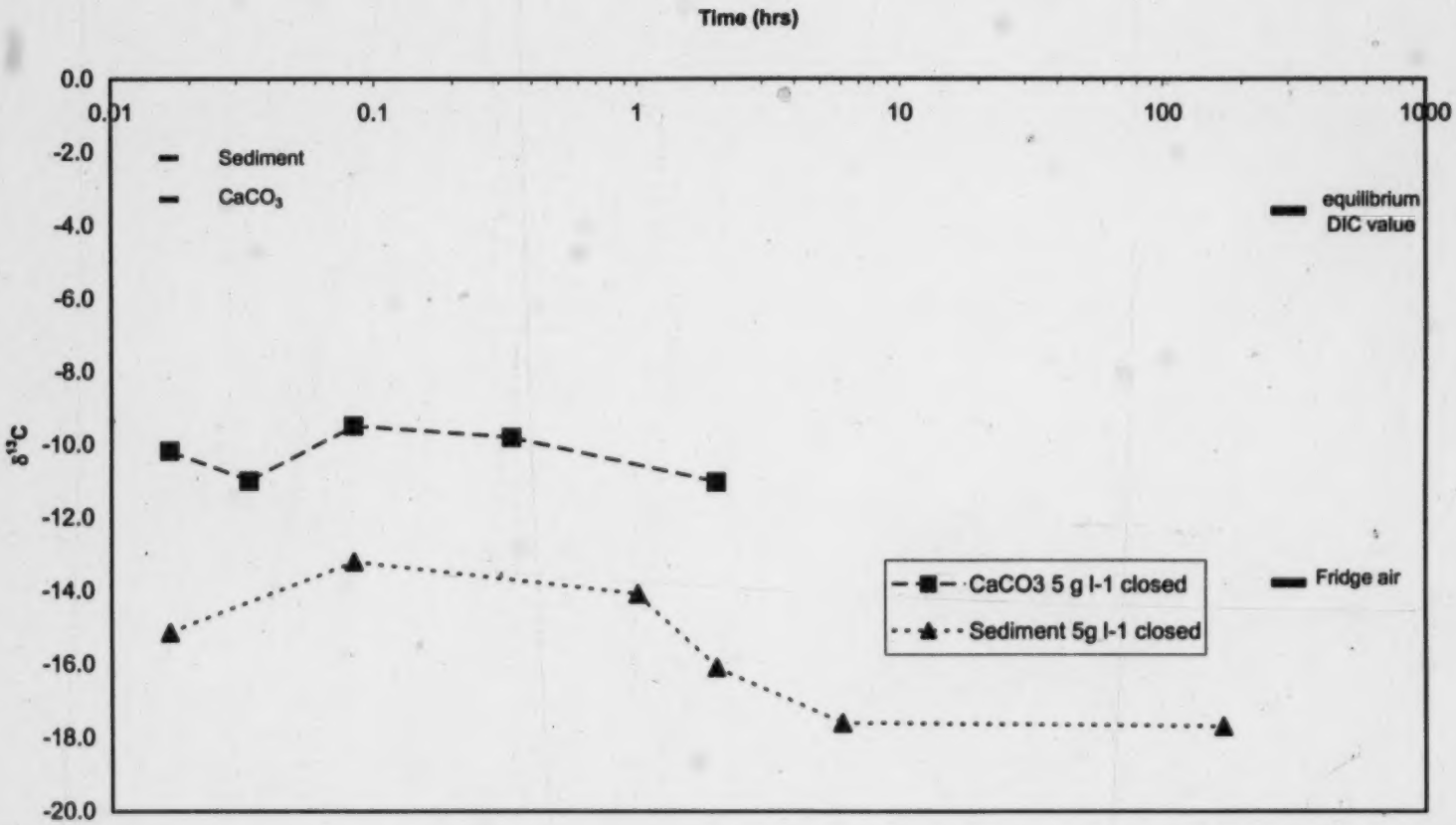

Fig. 4.4 c Closed system 5 g l^{-1} weathering experiments $\delta^{13}C$

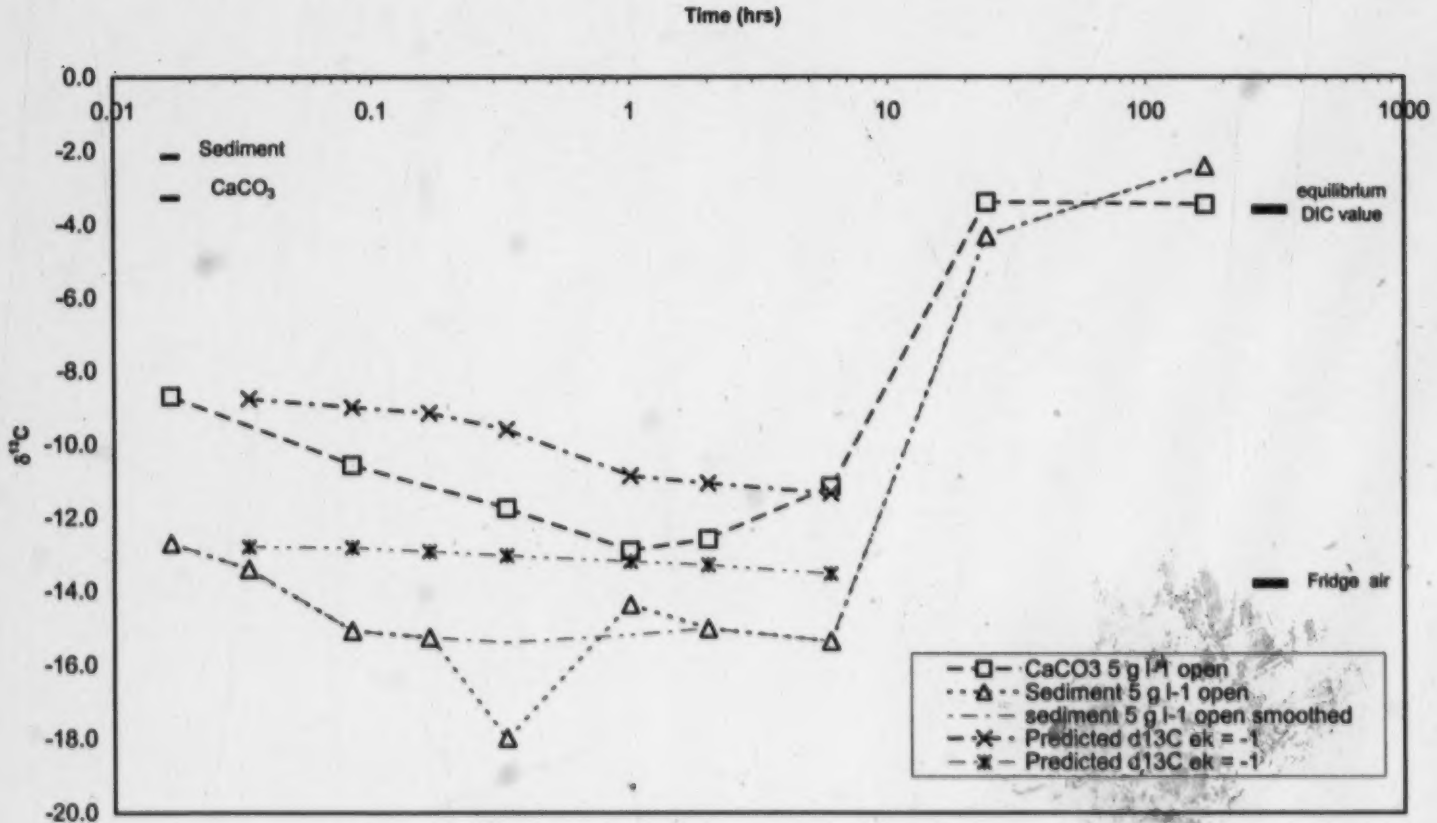

Fig. 4.4 d Open system 5 g l^{-1} weathering experiments $\delta^{13}C$

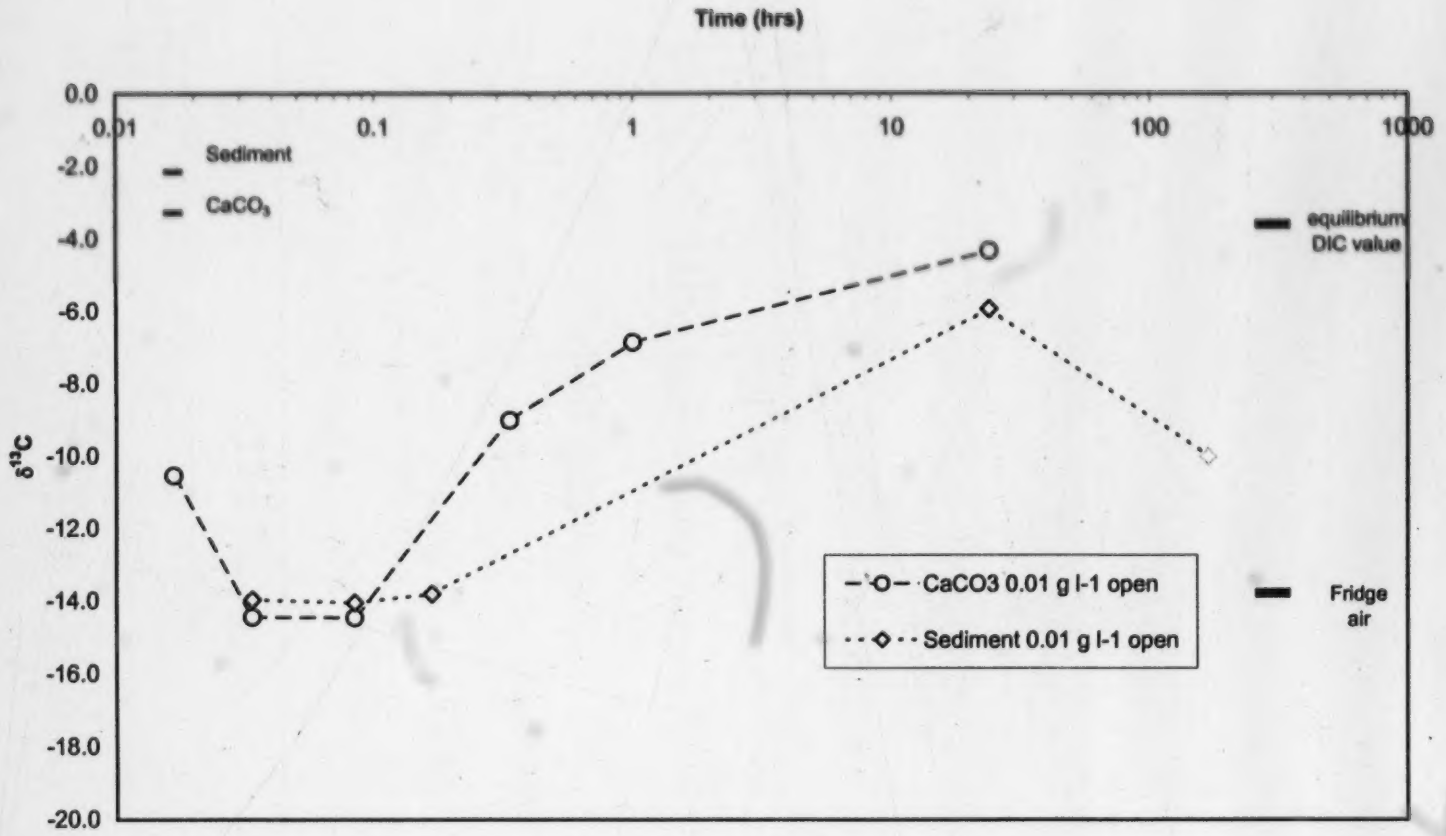

Fig. 4.4e Open system 0.01 g l^{-1} weathering experiments $\delta^{13}C$

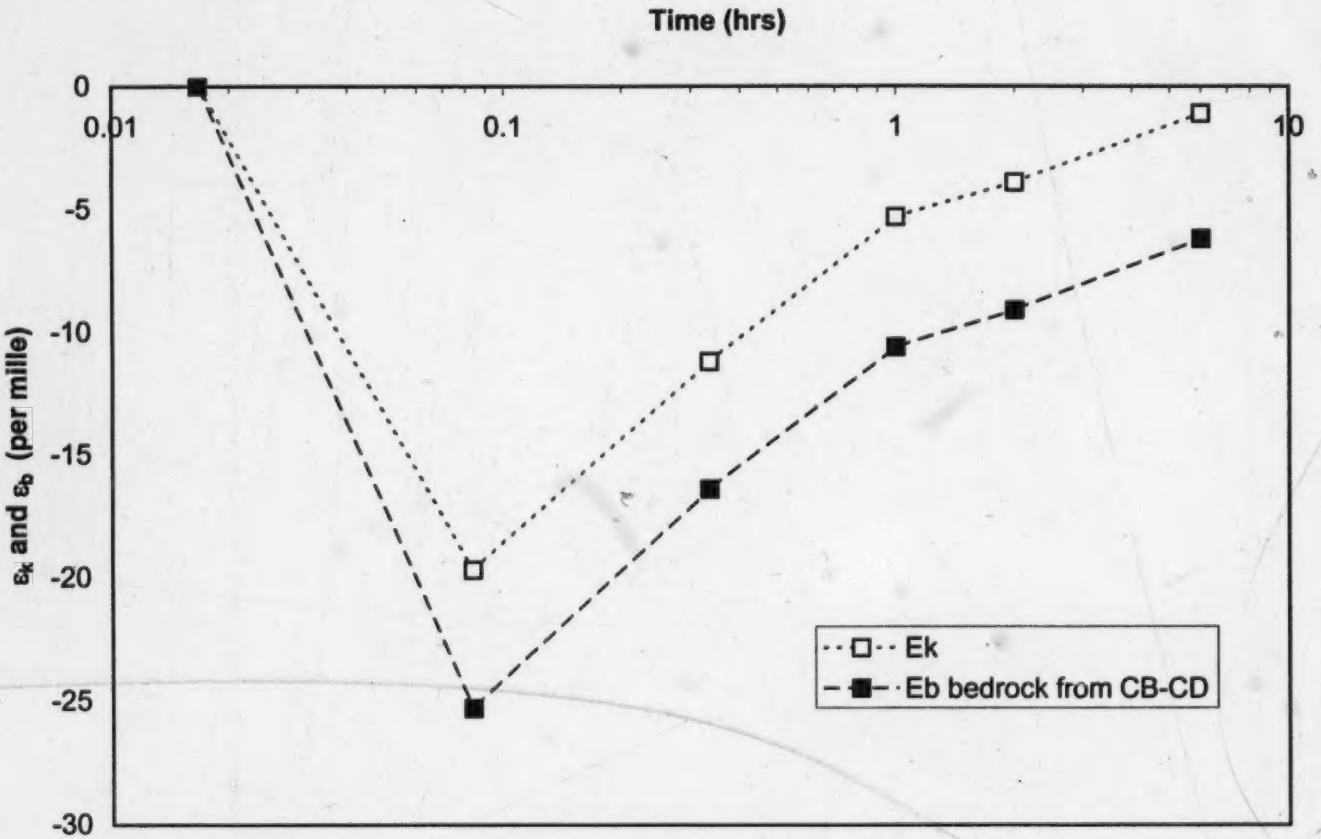

Fig. 4.5 5 g l^{-1} $CaCO_3$ experiment: ε_k and ε_b v t

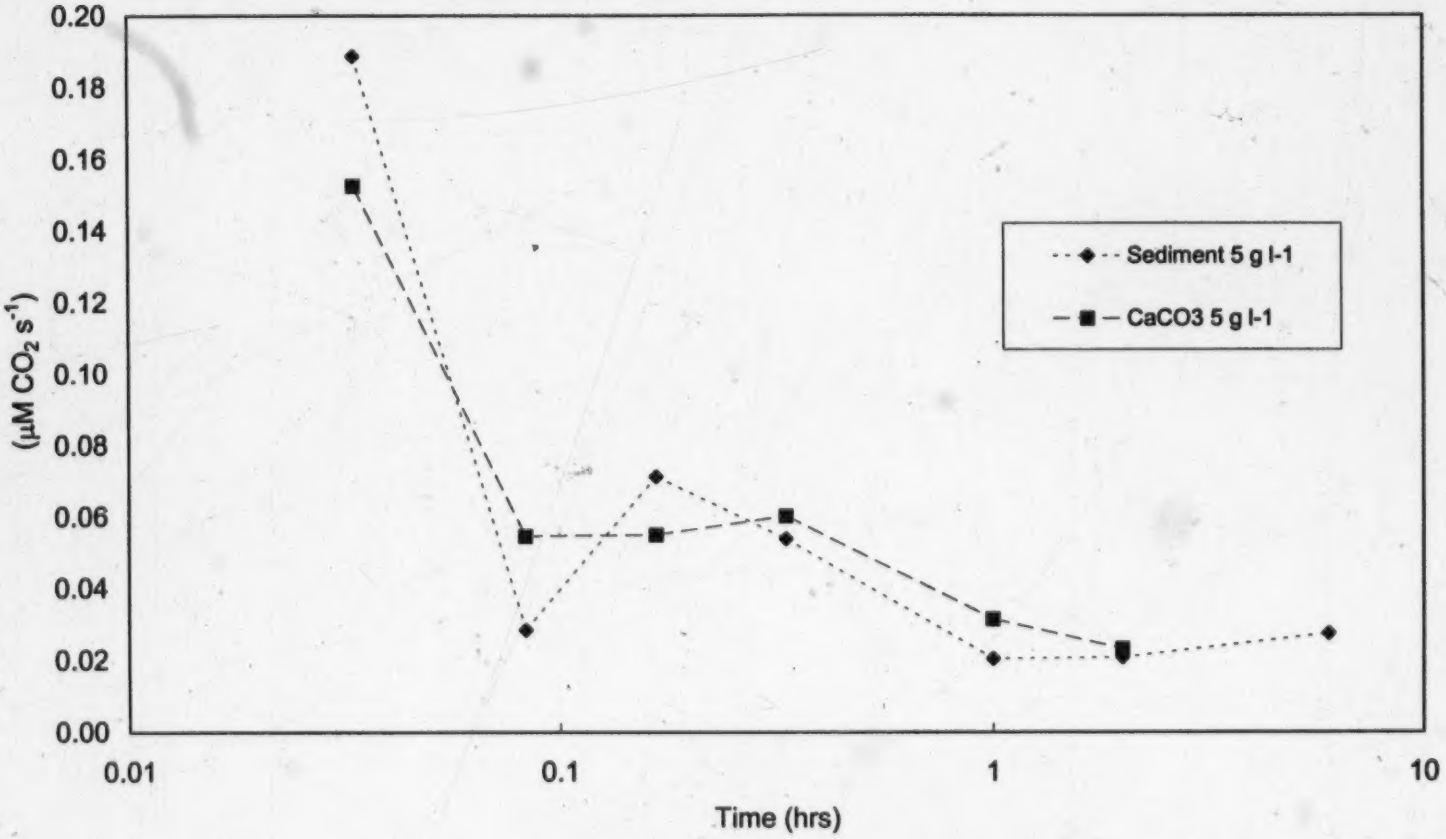

Fig. 4.6 dCO_2/dt for 5 g l^{-1} weathering experiments

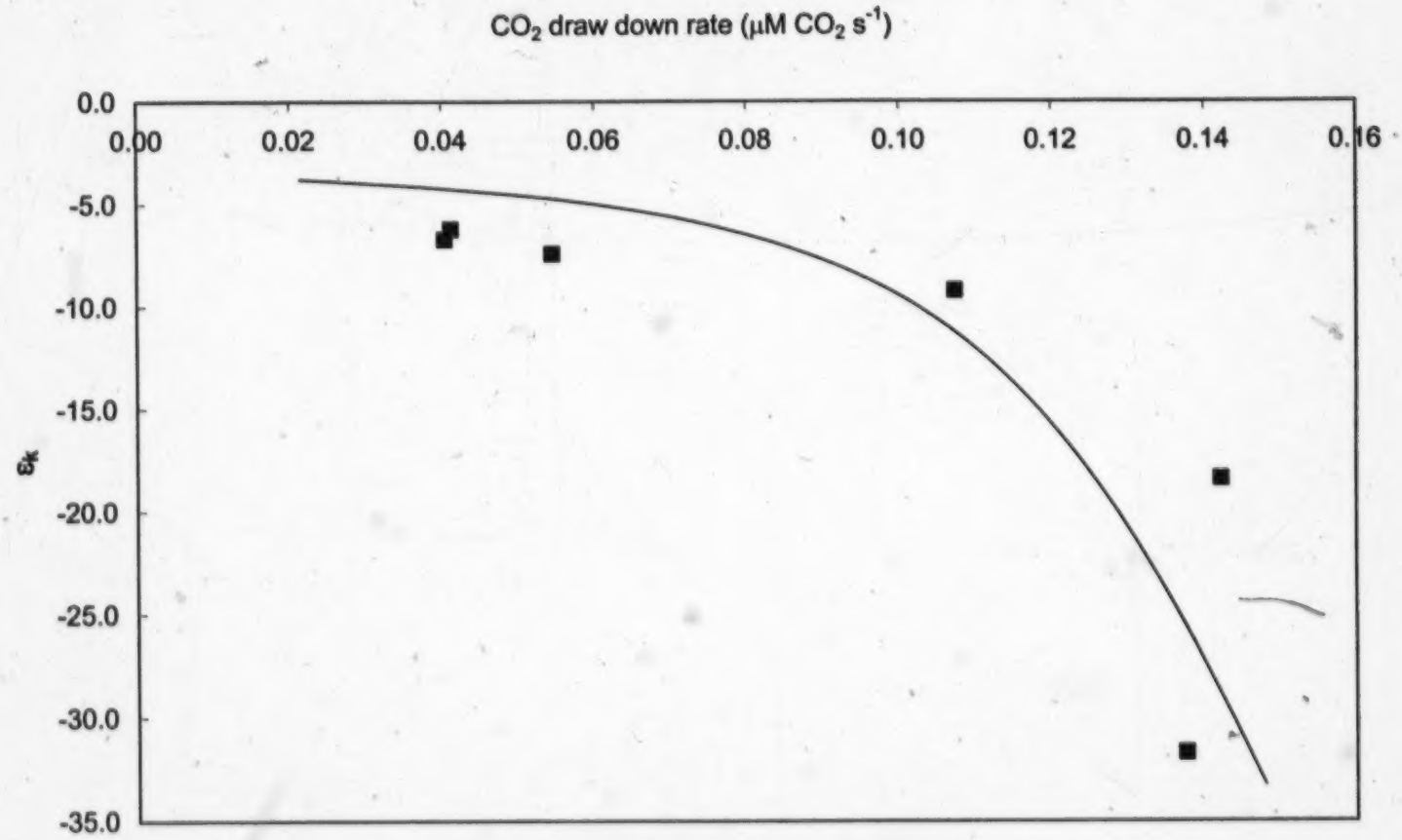

Fig. 4.7 5 g l^{-1} $CaCO_3$ ε_k v CO_2 draw down rate

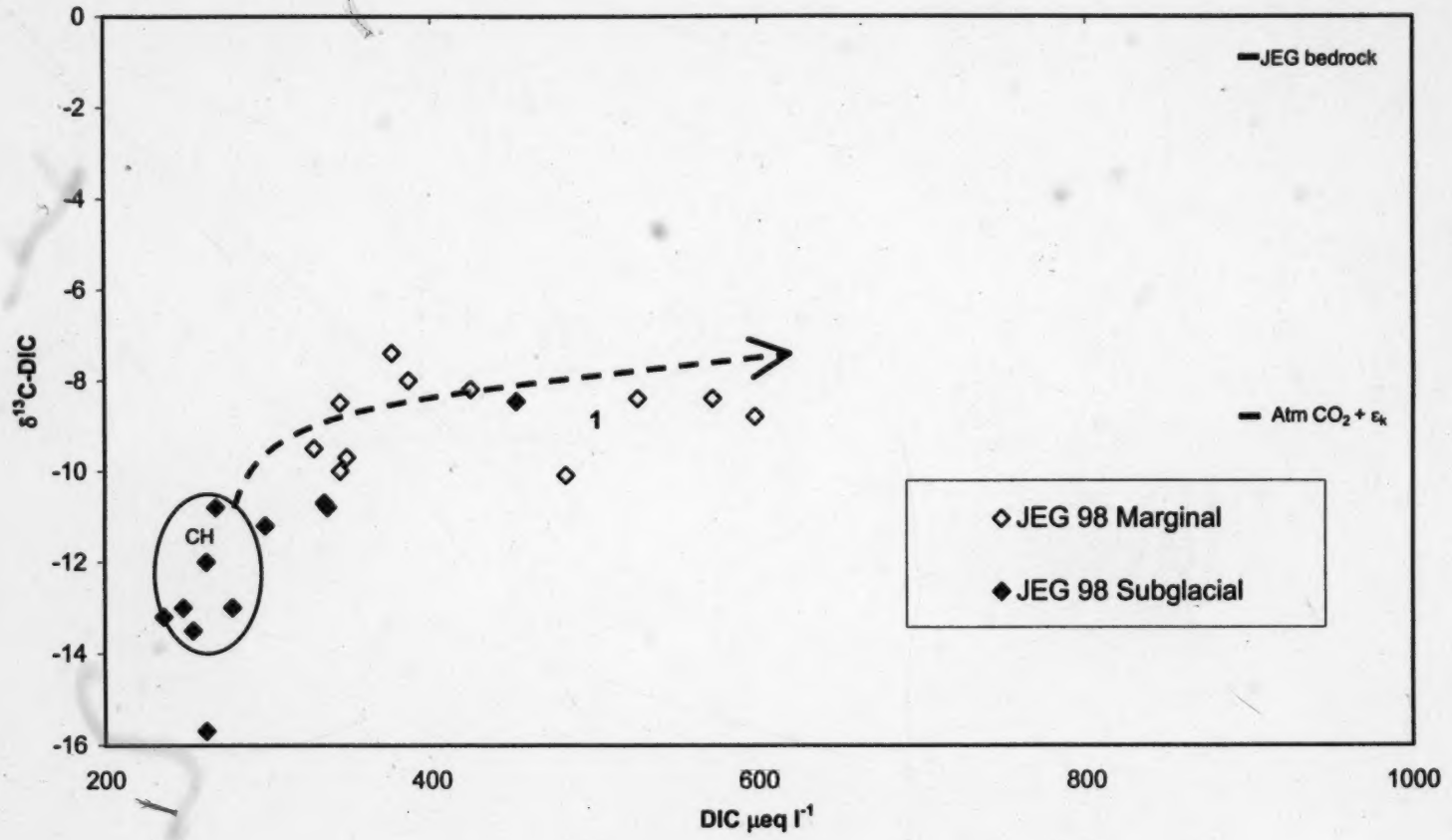

Fig. 4.8 a John Evans Glacier DIC v δ^{13}C-DIC

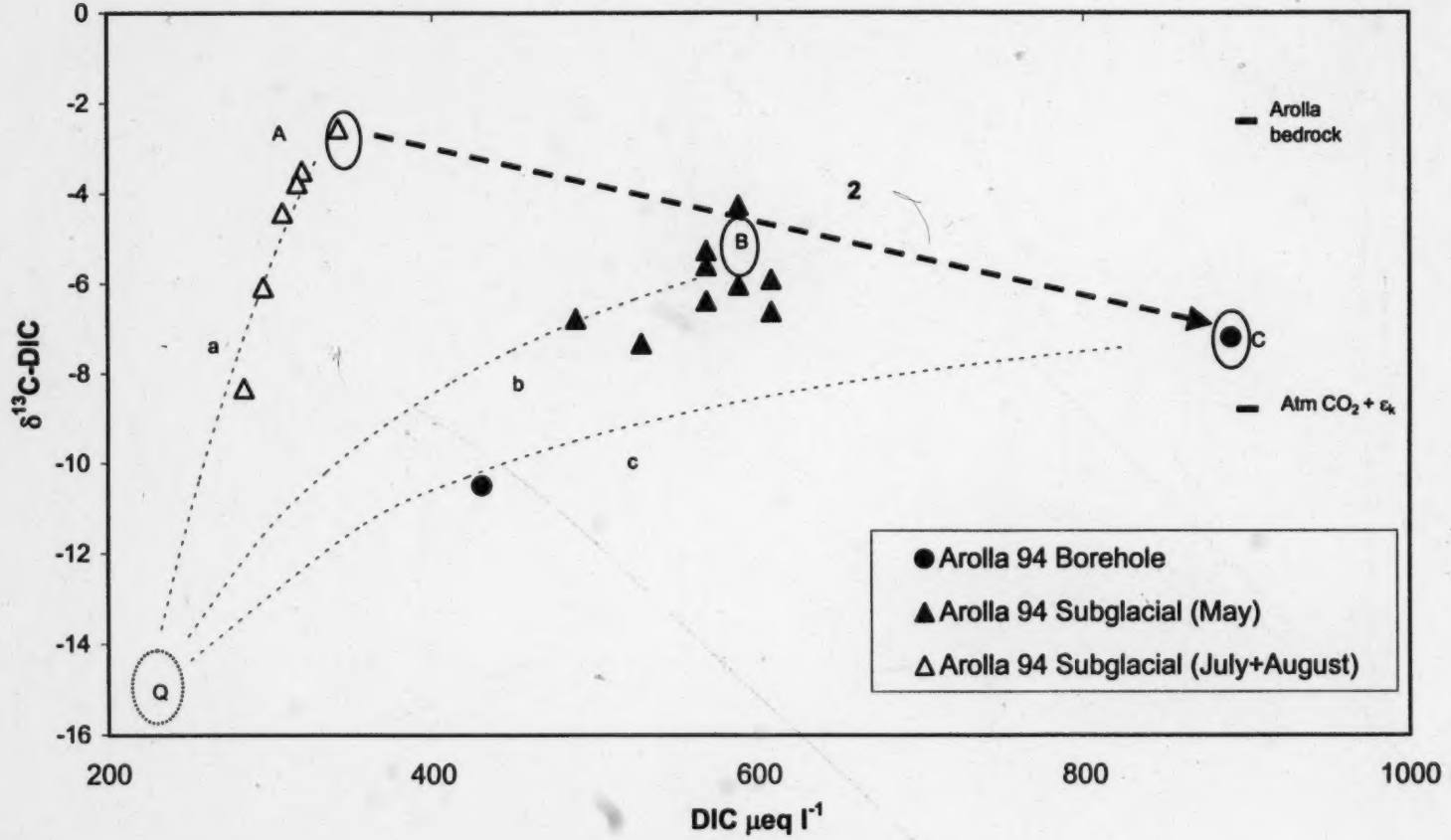

Fig. 4.8 b Haut Glacier d'Arolla DIC v δ^{13}C-DIC

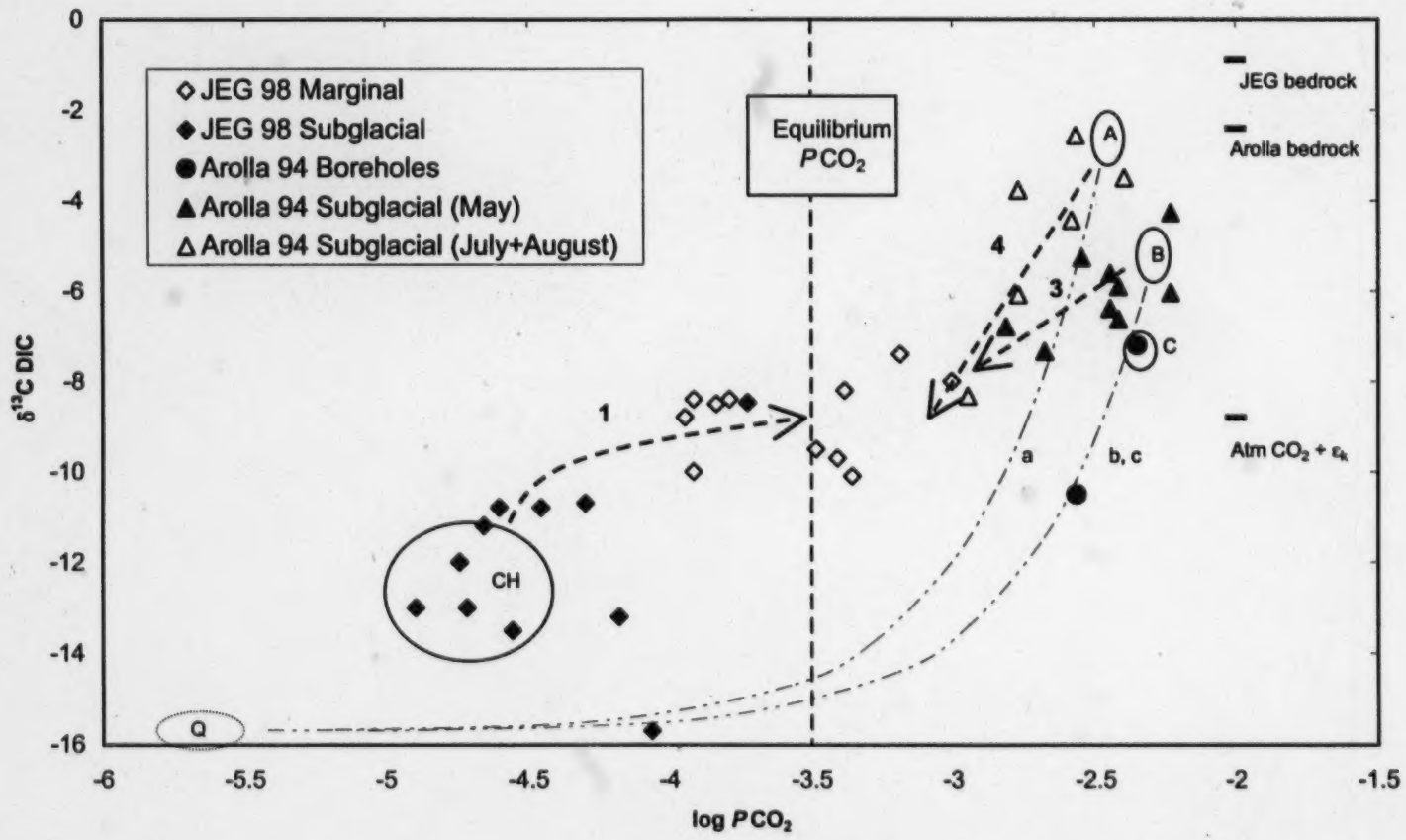

Fig. 4.9 δ^{13}C-DIC v log PCO_2

Appendix 4.1. Composition of rock samples collected at Haut Glacier d'Arolla, 1994.

	Carbonate	
Rock Type	Wt %	$\delta^{13}C$
Gabbro/diorite	0.084	-2.58
Gabbro/diorite	0.004	ND
Gneiss	0.031	-6.63
Gneiss	0.100	-2.65
Gneiss	0.041	-3.71
Schistose granite	0.007	ND
Schistose granite	0.000	ND
Schistose granite	0.002	ND
Schistose granite	0.500	-2.50
Schistose granite	0.160	-2.42
Schistose granite	0.580	-2.62
Amphibolite	0.330	-0.94
Weighted mean		-2.4

Chapter 5. Summary

The research has (a) significantly enhanced our knowledge of polythermal glacier hydrology, (b) demonstrated microbial activity at near *in situ* subglacial conditions, (c) highlighted the potential importance of redox processes and anoxic conditions in chemical weathering in distributed system subglacial environments and (d) demonstrated the importance of kinetic processes in subglacial weathering environments.

Skidmore and Sharp, (1999), (Chapter 2) is the first detailed study to document the pattern of subglacial drainage at a polythermal Arctic glacier, and its interannual variability. It demonstrates that subglacial drainage is established even in years when the melt season is extremely short, (~ 3 weeks in 1996). The generalised model for John Evans Glacier is as follows. Unlike temperate glaciers and other arctic polythermal glaciers (e.g. Finsterwalderbreen, Svalbard, Wadham, et al., 2001), subglacial drainage at John Evans Glacier ceases over winter. During fall/winter, a frozen seal is created at the (cold based) glacier terminus, which impedes subglacial drainage. This likely results in water storage at the glacier bed over winter (as indicated by high conductivity waters, and high concentrations of silicate mineral weathering products in the initial outburst waters). In spring when surficial melt begins, water is supplied to the subglacial environment and is stored until sufficient pressure builds up to break the frozen seal. Hence, subglacial drainage is initiated as an outburst event, ~ 3 weeks after the onset of the melt season. In 1994 and 1996, when temperatures and melt rates were low the subglacial water outflow was pulsed following the initial outburst. Field research in 1998, 1999 and 2000 generally supports the 1994 and 1996 observations, except that in those years, flow was continuous after the initial outburst, rather than pulsed. The continuous subglacial outflow in 1998, 1999 and 2000 is probably a result of greater and more sustained surface water inputs to the subglacial system than in 1994 and 1996 due to higher melt rates (Table 1.2.). This would affect the temporal continuity of subglacial flow, the size of conduits that develop during high melt periods, and thus the likelihood that they will close through ice deformation during periods of cold weather when runoff volumes are reduced. The unique chemical composition of the subglacial waters can be used to trace hydrological

links between the subglacial and marginal streams, demonstrating both lateral and downglacier movement of subglacial waters during outburst events. The research has significantly improved our understanding of polythermal glacier hydrology and provided the groundwork for subsequent studies at John Evans Glacier (Copland, 2001) which link the observed hydrological behaviour to variations in glacier dynamics, measured via surveying techniques.

Skidmore et al., (2000), (Chapter 3) demonstrate microbial activity at 0.3°C from John Evans Glacier subglacial sediments and the presence of strictly anaerobic bacteria in these sediments. This highlights the potential importance of redox reactions in subglacial weathering environments that hitherto have been given little consideration. Recent studies at Haut Glacier d'Arolla also demonstrate geochemically (Tranter et al., in press) and isotopically (Bottrell and Tranter, in press) that certain subglacial weathering environments are likely anoxic. The presence of strictly anaerobic bacteria (e.g. methanogens) in the basal sediments also argues that these bacteria are not washed in with oxygenated surface meltwaters, but are present in the subglacial environment.

This suggests that the subglacial environment beneath a polythermal glacier provides a viable habitat for life and that microbes may be widespread where the basal ice is temperate and water is present at the base of the glacier, and where organic carbon from glacially overridden soils is present. The observations raise the possibility that *in situ* microbial production of CO_2 and CH_4 beneath ice masses (e.g. the Northern Hemisphere ice sheets) is an important factor in carbon cycling during glacial periods. Moreover, this terrestrial environment may provide a model for viable habitats for life on Mars, since similar conditions may exist or have existed in the basal sediments beneath the Martian north polar ice cap.

To date this is the only study to unequivocally demonstrate microbial activity with simulated *in situ* subglacial conditions. Microbes have been detected in the accreted lake ice from Lake Vostok at the base of the Vostok Ice Core (Priscu et al., 1999, Karl et al., 1999). However, Priscu et al., (1999) do not demonstrate any metabolic activity in their samples. By contrast, Karl et al., (1999) demonstrate limited rates of metabolism at 3°C,

however, metabolic rates are significantly enhanced at 18°C, suggesting that the bacteria are psychrotrophic rather than truly psychrophilic. It is interesting that the bacteria have a temperature optimum of at least 18°C, given that the samples have been stored at temperatures below zero for c. 500,000 years whilst in transport in the ice and when (presumably) active in the lake water were operating in water temperatures of ≤ 0°C. It is also interesting that the samples which contain sediment inclusions, (Priscu et al, 1999), show no growth whereas the sediment free ice (Karl et al., 1999) shows microbial growth. This contrasts with the results from the Alpine and Arctic glacial samples, (Sharp et al., 1999; Skidmore et al., 2000) and Antarctic sea ice (Priscu et al., 1998).

It is theoretically possible that subglacial bacteria may operate within the ice at sub-freezing temperatures, in the liquid veins between ice crystals (Price, 2000). Our study did not demonstrate evidence for such activity after 66 days incubation at – 4.5°C to -1.5°C. However, there are reports of microbial activity at < 0°C from radiotracer investigations in other permafrozen environments (Rivkina et al., 2000; Carpenter et al., 2000). Rivkina et al., (2000) report metabolism at –5°C from Siberian permafrozen soils, with a 365 day incubation period, whereas Carpenter et al., (2000) from South Pole snow, at –12°C to –15°C with only an 18 hour incubation period. However, in both studies the levels of radioisotopic production are close to background levels and have large error bars associated with their measurements. Hence, the veracity of the data is potentially questionable. Moreover, it is surprising that Carpenter et al., (2000) did not attempt longer incubations to more clearly demonstrate metabolic activity. In light of the existing evidence, further studies are required to unequivocally demonstrate subfreezing microbiological activity.

Skidmore et al., (in prep.), (Chapter 4) demonstrate that in glacial environments kinetic weathering processes have an important impact on the water chemistry. Incorporation of KBF (kinetic bedrock fractionation) and KFC (kinetic fractionation of CO_2) processes into standard geochemical models is necessary to fully account for the field $\delta^{13}C$–DIC values. It is possible to clearly identify environments where light $\delta^{13}C$-DIC is a result of kinetic processes and where it is indicative of *in situ* subglacial microbial activity using

this combined approach. The field data reflect the experimental findings that kinetic fractionation processes have a greater overall impact on δ^{13}C-DIC where bedrock carbonate concentrations are higher. δ^{13}C–DIC values at John Evans Glacier are significantly lighter on average than Haut Glacier d'Arolla values, even though the bedrock carbonate values for John Evans Glacier are ~ 1.5 ‰ heavier. However, it is only in the distributed system waters at Haut Glacier d'Arolla that there is clear evidence of microbial CO_2 input, which ranges from 10-30 % of DIC. This agrees with Tranter et al., (in press), who argue from borehole geochemical data that anoxic conditions occur in the distributed subglacial system, which may be driven to anoxia by microbial mediated weathering reactions.

At John Evans Glacier there is strong evidence for viable microbial populations in the subglacial environment (Skidmore et al., 2000). However, since CH is the main subglacial weathering reaction, the impact of KBF on δ^{13}C-DIC makes it extremely difficult to detect microbial activity from the isotopic data.

Both this isotopic study and Tranter et al., (in press) indicate that the generation of DIC in subglacial environments is dominated by carbonate hydrolysis (CH), coupled sulphide oxidation-carbonate dissolution (SO-CD), and carbonation of carbonates driven by microbial respiration (MR-CD). Thus there is minimal atmospheric CO_2 consumption in subglacial environments at Haut Glacier d'Arolla and John Evans Glacier. In glaciated catchments, the key determinants on chemical denudation and transient CO_2 draw down rates are first, specific runoff (Anderson et al., 1997) and second, bedrock type (Hodson et al., 2000). However, Hodson et al., (2000) may substantially over estimate CO_2 draw down rates since they ignore both CH and MR-CD as weathering processes. They assume that all HCO_3^- is derived from the carbonation of carbonates driven by atmospheric CO_2 (CB-CD), and do not assess the PCO_2 values of the glacial waters. For example, at Haut Glacier d'Arolla the subglacial waters may have undergone two episodes of CH, but the addition of DIC from SO-CD and MR-CD, results in PCO_2 values that are greater than atmospheric thus leading to degassing on exposure to the atmosphere. This demonstrates that although CH does lower PCO_2 values, processes other than equilibration with

atmospheric CO_2 can lead to greater than equilibrium PCO_2 values. By contrast, at John Evans Glacier subglacial waters have PCO_2 values below atmospheric and thus chemical weathering in the proglacial zone will likely result in atmospheric CO_2 draw down. Therefore, this highlights the importance of considering both CH and MR-CD in CO_2 draw down calculations for glacial waters.

5.1. REFERENCES

Anderson S. P., Drever J. I., and Humphrey N. F. (1997) Chemical weathering in glacial environments. *Geology* **25**, 399-402.

Carpenter E. J., Lin S., and Capone D.G. (2000) Bacterial activity in South Pole snow. *Applied and Environmental Microbiology* **66** (10), 4514-4517.

Copland L. (2001) Polythermal glacier hydrology and ice flow dynamics. Ph.D. University of Alberta.

Hodson A., Tranter M., and Vatne G. (2000) Contemporary rates of chemical denudation and atmospheric CO_2 sequestration in glacier basins: and Arctic perspective. *Earth Surface Processes and Landforms* **25**, 1447-1471.

Karl D. M., Bird D. F., Bjorkman K., Houlihan T., Shackelford R., and Tupas L. (1999) Microorganisms in the accreted ice of Lake Vostok, Antarctica. *Science* **286**, 2144-2147.

Price P. B. (2000) A habitat for psychrophiles in deep Antarctic ice. *Proceedings of the National Academy of Sciences* **97** (3), 1247-1251.

Priscu J. C., Adams E. E., Berry Lyons W., Voytek M. A., Mogk D. W., Brown R. L., McKay C. P., Takacs C. D., Welch K. A., Wolf C. F., Kirshtein J. D., and Avci R. (1999) Geomicrobiology of subglacial ice above Lake Vostok, Antarctica. *Science* **286**, 2141-2144.

Rivkina E. M., Friedmann E. I., McKay C. P., and Gilichinsky D. A. (2000) Metabolic activity of permafrost bacteria below the freezing point. *Applied and Environmental Microbiology* **66** (8), 3230 - 3233.

Sharp M., Parkes J., Cragg B., Fairchild I. J., Lamb H., and Tranter M. (1999) Widespread bacterial populations at glacier beds and their relationship to rock weathering and carbon cycling. *Geology* **27** (2), 107-110.

Skidmore M., Foght J., and Sharp M. (2000) Microbial life beneath a high Arctic glacier. *Applied and Environmental Microbiology* **66** (8), 3214-3220.

Skidmore M. L. and Sharp M. J. (1999) Drainage behaviour of a high Arctic polythermal glacier. *Annals of Glaciology* **28**, 209-215.

Skidmore M. L., Sharp M. J., Tranter M., and Bottrell S. (in prep.) Fractionation of carbon isotopes during the weathering of carbonates in glaciated catchments: Implications for subglacial microbial activity. *Geochimica et Cosmochimica Acta*.

Tranter M., Sharp M. J., Lamb H. R., Brown G. H., Hubbard B. P., and Willis I. C. (in press) Geochemical weathering at the bed of Haut Glacier d'Arolla, Switzerland - a new model. *Hydrological Processes*.

Wadham J. L., Hodgkins R., Cooper R. J., and Tranter M. (2001) Evidence for seasonal subglacial outburst events at a polythermal glacier, Finsterwalderbreen, Svalbard. *Hydrological Processes* ***15***, 2259-2280.